STIAN LYDERSEN

RELIABILITY TESTING BASED ON DETERIORATION MEASUREMENTS

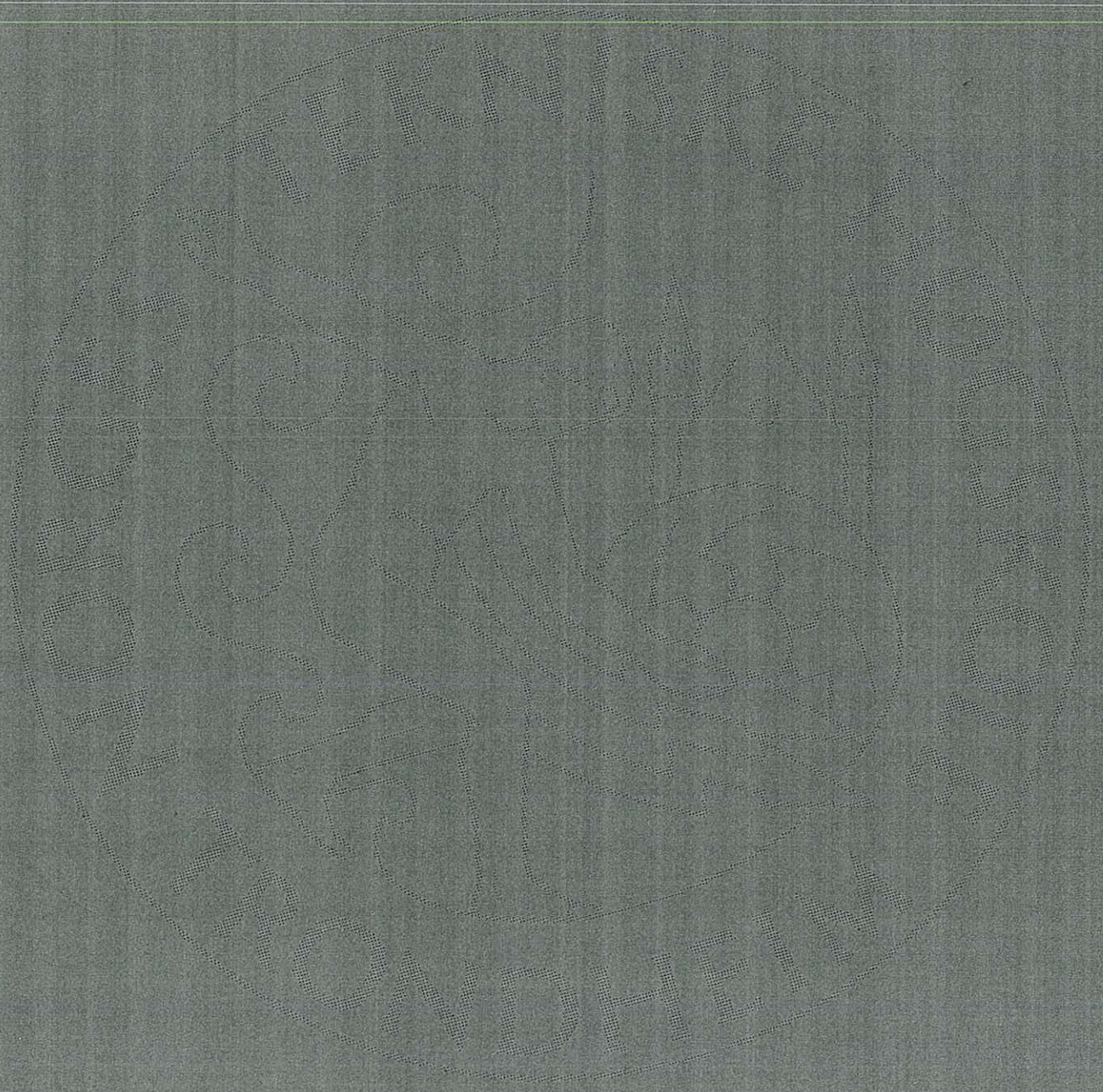

NTH
UNIVERSITETET I TRONDHEIM
NORGES TEKNISKE HØGSKOLE

DOKTOR INGENIØRAVHANDLING 1988:32
INSTITUTT FOR MATEMATISKE FAG
TRONDHEIM 1988

STIAN LYDERSEN

RELIABILITY TESTING BASED ON DETERIORATION MEASUREMENTS

DOKTOR INGENIØRAVHANDLING 1988:32
NTH, INSTITUTT FOR MATEMATISKE FAG
TRONDHEIM 1988

PREFACE

This doktor ingeniør thesis consists of 3 separate parts:

- Part I: Reliability Testing and Deterioration Measurements-General Theory.

- Part II: Deterioration of Hydraulic Control Valves

- Part III: Heat Ageing of Elastomer Foil

The three parts I - III have been edited to make it possible to read one part without reading the others. Note that most of the references are included in part I, while Part II and Part III include only literature direct connected to those parts. Each part includes a list of contents for that part only. Part I, which includes most of the general theory, also has a list of symbols and abbreviations.

The topic area for my doktor ingeniør study has been "Statistical Methods in Accelerated Life Testing (ALT)". Within this area, "Accelerated Life Testing Based on Deterioration Measurements" was chosen as working title for the thesis. However, several of the main results in the thesis are not only directed towards accelerated life testing, but rather towards wider parts of a reliability management programmes. This is especially true for the acceptance test procedure developed in Part II. The title "Reliability Testing Based on Deterioration Measurements" was felt to be more adequate for the thesis. Still, most of the emphasis has been laid on ALT applications.

The study has been carried out at the Norwegian Institute of Technology, Department of Mathematical Statistics (Norges Tekniske Høgskole, Institutt for Matematisk Statistikk) from October 1984 to July 1988. Professor Emil Spjøtvoll has been major research advisor (hovedfaglærer) for the study.

Before and in parallel with the doktor ingeniør study, I have participated in several projects including accelerated life testing (ALT) at SINTEF (Stiftelsen for Industriell og Teknisk Forskning ved Norges

Tekniske Høgskole - The Foundation for Industrial Research at the Norwegian Institute of Technology). The projects including ALT are:

- Mechanical Reliability, 1982 - 1985. Sponsor: NTNF - The Royal Norwegian Council for Scientific and Technical Research. VF-Committee.

- SERA - Subsea Equipment Reliability and Availability, 1985 - 1988. Sponsor: NTNF - The Royal Norwegian Council for Scientific and Technical Research, Sikkerhet og Beredskapskomitéen.

- Reliability of Subsea Gate Valves. Phase I, II, and III, 1984-1988. Sponsor: Norske Shell, Statoil, Hydro.

- Subsea Control Valves, Accelerated Life Testing. Phase I and II, 1985 - 1986. Sponsor: Saga Petroleum.

- Accelerated Life Testing of Pilot Valves, 1986 - 1987. Sponsor: Statoil.

The background and experience provided through these studies has been important during the work on the thesis. Some results from the NTNF projects have been included in the thesis. Although no results from the industry projects have been included in the thesis, they have provided practical insight during the study. Vice versa, work performed as part of the doktor ingeniør study, has been beneficial to these projects.

During the study, I received a university scholarship at the Norwegian Institute of Technology for 2 1/2 years. For the rest of the time, I have been employed as research scientist at SINTEF, Division of Safety and Reliability. Further, NTNF provided a direct support of NOK 50 000,- to the doktor ingeniør study in 1988, through the SERA research programme.

Among those who have contributed to the technical contents of the study, I particularly wish to thank:

- Division Manager Marvin Rausand at SINTEF, Division of Safety and Reliability. He initiated a major part of the activities on ALT at SINTEF. Further, he contributed to the initiation of this Doktor Ingeniør study.

- Professor Emil Spjøtvoll, for interesting and inspiring guidance during the study.

- Norges Tekniske Universitetsbibliotek (NTUB), for providing professional and efficient library services which are necessary to carry out a study like this one.

Trondheim, 26 July 1988,

Stian Lydersen

Stian Lydersen

STIAN LYDERSEN

RELIABILITY TESTING BASED ON DETERIORATION MEASUREMENTS

PART I: RELIABILITY TESTING AND DETERIORATION MEASUREMENTS - GENERAL THEORY

DOKTOR INGENIØRAVHANDLING 1988:32
NTH, INSTITUTT FOR MATEMATISKE FAG
TRONDHEIM 1988

ABSTRACT

In traditional reliability life testing and accelerated life testing, usually only the failure mode and the lifetime upon failure or censoring, are recorded. The information obtained from such testing may be significantly improved by also recording one or more measures of deterioration, such as wear depth, crack length, leakage rate, etc. Failure occurs when a measure of deterioration, or a combination of them, reach a critical value. This approach calls for refined reliability models and estimation techniques.

Established deterministic models for some physical deterioration mechanisms are described. Alternative approaches for stochastic models are studied, such as cumulative stochastic processes, Wiener processes, regression models with random coefficients, Wiener processes with random drift, and the Bernstein distribution and related models. Special attention is attached to models where a parameter set in the stochastic process is considered as a stochastic variable with one realization per specimen. Maximum likelihood estimators are studied and compared for the Wiener process model, and the Wiener process with random drift.

Contents Part I

LIST OF SYMBOLS AND ABBREVIATIONS

This list includes some of the symbols and abbreviations used in this report. Symbols and abbreviations are also defined in the text at their first appearance.

ALPHANUMERIC SYMBOLS AND ABBREVIATIONS

Symbol or abbreviation	Meaning
ALT	Accelerated life testing
BS	Birnbaum-Saunders distribution. The c.d.f. of the BS distribution with parameters (α,β) is $F(t) = \Phi\left[\frac{1}{\alpha} \left(\sqrt{\frac{t}{\beta}} - \sqrt{\frac{\beta}{t}} \right) \right]$
c.d.f.	Cumulative distribution function. The c.d.f. F for a stochastic variable T is defined as $F(t) = P(T \leq t)$.
$\underline{d}_c = (d_{c,1}, d_{c,2}, \ldots, d_{c,h})'$	Critical deteriority values for occurrence of failure.
$\underline{D}(t) = (D_1(t), D_2(t), \ldots, D_h(t))'$	Deteriority vector at time t.
$F(t)$	Cumulative distribution function (c.d.f.)
$f(t)$	Probability density function (p.d.f.) $f(t) = \frac{d}{dt}F(t)$
$\Phi(x)$	C.d.f. for the standard normal distribution, N(0,1), $\Phi(x) \stackrel{\text{def}}{=} \int_0^x \frac{1}{\sqrt{2\pi}} \exp(-\frac{1}{2}t^2)dt$
$h(\underline{D}(t)) = h((D_1(t), D_2(t), \ldots, D_h(t))')$	Increasing function of the deteriority vector, indicating when failure occurs.

Symbol or abbreviation	Meaning
h_c	Critical value for occurrence of failure.
$\underline{h}_c = (h_c^1, h_c^2, \ldots, h_c^k)'$	Critical values for occurrence of failure modes $M_1, \ldots, M_k$.
$I(\cdot)$	The indicator function. $I(A)$ equals 1 (0) if the event A is true (false).
$IG(\delta,\nu)$	Inverse Gaussian distribution with parameters (δ,ν). The probability density is $g(t) = \frac{1}{\sqrt{2\pi\nu}\, t^{3/2}} \exp\left[- \frac{(1-\delta t)^2}{2\nu t} \right]$
$k(\cdot)$	The killing rate, as defined in the model in Section 2.2.1.
$\log(\cdot)$	Logarithm with base e = 2.71828... (natural logarithm)
$\log_{10}(\cdot)$	Logarithm with base 10
$\underline{m}(t) = (m_1(t), m_2(t), \ldots, m_h(t))'$	Deterioration vector, modelled as a deterministic process.
$M_1, \ldots, M_k$	Failure modes.
MLE	Maximum Likelihood Estimator(s)
$N(\mu,\sigma^2)$	Normal distribution with mean μ and variance σ^2.
$R(t)$	Survivor function or survival probability. $R(t) = P(T > t) = 1 - F(t)$
T	Lifetime of a unit upon failure or censoring
$\underline{x} = (x_1, x_2, \ldots, x_p)'$	Stressors
$Y = \log(T)$	Log lifetime
$z(\cdot)$	Failure rate $z(t) = \frac{f(t)}{1 - F(t)}$

OTHER SYMBOLS AND NOTATION

A vertical line, |, is used in the usual way in conditional probabilities, distributions etc. The notation

$$X|y \sim N(a(y), b(y)^2),$$

for example, means that the conditional distribution of X given Y=y is normal with mean a(y) and variance $b(y)^2$.

An underlined symbol denotes a vector, for example,
$\underline{x} = (x_1, x_2, \ldots, x_p)'$.

For two vectors $\underline{a} = (a_1, \ldots, a_n)'$ and $\underline{b} = (b_1, \ldots, b_n)$, the notation $\underline{a} \leq \underline{b}$ means that $a_i \leq b_i$ for $i = 1, \ldots, n$.

In some cases, bold types are used to denote matrices, such as A below.

The transpose of a matrix is denoted by an apostrophe. For example, if

$$\mathbf{A} = \begin{bmatrix} a_{11} & a_{12} & \cdots & a_{1m} \\ a_{21} & a_{22} & & a_{2m} \\ \vdots & & & \vdots \\ a_{n1} & a_{n2} & \cdots & a_{nm} \end{bmatrix},$$

then

$$\mathbf{A}' = \begin{bmatrix} a_{11} & a_{21} & \cdots & a_{n1} \\ a_{12} & a_{22} & & a_{n2} \\ \vdots & & & \vdots \\ a_{1m} & a_{2m} & \cdots & a_{mn} \end{bmatrix}.$$

SUMMARY AND CONCLUSIONS

A number of today's technologies require extremely high component reliability. It is often necessary to perform reliability testing before choosing components and setting them into operation. The testing may be performed under simulated normal use conditions, or as accelerated life testing (ALT). The latter is achieved by testing the item under more severe stresses than those encountered during normal use. In this way, failures may occur during a realistic testing time. Test results are extrapolated, to estimate the reliability under normal use conditions. Chapter 1 of this report gives a short introduction to reliability testing and ALT.

From a traditional reliability point of view, a component is assumed to have two states - functioning or failed. However, many component types deteriorate gradually. Associated with the failure modes, there may be one or more physical measures describing the degree of deterioration, such as:

- Wear depth
- Crack length(s)
- Leakage rate
- Degree of corrosive attack
- Material properties, such as: Mass loss, elasticity, compressibility, fracture strength, etc.

The deterioration may, thus, be described in terms of some (possibly vector valued) stochastic process, i.e.

$$\underline{D}(t) = (D_1(t), D_2(t), \ldots, D_h(t))'. \tag{1}$$

Let T denote the lifetime for an observed specimen, and let M denote the failure mode if it failed at time T, M = 0 denotes censoring. In the traditional approach, only

$$T, M \tag{2}$$

would be recorded as outcome of the test, and estimates would be based on these values. In an extended approach, the deterioration vector at T may also be recorded. That is, the information obtained for each specimen would be

$$T,\ M,\ D_1(T),\ D_2(T),\ \ldots,\ D_h(T). \tag{3}$$

Obviously, (3) may contain much more information than (2). Depending on the component type, it may also be possible to measure one or more of the deteriorations during the testing before it fails or is removed from the test.

In the case of ALT, the stress levels for each specimen is recorded as a (vector of) stressor(s) $\underline{x}$.

If only one deterioration is relevant for a specific failure mode, failure may occur when D(t) exceeds some critical value d_c. This is illustrated in Figure 1.

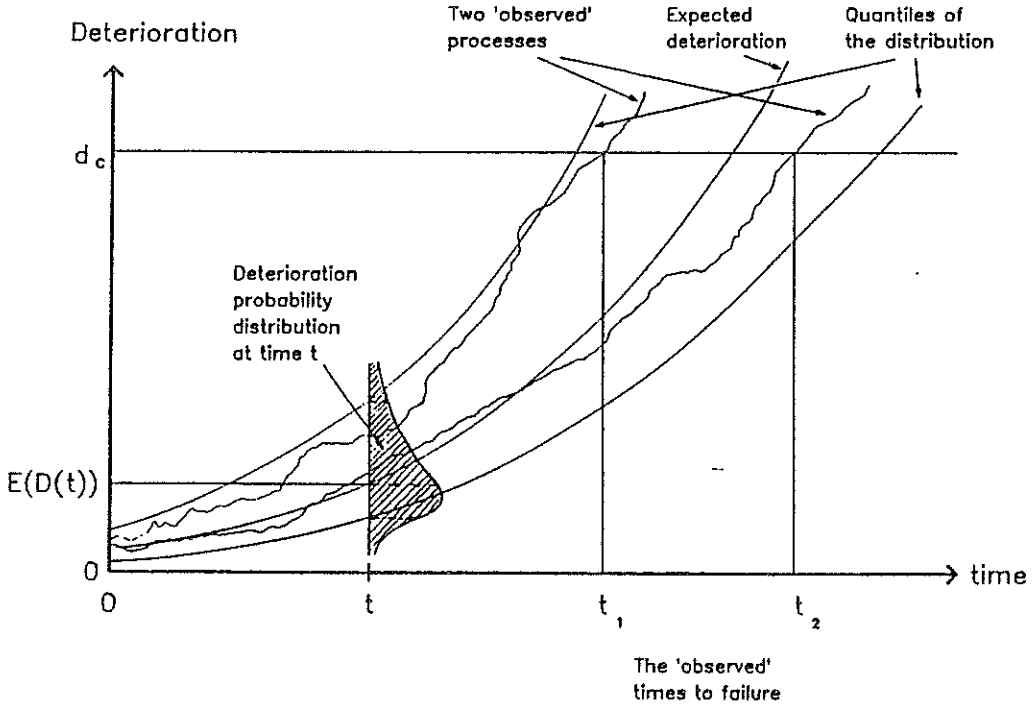

Figure 1. A one-dimensional deterioration process leading to failure.

Generally, failure may be said to occur if

$$h(\underline{D}(t)) > h_c, \tag{4}$$

where

$$h(\underline{D}(t)) = h(D_1(t), D_2(t), \ldots, D_h(t)) \tag{5}$$

is a given function increasing in each argument. The quantity h_c is a critical value corresponding to the failure mode(s) considered.

Some authors propose to include the possibility of failure also before the critical value is reached (Lemoine and Wenocur, 1985, Lemoine and Wenocur, 1986, Giglmayr, 1987). In these models, the probability that an item which is functioning at time t with $\underline{D}(t) = \underline{d}$, will fail within the time interval $(t, t+\Delta t]$, is

$$P(T \leq t+\Delta t \mid ((T > t) \cap (\underline{D}(t) = \underline{d}))) = k(\underline{d}) \cdot \Delta t + o(\Delta t), \tag{6}$$

where

$$\lim_{\Delta t \to 0} \frac{o(\Delta t)}{\Delta t} = 0.$$

The function $k(\underline{d})$ is called the killing rate. If the process $\underline{D}(t)$ is deterministic, then the killing rate at $\underline{D}(t)$ equals the failure rate at t. The present report mainly discusses deterioration models where failure occurs only when the critical value is reached.

Systematic use of reliability testing including deterioration measurements seems to have been little used, except for modelling for fatigue crack failure, and a few other examples. Basic ideas for reliability modelling based on deterioration measurements are presented in Chapter 2.

In many engineering disciplines, equations for physical deterioration processes have been established. Generally, these equations describe the

deterioration as some deterministic process $\underline{m}(t,\underline{x})$. That is, for a given stressor $\underline{x}$, then $\underline{m}(t,\underline{x})$ is a function of t which predicts the exact deterioration at time t. In Chapter 3 of this report, mechanical wear between two surfaces, fatigue crack growth, corrosion, and chemical ageing are discussed from this viewpoint. The deterministic equation for $\underline{m}(t,\underline{x})$ is often given in terms of the deterioration rate, which is the derivative of $m(t,\underline{x})$ with respect to t. Table 1 summarizes some models which are discussed in Chapter 3. As seen in Table 1, in many of the models the deterioration rate is independent of t.

Table 1. Deterministic deterioration models considered in this report.

Deterioration mechanism	Deterioration rate $\frac{\partial m(t,\underline{x})}{\partial t}$	Stressors included
Wear depth, mechanical wear between two surfaces	$k_0 x_1 x_2$	x_1 = average sliding length per unit time x_2 = pressure between surfaces
Fatigue crack length	$k_0 \Delta K(\underline{x}, m(t,\underline{x}))^{k_1}$	$\underline{x}$ includes tensile stress and torsion. The stress intensity factor ΔK depends on $\underline{x}$, and, to some extent, on $m(t,\underline{x})$.
General corrosion on metal in liquid	$k_0 \exp(k_1/x_1 + k_2 x_2/x_1)$	x_1 = absolute temperature x_2 = oxygen concentration in the liquid
Arrhenius law for chemical degradation	$k_0 \exp(-k_1/x_1)$	x_1 = absolute temperature
Eyring law for chemical degradation	$x_1 k_0 \exp(-k_1/x_1)$	x_1 = absolute temperature
Generalized Eyring law for chemical degradation	$x_1 k_0 \exp(-k_1/x_1 + k_2 x_2 + k_3 x_2/x_1)$	x_1 = absolute temperature x_2 = a non-thermal stressor, e.g. voltage

Models for the stochastic nature of $\underline{D}(t)$ are discussed in Chapter 4. At least on the macroscopic level, it is usually most natural to consider processes which are continuous both in time and state space. Other authors have used the theory of martingales to study the stochastic

nature of $\underline{D}(t)$. Further, deterministic models of deterioration mechanisms are frequently given in terms of differential equations. Hence, the theory of stochastic differential equations could prove useful. In this report, however, an approach based on the more basic theory of stochastic processes is used.

Section 4.2 covers some classes of cumulative stochastic processes, that is, processes where always $D(t_2) \geq D(t_1)$ if $t_2 \geq t_2$. The class of cumulative stochastic processes suggested by Pieper and Tiedge (1983) is discussed in Section 4.2.1. In their model class, the item is exposed to "shocks" at the points in time X_1, $X_1 + X_2$, ... The shocks cause the deterioration to increase with Y_1, Y_2, ..., respectively. The random vectors (X_1, Y_1), (X_2, Y_2), ..., are assumed independent, identically distributed, while X_i and Y_i may be stochastically dependent.

Discrete models are especially interesting when they may be used as approximations for continuous processes. The Poisson process has been studied from this viewpoint in Section 4.2.2. It has not been found suited for approximations to continuous deteriorations processes. Such models, give a coefficient of variation for the time to failure distribution which is far too small for practical applications.

The theory of Markov processes is attractive from its mathematical convenience. For example, the class of "B-models" suggested by Bogdanoff and Kozin (1985) belong to the class of Markov processes. They are cumulative stochastic processes where the transition matrix is allowed to be time- and state dependent. The basic features of B-models are summarized in Section 4.2.3.

The Wiener processes are a mathematically convenient class of continuous Markov processes. In a Wiener process with drift μ and infinitesimal variance σ^2, the increment $D(t_2)-D(t_1)$ over the time interval (t_2,t_1) is assumed normally distributed with mean μ and variance $\sigma^2(t_2-t_1)$. In this case, the time to first reach a fixed value d_c is inverse Gaussian (IG) distributed. The Wiener process and corresponding IG distribution are described with some generalizations in Section 4.3. Not only are these models important as such, but they may be extended to a model class

where the drift and, possibly other parameters, have different values for each specimen.

Although there are situations where Markov processes provide a good framework for stochastic deterioration processes, there are cases where Markov processes fail to provide an acceptable description. Two important reasons are mentioned in this report:

First, a complete description of the "state" of a component at time t would usually require a large number of physical measures. Some of these measures influence the deterioration rate with respect to other measures. If only one, or a few, deteriorations are included in $\underline{D}(t)$, then $\underline{D}(t)$ cannot be expected to possess the Markov property.

The second reason is connected to an underlying deterministic model $\underline{m}(t,\underline{x})$, which describes some "typical path", for example the expectation, of $\underline{D}(t)$. The model for $\underline{m}(t,\underline{x})$ contains a set of parameters, say, $\underline{k} = (k_0, k_1)$ as in Table 1. In some cases, the parameter vector $\underline{k}$ is seen to differ significantly from specimen to specimen, even for specimens from the same production lot. Satisfactory models for a number of situations are obtained by considering $\underline{k}$ as a stochastic vector with one (not directly observable) realization per specimen. This has been the case for leakage through control valves, fatigue crack growth in an aluminum alloy and in steel, and accelerated life testing of metallic layer resistors at elevated temperatures. Several of these cases have been modelled assuming Markov processes conditionally given $\underline{k}$. However, unconditionally, such models are not Markov processes.

In Section 4.5, a Wiener process model with random drift is studied. That is, conditionally given the drift parameter μ, then D(t) is a Wiener process, and the time to failure (first crossing of d_c) is conditionally inverse Gaussian distributed.

Although regression models with random coefficients do not describe the path of $\underline{D}(t)$, these models do provide useful models for the measurements of $\underline{D}(t)$ at a limited number of t values. A survey of such models is given in Section 4.4.

If $\underline{D}(t)$ is assumed to follow a deterministic function conditionally given $\underline{k}$, then the Bernstein life distribution and related models described in Section 4.6. evolve. These models can not be used to model measurements of $\underline{D}(t)$ if it is measured at more than one point in time per specimen.

In Chapter 5, maximum likelihood estimators (MLE) are derived for two models:

i) The Wiener process / inverse Gaussian model.

ii) The Wiener process with random drift. In this model, the drift parameter μ is assumed to follow a normal distribution with mean θ and variance λ, truncated at 0. Conditionally given μ, then D(t) is assumed to follow a Wiener process with drift μ and infinitesimal variance σ^2.

MLE are derived for the case when, for each specimen, either the failure time t_i, or a censored lifetime t_i with corresponding deteriority d_i, is recorded.

In the first model, the MLE for μ is found to be

$$\hat{\mu} = \frac{\Sigma\, d_i}{\Sigma\, t_i}, \tag{7}$$

where all sums are taken over i=1,...,n.

In the second model, the maximum likelihood equations can not be solved explicitly. The MLE must be obtained by numerical methods for each given data set. The MLE for θ is approximately equal to

$$\hat{\theta} = \frac{\Sigma \dfrac{d_i}{\hat{\lambda} t_i + \hat{\sigma}^2}}{\Sigma \dfrac{t_i}{\hat{\lambda} t_i + \hat{\sigma}^2}}, \tag{8}$$

where $\hat{\lambda}$ and $\hat{\sigma}^2$ are the MLE for λ and σ^2, respectively. The estimator (8) may also be written in the form

$$\hat{\theta} = \frac{\Sigma v_i (d_i/t_i)}{\Sigma v_i}, \tag{9}$$

where

$$v_i = \frac{t_i}{\hat{\lambda} t_i + \hat{\sigma}^2}, \quad i = 1, 2, \ldots, n.$$

In the first and second model, E(D(t)) equals μt and θt, respectively. In this respect, both (7) and (9) are estimators for E(D(t))/t.

If the t_i's are all equal, it is not possible to estimate both λ and σ^2. If the t_i's are not equal, most weight in (9) is assigned to the (d_i/t_i) with highest t_i. This is natural, since the data with higher t_i contain more information on the unobservable μ_i than the data with shorter t_i.

1. INTRODUCTION

1.1 RELIABILITY TESTING AND ACCELERATED LIFE TESTING

A number of today's technologies require extremely high component reliability. This especially applies to systems where modest component reliability cannot be compensated for by extended maintenance. Examples of such systems are aerospace vehicles and subsea production systems for oil and gas. Before setting them into operation, it may be required to:

a) Compare alternatives to identify which is best.
b) Verify that specified reliability requirements are met.
c) Predict the reliability
d) Identify weak point in design which need improvement.

Typically, the tasks above are included in the reliability management programme, in the cases where such a programme has been established. In order to fulfill tasks like a) to d) above, knowledge may be obtained from four sources:

i) Field performance data: Reliability experience from identical or comparable equipment types, under identical or comparable operational and environmental conditions.

ii) Mechanical evaluations of the equipment types in question, using "engineering judgment" to make statements on expected reliability performance.

iii) Acceptance tests for the items to be deployed. These are typically rather simple, non-destructive function tests. Only the items who pass the test are deployed, the rest are "thrown away".

iv) More extensive tests, like accelerated life tests (ALT).

If enough relevant field performance data are available, this is the best, and perhaps the cheapest, information source. In many cases, available and relevant field performance data is rather limited. Mechani-

cal evaluations and acceptance tests do not always provide enough supplementary information. In these cases, some sort of reliability testing seems to be the only feasible approach. Reliability testing may be performed under simulated normal use conditions, or as accelerated life testing (ALT). The latter is achieved by testing the item under more severe stresses than those encountered during normal use. In this way, failures may occur during a realistic testing time. Test results are extrapolated, to estimate the reliability under normal use conditions. As a result, ALT may provide knowledge that is not obtainable in any other way within realistic time schedules, to give a basis for decisions.

Cohen & Al (1987) describe how to establish a comprehensive reliability programme for new products, bearing integrated circuits in mind. ALT constitutes a major part of their suggested programme. However, their scheme includes testing of a large number, say 1000, components. This is only possible where the components themselves, as well as the tests, are rather cheap, such as the case is for many integrated circuits. Lydersen and Rausand (1987) describe a systematic procedure for carrying out ALT programmes, including all available information in the test planning and evaluation of test results. Their procedure is primarily intended for more complex types of equipment, or equipment where a large number of tests is not possible in practice.

More comprehensive surveys of ALT methods and models are found in the literature study preceding this thesis (Lydersen, 1986), and in an article by Ahmad and Sheikh (1985). The latter also includes a comprehensive lists of references, but, surprisingly, does not mention the proportional hazards model class suggested by Cox (1972).

1.2 DEFINITION OF BASIC CONCEPTS

This section defines some basic concepts of reliability theory and accelerated life testing. Readers who are familiar with these concepts, may skip the section. For a more thorough treatment, see e.g. Lydersen (1986).

Generally, the **reliability** of an item may be defined as (British Standard BS 4778):

> "the ability to perform a required function under stated conditions for a stated period of time."

Let T be the time to failure for the item in question. This is the time from it is activated in service until the first time it is unable to perform the required function as stated in the definition. The time T is considered as a stochastic variable. Quantitatively, the reliability may be expressed in several ways, in terms of:

- The probability distribution F(t), also called the life distribution function. This is the probability that the item fails before time t:

$$F(t) = P(T \leq t) \tag{1.2.1}$$

- The survivor function R(t), also called survival probability or reliability. This is the probability that the item will not fail before time t:

$$R(t) = P(T > t) \tag{1.2.2}$$

- The failure rate z(t). Consider an item with age t, which is functioning. The probability that it fails within a small time interval Δt, is approximately $z(t)\cdot\Delta t$:

$$P(T \leq t+\Delta t \mid T > t) \approx z(t)\cdot\Delta t \tag{1.2.3}$$

The formal definition of z(t) is

$$z(t) = \lim_{\Delta t \to 0} \frac{P(t < T \leq t + \Delta t \mid T > t)}{t}. \tag{1.2.4}$$

Alternatively, it may be written

$$z(t) = \frac{f(t)}{R(t)} = \frac{f(t)}{1 - F(t)} = -\frac{d}{dt} \ln R(t), \tag{1.2.5}$$

where $f(t) = F'(t)$.

- The availability A(t). This is the probability that the item is functioning as demanded at time t. For items that are not repaired or replaced, $A(t) = R(t)$.

- The expected lifetime (Mean Time to Failure, MTTF):

$$MTTF = E(T) = \int_0^\infty tf(t)dt = \int_0^\infty R(t)dt. \tag{1.2.6}$$

Other quantities or functionals of F(t) may also be of interest. For example, consider an item which is suppposed to be operating for a specific mission, and then to be condemned. In this case, the probability of surviving the specified mission time will be the main quantity of interest.

When ALT is performed, it is usually assumed that the life distribution function, F(t), belongs to some parametric class of distributions. That is, the distribution function is assumed to be of the form

$$P(T \leq t) = F(t;\underline{\theta}), \tag{1.2.7}$$

where

$$\underline{\theta} = (\theta_1, \theta_2, \ldots, \theta_r)', \qquad r \geq 1 \tag{1.2.8}$$

is (are) unknown parameter(s). Generally, the life distribution depends on a number of environmental and operational factors, such as

x_1 = temperature
x_2 = pressure
⋮
etc.

These values of factors are commonly referred to as stressors. The relevant stressors will be denoted

$$\underline{x} = (x_1, x_2, \ldots, x_p)'. \tag{1.2.9}$$

The life distribution is usually assumed to belong to the same distribution class (1.2.7) when the stressors have different values. That is, the life distribution at stressor level $\underline{x}$ is assumed to be of the form

$$P(T \leq t) = F(t;\underline{\theta}(\underline{x})), \tag{1.2.10}$$

where

$$\underline{\theta}(\underline{x}) = (\theta_1(\underline{x}), \theta_2(\underline{x}), \ldots, \theta_r(\underline{x}))', \tag{1.2.11}$$

as long as $\underline{x}$ is within the region where (1.2.10) gives a good enough approximation to reality. The functions $F(\cdot)$ and/or $\underline{\theta}(\cdot)$ in (1.2.10) may include one or more parameters to be estimated.

The relation between the stressors and the life distribution function may be expressed in numerous ways. In most practical applications, this relation is modelled with an accelerated time model or a proportional hazards model.

Accelerated time models may be defined as follows: Let the lifetime distribution under normal operating conditions, that is, $\underline{x}=\underline{x}_0$, be denoted $F_0(t)$. In general, an accelerated time model may then be written on the form

$$F(t;\underline{x}) = F_0(at), \tag{1.2.12}$$

where

$$a = a(\underline{x}) \tag{1.2.13}$$

is commonly referred to as the acceleration factor. For example, the frequently used location-scale models for log-lifetime constitute a subclass of accelerated time models (Lydersen, 1986).

Proportional hazards (PH) models may be defined in terms of the failure rate:

$$z(t;\underline{x}) = z_0(t)\, h(\underline{x}). \tag{1.2.14}$$

Equivalently, the class may be defined in terms of the survival probability:

$$R(t;\underline{x}) = R_0(t)^{h(\underline{x})} \tag{1.2.15}$$

The functions $z_0(\cdot)$ or $R_0(\cdot)$, and/or $h(\cdot)$, may include one or more parameters to be estimated.

An important subclass of the PH models are the so-called Cox-models (Cox, 1972), in which

$$h(\underline{x}) = \exp(\underline{\beta}\cdot\underline{x}) = \exp\Big(\sum_{i=1}^{p} \beta_i x_i\Big). \tag{1.2.16}$$

An attractive property of the Cox models is the existence of methods for estimation and inferences on the parameters $\underline{\beta}$ without assuming any special distribution class for $z_0(t)$ or $R_0(t)$. For some extensions and further properties of the Cox models, see Lydersen (1986) and references therein, or Cox and Oakes (1984).

The accelerated time models and the proportional hazards models are conceptually different. They coincide if, and only if, the lifetime distribution belongs to the two-parameter Weibull type (Newby, 1988,

Solomon, 1984). The effect of erroneously specifying one of these models if the other is in fact true, is studied by Solomon (1984).

1.3 DETERIORATION MEASUREMENTS

Usually, times to failure or censored lifetimes is the only utilized outcome of field performance or laboratory tests, when reliability is to be estimated. In many cases, however, there exist one or more physical measures describing the degree of deterioration. Adding such measurements to the recorded data, increases the available information significantly. This is especially true in cases where ALT is performed. In these cases, existing lifetime data are usually scarce, testing "many" specimens may be too expensive, and there are several other sources of uncertainty (Lydersen, 1986, Lydersen and Rausand, 1987).

According to the literature on ALT, the approach including deterioration measurements seems to have been little used, except for modelling for fatigue crack failure, see e.g. Birnbaum and Saunders (1969) or Saunders (1975). The total crack length is then set equal to crack increments resulting from individual stress cycles. Fatigue failure occurs when accumulated crack length exceeds a critical length. Some rather straightforward analyses of ALT including deterioration measurements for other failure mechanisms have been performed by Nelson (1981) and Maskalick (1975). These are further commented in Lydersen (1986). Heat ageing of elastomer materials seems to be a fruitful application for ALT including deterioration measurements. This is commented towards the end of Section 2.1. In part II of this thesis, data from an ageing experiment (Renolen, 1979) is analyzed using this approach.

A recent book by Bogdanoff and Kozin (1985) proposes a class of probabilistic models for cumulative damage. Their main ideas will be discussed later in this report. Failure modelling including deterioration in one dimension has been discussed by Gertsbakh and Kordonsky (1969). Some of the fundamental principles presented in Chapter 2 in this report were presented by this author in Lydersen (1986) and in Lydersen and Rausand

(1987). A few similar ideas have been presented, independent of this author, by Knezevic (1987).

A recent article on statistical methods for reliability improvement (Amster and Hooper, 1986, p 73), states that there appear to be at least two fruitful directions for future reliability technology in order to build high reliability into products in a cost-effective way. The first involves a closer coupling between the physics of failure and reliability models. The second concerns measured degradation data.

The working title of the present thesis was "Accelerated life testing based on deterioration measurements". The area seems to have important practical applications. The choice of topic was further influenced by the fact that this author has taken part in several practical ALT projects where this kind of modelling seemed fruitful. These projects include ALT of subsea gate valves (Rausand & Al, 1985, Ørjasæter & Al, 1986, Ørjasæter & Al, 1987, and Ørjasæter & Al, 1988), subsea control valves (Kielland & Al, 1985, Lydersen & Al, 1986), and pilot valves (Lydersen & Al, 1987).

The basic theoretical framework for accelerated testing based on deterioration measurements is defined and described in Chapter 2. Lemoine and Wenocur (1985) suggest an approach for failure modelling similar to the one presented here. Their model, with some special cases, is described and commented in Section 2.2. Chapter 3 gives examples of how the deterministic part of the deterioration processes may be modelled. Chapter 4 concerns how to extend these the deterministic models into stochastic models, and in Chapter 5, estimation methods for some special cases are discussed. In Part II and III of this thesis, the models and methods are applied to practical ALT results of elastomer foil and control valves, respectively.

2. DETERIORATION AND FAILURE MODELLING

2.1 STOCHASTIC MODELLING INCORPORATING DETERIORATION AND FAILURE

Usually, ALT modelling has been concerned with components with two states - functioning or failed. However, many components deteriorate gradually. A refined model may incorporate this fact. Associated with the failure modes, there may be one or more physical measures describing the degree of deterioration. Such measures may be:

- Wear depth
- Crack length(s)
- Leakage rate
- Degree of corrosive attack
- Material properties, such as: Mass loss, elasticity, compressibility, fracture strength, etc.

The deterioration may, thus, be described in terms of some (possibly vector valued) stochastic process, i.e.

$$\underline{D}(t) = (D_1(t), D_2(t), \ldots, D_h(t))'. \qquad (2.1.1)$$

$\underline{D}(t)$ will be referred to as the **deteriority vector** at time t, and its entries will be referred to as **deteriorities**.

In many practical cases, the deteriority vector represents a state of cumulative damage. In many physical deterioration processes, damage will not recover once it has occurred. This implies that the deteriorities become non-decreasing functions of time. Still, a series of measured values may show some jumps due to measurement errors. A measured value $\underline{M}(t)$ for the deterioration may be modelled as

$$\underline{M}(t) = \underline{D}(t) + \underline{\varepsilon}, \qquad (2.1.2)$$

where $\underline{D}(t)$ is the true value at the time when measuring, and $\underline{\varepsilon}$ is a random error which can take both positive and negative values. Except

otherwise is stated, we shall assume that $\underline{\varepsilon}$ is of negligible magnitude and consider only $\underline{D}(t)$.

There are also examples of deterioration processes where even the true deterioration $\underline{D}(t)$ may show temporary improvements. An example, with a plausible explanation, is provided in Part II of this thesis. We shall, however, assume that the deteriorities are non-decresaing functions unless otherwise is stated.

Looking at the one-dimensional case, h=1, failure may be said to occur when D(t) exceeds some critical value d_c. This is illustrated in Figure 2.1.1.

In the general case, the initial deteriority $\underline{D}(0)$ may be a random variable. The random nature of $\underline{D}(0)$ is generated by variable manufacturing, quality control, deterioration before setting the item into service, and so forth.

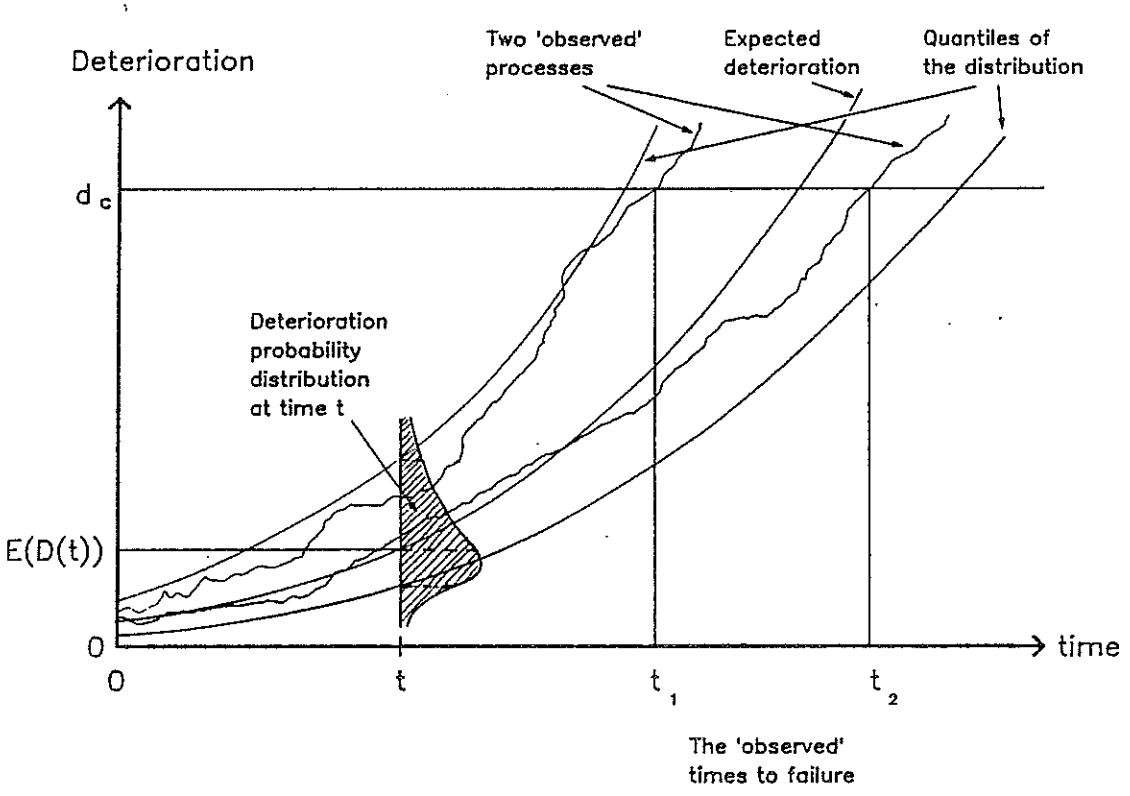

Figure 2.1.1. A one-dimensional deterioration process leading to failure.

In the multidimensional case, d_c may be viewed upon as some vector:

$$\underline{d}_c = (d_{c,1}, d_{c,2}, \ldots, d_{c,h})'. \tag{2.1.3}$$

In a simple model, failure may be said to occur as soon as at least one of the critical values is exceeded, that is,

$$D_i(t) > d_{c,i} \quad \text{for at least one } i,\ i=1,2,\ldots,h. \tag{2.1.4}$$

Note that in one sense, (2.1.4) only considers one D_i at a time: Failure occurs when $D_i(t) > d_{c,i}$, no matter what the other deteriorities are, as long as they are less than their respective critical values. This may be a too simple model for failure occurrence. For example, a critical leakage in a valve may occur if some combination of wear depths at several places, packing material deterioration etc. becomes critical. Generally, failure may be said to occur if

$$h(\underline{D}(t)) > h_c, \tag{2.1.5}$$

where

$$h(\underline{D}(t)) = h(D_1(t), D_2(t), \ldots, D_h(t)) \tag{2.1.6}$$

is increasing in each argument. The quantity h_c is a critical value corresponding to the failure mode(s) considered.

The model (2.1.4) is a special case of (2.1.6). Assume that (2.1.4) holds. Let $h(\underline{D}(t)) = \max(D_1(t)/d_{c,1}, \ldots, D_h(t)/d_{c,h})$. This means that failure occurs when $h(\underline{D}(t))>1$, which is (2.1.6) with $h_c=1$.

These models may easily be extended to the case with several failure modes, say $M_1, \ldots, M_k$. Failure mode M_i may then be said to occur if

$$h^i(\underline{D}(t)) > h_c^i. \tag{2.1.7}$$

Another generalization may allow $\underline{d}_c$, or $\underline{h}_c=(h_c^1,h_c^2,\ldots,h_c^k)'$, to have different values for each specimen. That is, $\underline{d}_c$, or $\underline{h}_c$, is considered to be stochastic.

The deteriority vector $\underline{D}(t)$ represents a state description in which increasing values of its entries represent a reduction in state quality. In some practical situations, it is more logical or convenient to use state measures where high values correspond to high quality, for example tread depth on an automobile tyre. This represents no practical restriction. The ideas presented above still apply, with the appropriate changes in sign.

It should be noted that the most models and estimation methods for ALT, only include the failure or censor time for each unit tested (Lydersen, 1986). In many situations, a laboratory test may yield much more information. Viewing the deterioration as a vector of physical measures, these values may provide useful information in addition to the mere lifetimes. Instead of recording only the mere lifetimes, the deteriority vectors at failure or censoring may be recorded. Let T denote the failure time or censored lifetime for an item. Further, let M denote the failure mode if the item fails at T, M=0 denotes censoring. In the "conventional" procedure, only

$$T,\ M \tag{2.1.8}$$

would be recorded, and estimates would be based on these values. In the extended procedure indicated here, one would also record the deteriority vector at failure or censoring. That is, the information recorded for each test item would be

$$T,\ M,\ D_1(T),D_2(T),\ldots,D_h(T). \tag{2.1.9}$$

Obviously, (2.1.9) may contain much more information than (2.1.8). Depending on the item to be tested, it may even be possible to measure one or more of the deteriorities during the testing, before failure or censoring. If this is the case, (2.1.9) may be extended to include one or

more of the components of $\underline{D}(t)$ for some t values between 0 and T. In some situations, not all deteriorities can be measured after failure.

Heat ageing of polymeric materials provides an example where a deteriority vector is measured. On the basis of deformation kinetics, the Arrhenius model may be shown to hold for this situation, see e.g. Valanis and Peng (1982) or Peng (1985). Heat ageing of such materials are typically performed in the following way, see e.g. Renolen (1975):

A large number of specimens are kept at various temperatures. At some instants, some of them are taken out and tested destructively. Properties such as elasticity, fracture length, relative mass change, etc, are measured. A packing may, for example, be said to be in a failed state if its fracture length is less than a defined value. Data for time to failure seem to fit well with the Arrhenius model (Renolen, 1975). However, estimation methods including the whole deteriority vector do not seem to have been used. In Part III of this thesis, test results from heat ageing of elastomer foil (Renolen, 1979) are analyzed in this way.

The approach outlined here calls for refined estimation techniques, incorporating the deterioration vector for the items tested. In the literature on ALT, such refined techniques have not been much discussed.

2.2 DETERIORATION MODELS WITH KILLING RATE

2.2.1 General description

Lemoine and Wenocur (1985) suggest an approach for failure modelling similar to the one presented above. One of their models and some related models will be briefly described in terms of the terminology used in this report, and commented.

In their article, Lemoine and Wenocur (1985) consider a one-dimensional deterioration process D(t). Associated with each state d there is a

killing rate k(d), defined as follows: Assume that the unit is functioning at time t, with deterioration d. The killing rate is defined as

$$k(d) = \lim_{\Delta t \to 0} \frac{P(T \leq t+\Delta t \mid D(t)=d \cap T > t)}{\Delta t} . \qquad (2.2.1)$$

Note the analogy between the killing rate, as defined above, and the failure rate. Actually, if the wear process is deterministic, i.e. given as a function d(t), the failure rate at time t equals the killing rate at state d(t):

$$z(t) = k[d(t)] \qquad (2.2.2)$$

Further, Lemoine and Wenocur (1985) assume the possibility of a critical value d_c, such that the unit is certain to fail when D(·) passes d_c.

For example, consider the thickness of tread on a tyre. The killing rate is associated with tread thickness d. The tyre is condemned when the tread passes below some safe level d_c. It may also fail before that time, if it encounters i.e. a sharp piece of road surface. The killing rate k(d) in this example is an increasing function of d.

Let τ denote the time of first passage of the D process to d_c. The probability of surviving beyond time t is given by

$$P(T > t) = E(\exp\{-\int_0^t k[D(u)]du\} \; I(\tau > t)), \qquad (2.2.3)$$

where the expectation is taken over the distribution of D(·). The function I(·) is the indicator function, I(A) is 1 (0) if A is true (false).

The failure model described above, will be referred to as the Lemoine-Wenocur model. This model may be generalized to multidimensional deterioration processes $\underline{D}(t)$, with an associated killing rate $k(\underline{d})$. In this generalization, failure will occur at the first shock in the "killing rate" process, or when $\underline{D}(t)$ reaches a critical level, whichever occurs

first. The critical level for $\underline{D}(t)$ may be defined in terms of (2.1.4) or (2.1.5).

If the killing rate and the distribution of the process $D(\cdot)$ are given, it is of interest to perform the integration and find the expectation in (2.2.3). This is not necessarily a straight-forward matter.

Section 2.2.2 and Section 2.2.3 below each describe a subclass of the Lemoime-Wenocur model, with references.

2.2.2 A Shot-Noise Model

Solutions for (2.2.3) are given for some special cases by Lemoine and Wenocur (1986). The cases given in Lemoine and Wenocur (1986) include a special form of the deterioration process $D(\cdot)$: The specimen is subjected to shots or jolts according to a homogeneous or non-homogeneous Poisson process. Jolt number n occurs at time t_n, has size J_n, and is assumed independent of the history up to t_n. Its contribution to the deteriority at time $u+t_n$ is $J_n h(u)$, where h is a non-negative function which vanishes on $(-\infty,0)$ and tends to 0 as $t \to \infty$, for example

$$h(u) = \begin{cases} e^{-au} & \text{if } u \geq 0 \ ; \ a > 0 \\ 0 & \text{if } u > 0. \end{cases} \tag{2.2.4}$$

This gives

$$D(t) = \sum_{n=1}^{\infty} J_n h(t-t_n) \tag{2.2.5}$$

These assumptions imply that the damage caused by the jolt will recover completely in time. Lemione and Wenocur (1986) comment that this may be a reasonable model class in some medical applications, where D(t) represents the "state" of a patient.

2.2.3 Killing Rate Without a Failure Limit

Giglmayr (1987) treats the Lemoine-Wenodur model type for the case where no limit d_c exists. That is, an item can only fail from the first shock in the "killing rate process". His two main assumptions are:

i) The deterioration process D(t) is either

- a step-function following a Poisson process, possibly with time- and state- dependent rate of occurrences,

or,

- a Gaussian diffusion process, where infinitesimal mean and variance are allowed be time- and state- dependent. (Such processes are briefly described in Chapter 4 of this report.)

ii) The killing rate is allowed be time- and state dependent.

Giglmayr (1987) does not refer to Lemoine and Wenocur (1985), and the two articles seem to have been written independent of each other. Giglmayr (1987) presents the general mathematical framework for his model classes, including integro differential equations and partial differential equations for transition probabilities and other quantities of interest.

3. DETERMINISTIC DETERIORATION MODELS

3.1 INTRODUCTION

The deterioration process $\underline{D}(t)$ in the extended model outlined in Chapter 2 is a stochastic process. It is instructive to start by looking at some deterministic deterioration process,

$$\underline{m}(t,\underline{x}) = (m_1(t,\underline{x}),\ m_2(t,\underline{x}),\ \ldots,\ m_h(t,\underline{x}))' \qquad (3.1.1)$$

That is, for a given stressor $\underline{x}$, then $\underline{m}(t,\underline{x})$ is a function of t which predicts the exact deterioration at time t.

Often, $\underline{m}(t,\underline{x})$ may be given implicitly, in terms of a differential equation. For simplicity, consider the one-dimensional case, h=1, and a first order differential equation:

$$m'(t) = f(\underline{x},t,m(t)) \qquad (3.1.2)$$

The function $f(\cdot)$ may also include one or more unknown parameters, to be estimated in a given situation.

From a physical point of view, many deterioration processes are initially modelled in terms of deterministic models. That is, the functional form of $\underline{m}(t,\underline{x})$ is determined. The function may be given explicitly, or in terms of a differential equation. Some examples are given below. Afterwards, a stochastic model for $\underline{D}(t)$ may be built around $\underline{m}(t,\underline{x})$.

3.2 WEAR

In this section, mechanical wear between two surfaces sliding against each other is considered. Experts distinguish between several wear mechanisms. These are two-body and three-body wear, together with adhesive, abrasive and other types. Experience shows that the wear depth is proportional to the total sliding lengths and to the pressure between

the two surfaces. This model holds if the pressure is below certain limits, above which the wear tends to increase more than proportionally with the pressure. In the proportional region, one may thus write

$$m'(t) = k\, l\, p, \tag{3.2.1}$$

where k is a constant depending on surface finish, material types, etc, l is average sliding length per unit time, and p is pressure between the surfaces.

3.3 FATIGUE CRACK GROWTH

Fatigue failure in a metal part may occur when it is exposed to a series of stress cycles or oscillations. Each stress cycle is below the fracture strength limit for the part or the construction. The large number of repetitions cause an accumulation of microscopic crack increments, and finally, fracture. Typical number of oscillations to failure are in the range 10^3 to 10^{10} (Haagensen, 1973).

A crack increment during a stress cycle results from broken atomic bounds, such that new surfaces are created. For each oscillation with high enough stress, there will be some increment in crack size on atomic level. This is illustrated in Figure 3.3.1.

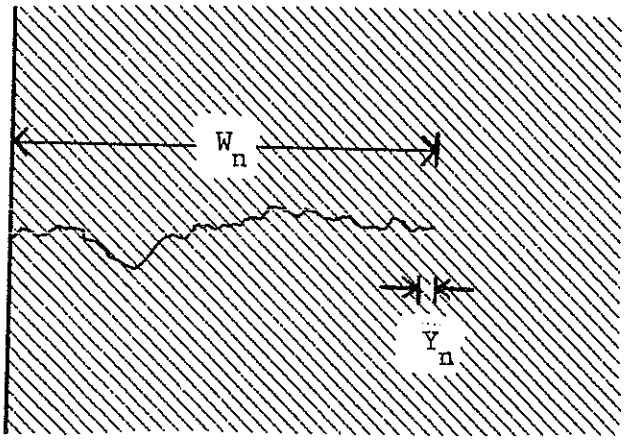

Figure 3.3.1. Fatigue crack growth, where W_n is the total crack length after n cycles, and Y_n is the crack increment caused by cycle number n.

Three stages of fatigue crack growth are distinguished: Initiation, crack propagation, and final fracture. Initiation is the time until an observable crack has developed. The duration of this stage is, to some extent, a matter of definition, depending on the observation method, for example how good the microscope is.

Initiation usually goes faster in notched specimens than in un-notched specimens (i.e. with a smooth surface). A notch may e.g. be a weld, a narrowing, or a thickening, causing high stress concentrations around it.

The second stage is called the crack propagation stage, or the growth stage. The crack is growing more or less regularly, as indicated in Figure 3.3.1. Crack propagation continues until the remaining thickness is too small to resist the stress cycles, and final fracture occurs.

The lifetime of a specimen equals the sum of crack initiation time and crack propagation time. Final fracture normally takes negligible time compared to these. The fraction of the lifetime consumed by the initiation depends on several factors: The specimen shape, material, and the

stress cycles history. Usually, crack initiation gives the largest contribution to the total failure time. If the stress cycles amplitude is so small that a relatively long lifetime is expected, initiation may last several times as long as crack propagation (see e.g. Haagensen, 1973, p 8). This is also experienced for fatigue tests on smooth specimens.

Crack length as a function of time is illustrated in Figure 3.3.2, for two situations. In the crack propagation phase, the crack growth rate approximately follows Paris' Law:

$$\frac{dm(t)}{dt} = C(\Delta K)^m, \tag{3.3.1}$$

where ΔK is the stress intensity factor, and C and m are material constants. Paris' Law was first suggested by Paris (Paris and Erdogan, 1963), and is described in most textbooks on metal fatigue, see i.e. Fuchs and Stephens (1980). The stress intensity factor ΔK is a function of tensile stress and torsion, and of the specimen shape. Hence, ΔK is also a function of the crack length. However, for some combinations of geometry and material, ΔK is approximately independent of crack length before fracture.

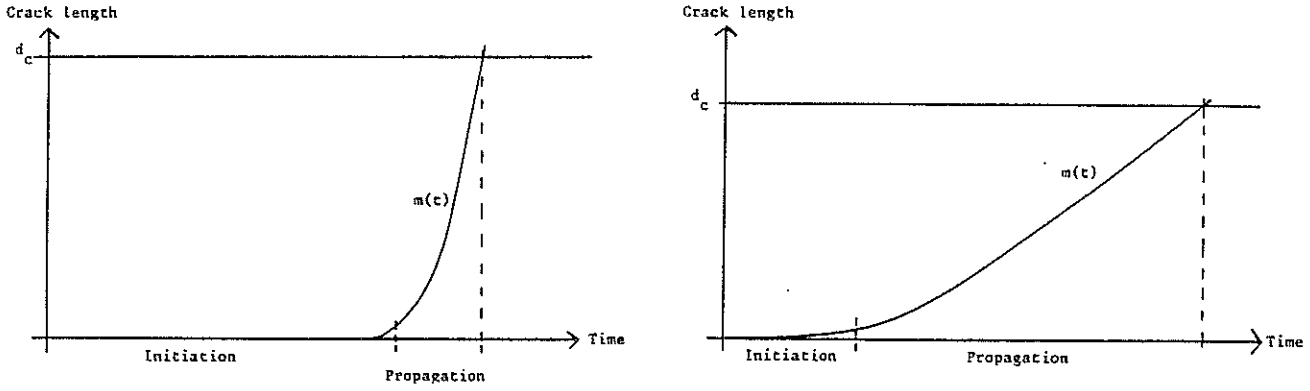

Figure 3.3.2. Crack length as a function of time (number of stress cycles). Small stress cycle amplitude or smooth specimen (a) and large stress cycle amplitude or notched specimen (b).

The lognormal distribution is frequently to describe time to fatigue failure. It agrees well with empirical data, and is computationally convenient. Birnbaum-Saunders distribution (see Chapter 4) for the propagation phase may be derived from rather general assumptions on the crack growth process. Both these distributions belong to the so-called ξ-normal family (Saunders, 1975):

$$P(T \leq t) = \Phi[\frac{1}{\alpha}\xi(\frac{t}{\beta})], \tag{3.3.2}$$

where $\alpha > 0$ and $\beta > 0$ are parameters, and ξ is a twice differentiable function on $(0,\infty)$ such that $\xi'' > 0$ and

$$\xi(\frac{1}{t}) = -\xi(t), \quad \text{for all } t > 0. \tag{3.3.3}$$

Saunders (1975) sets T_1, T_2 and T_3 equal to initiation time, propagation time and time for final fracture, respectively. He shows that if T_1, T_2, T_3 are independent, ξ-normal with the same ξ and possibly different parameters, then their sum is approximately ξ-normal, possibly with a different ξ.

3.4 CORROSION

Corrosion may be influenced by several mechanisms, resulting in different corrosion types according to the look of the corrosion attack. The following electrochemical corrosion forms may be defined (Bardal, 1985):

1) Uniform (general) corrosion
2) Galvanic or two metal corrosion
3) Thermogalvanic corrosion
4) Crevice corrosion and deposit corrosion
5) Pitting, pitting corrosion
6) Intergranular corrosion
7) Selective attack, selective leaching
8) Erosion corrosion
9) Cavitation corrosion
10) Fretting corrosion
11) Stress corrosion cracking
12) Corrosion fatigue

The terms used for these corrosion types are according to Fontana and Green (1967), and Treseder (1980). The rest of this section has, to some extent, been based on Bardal (1985).

General corrosion causes an approximately uniform corrosion depth, as illustrated in Figure 3.4.1. The relationship between corrosion current density and corrosion rate (corrosion depth increment per time unit) is given by:

$$\frac{\Delta S}{\Delta t} = \frac{i_{corr} \cdot M}{z \cdot F \cdot \rho} \qquad (3.4.1)$$

where

$\frac{\Delta S}{\Delta \tau}$ = corrosion rate

ΔS = average corrosion depth increment during time Δt

i_{corr} = corrosion current density

M = metal mole mass

z = number of electrons per metal atom, according to the reaction equation

F = Faraday's constant = 96 485 As

ρ = metal density (mass per volume)

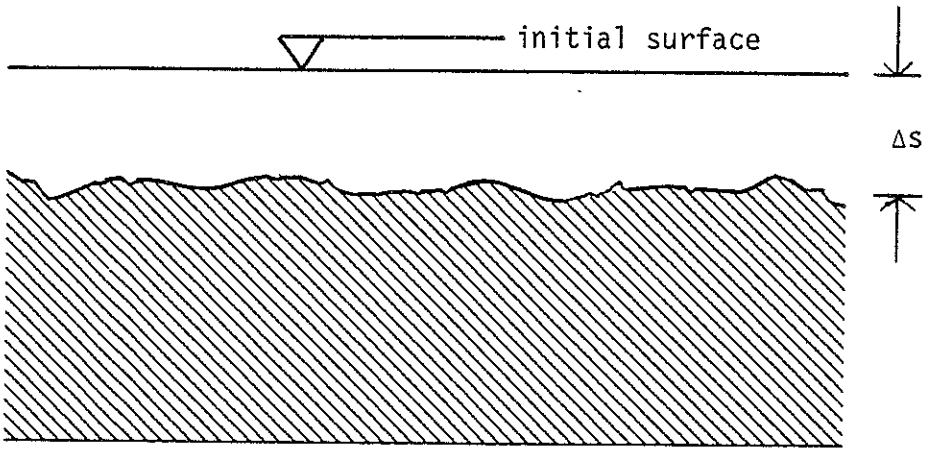

Figure 3.4.1.: General (uniform) corrosion.

General corrosion type may be dominating if these conditions are present:

1) Electrochemical corrosion is the only deterioration process.
2) Anodic and cathodic reactions occur on the entire surface, but not at the same place at the same time.
3) There are no significant concentration gradients in the electrolyte along the metal surface, and the metal is homogeneous.

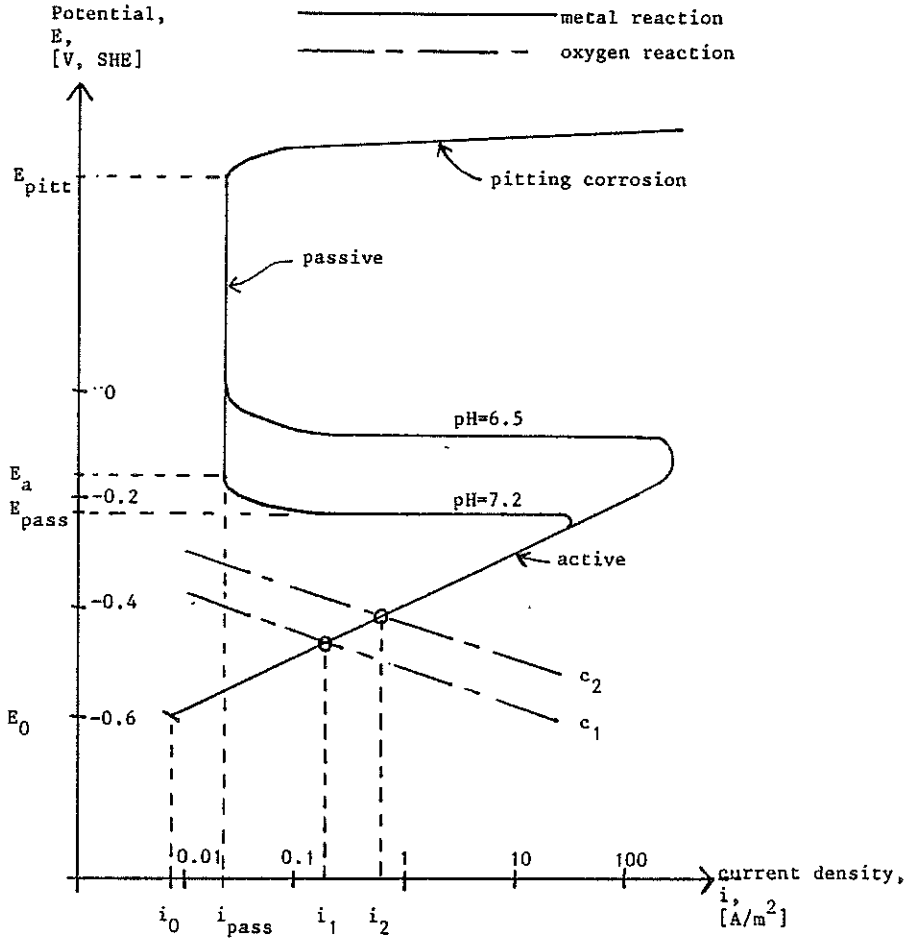

Figure 3.4.2.: Relationship between the metal surface potential and current density. The given E - i values are typical for iron in water. The potential is given with reference to the standard hydrogen electrode (SHE).

Figure 3.4.2 shows a typical relationship between the current density, and the metal surface potential. If $E < E_o$, immunity is present, that is, virtually no corrosion will take place. For $E_o < E < E_{pass}$, the current density is given by

$$E = E_0 + b_a \cdot \log_{10} \frac{i}{i_0} \tag{3.4.2}$$

where b_a is the so called tafel gradient for the actual metal/environment combination, and i_0 corresponds to E_0 (see Figure 3.4.2). The tafel gradient is given by

$$b = \frac{2.303 \cdot RT}{a \cdot zF} \tag{3.4.3}$$

where R is the gas constant, T is absolute temperature, and a is determined by the energy barrier to be exceeded by the reaction. Typical values of b_a around 20°C are 0.05 - 0.15 V/decade.

E_a is called the activation potential, and is slightly more positive than E_{pass}. For E between E_a and E_{pitt}, the metal is passive. That is, the corrosion products form an oxide film closely connected to the metal structure. Such films prevent metal ions from passing through. The corrosion rate is relatively low and independent of the potential. If E exceeds E_{pitt}, pitting corrosion will take place.

At a laboratory test, the metal surface potential may be regulated by means of a potentiostate. In other situations, the potential will stabilize at an equilibrium between the anodic reaction(s) as described, and the cathodic reaction(s). A common cathodic reaction is oxygen reduction,

$$O_2 + 4H^+ + 4e^- \rightarrow 2H_2O. \tag{3.4.4}$$

The E - i relationship for this reaction depends on a number of factors. If the oxygen concentration in the electrolyte is high enough, oxygen

transport towards the metal surface will not limit the reaction rate. Under these conditions, the E - i relationship is analogue to (3.4.2):

$$E_k = E_{0,k} - b_k \cdot \log_{10} \frac{i_k}{i_{0,k}} \tag{3.4.5}$$

This relationship is shown in Figure 3.4.2 for two concentrations $c_1 < c_2$, along with the corrosion current densities i_1 and i_2 at these conditions.

Let m(t) denote the average corrosion depth at time t. We shall derive a relationship between the corrosion rate m'(t) and the two stressors temperature and oxygen concentration, for the situation where equations (3.4.2) and (3.4.5) are valid. The potential and current density stabilize such that the potential for the two reactions equal:

$$E_{0,k} - b_k \log_{10} \frac{i}{i_{0,k}} = E_0 + b_a \log_{10} \frac{i}{i_{0,a}} \tag{3.4.6}$$

Solving this equation for $\log_{10} i$ yields

$$\log_{10} i = \frac{1}{b_a+b_k} [(E_{0k}-E_0) + b_a \log_{10} i_{0,a} + b_k \log_{10} i_{0,k}] \tag{3.4.7}$$

For a range of oxygen concentrations, $E_{0,k}$ may be considered as an approximately linear function of the concentration c. Since E_0 is independent of c, we may write

$$E_{0,k} - E_0 = k_1 + k_2 c, \tag{3.4.8}$$

where k_1 and k_2 are constants. Further, b_a and b_k are proportional to T according to (3.4.3), such that

$$b_a = b_1 T \tag{3.4.9}$$

$$b_k = b_2 T \tag{3.4.10}$$

Inserting (3.4.8) to (3.4.10) into (3.4.7) gives

$$\log_{10} i = \frac{k_1 + k_2 c}{(b_1+b_2)T} + \frac{b_1}{b_1+b_2} \log_{10} i_{0,a} + \frac{b_2}{b_1+b_2} \log_{10} i_{0,k} \quad (3.4.11)$$

Only the first term in (3.4.11) depends on c or T, the rest are constants. The corrosion rate, here denoted m'(t), is proportional to i, according to (3.4.1). Using this fact, and by redefining and combining some constants in (3.4.11), the following expression is obtained:

$$m'(t) = K_1 \exp(K_2/T + K_3 c/T) \quad (3.4.12)$$

3.5 CHEMICAL DEGRADATION

The Arrhenius and Eyring models are widely used for the reaction rate of chemical degradation processes. The reaction rate is given as a function of temperature, or as a function of temperature and a non-thermal stressor in the generalized Eyring model. These models may be written as follows, noting that other equivalent parametrizations are also encountered:

Arrhenius model:

$$m'(t) = A \exp(-B/\theta), \quad (3.5.1)$$

Eyring model:

$$m'(t) = \theta \exp(A-B/\theta), \quad (3.5.2)$$

Generalized Eyring model:

$$m'(t) = \theta A \exp(-B/\theta) \exp(CV + V/\theta). \quad (3.5.3)$$

In the equations above,

$m'(t)$ is the reaction rate,
θ is the absolute temperature,
V is a non-thermal stressor, e.g. voltage
$A > 0$, $B > 0$, and C are constants.

3.6 CONCLUDING REMARKS

In the preceding sections, deterministic models of the type

$$m'(t) = f(\underline{x},t,m(t)) \tag{3.6.1}$$

have been studied for some physical deterioration processes. Most of the models considered so far, are rather simple. Except for the fatigue crack growth model illustrated in Figure 3.3.2, we have been looking at models where the right hand side of (3.6.1) depends on $\underline{x}$ only, as long as $\underline{x}$ is within certain limits. That is, in these simple models, (3.1.2) reduces to

$$m'(t) = f(\underline{x}). \tag{3.6.2}$$

The functional forms of the simple models from the preceding sections may be summarized as follows:

Mechanism/model	Functional form	
Wear	$f(x) = kx_1$	(3.6.3)
Corrosion	$f(\underline{x}) = k_0 \exp(k_1/x_1 + k_2x_2/x_1)$	(3.6.4)
Arrhenius	$f(x) = k_0 \exp(-k_1/x_1)$	(3.6.5)
Eyring	$f(x) = x_1 k_0 \exp(-k_1/x_1)$	(3.6.6)
Generalized Eyring	$f(\underline{x}) = x_1 k_0 \exp(-k_1/x_1 + k_2x_2 + k_3x_2/x_1)$.	(3.6.7)

The model (3.6.3) is a special case of the model class

$$f(\underline{x}) = \beta_0 x_1 x_2 \ldots x_p. \tag{3.6.8}$$

The models (3.6.4) and (3.6.5) belong to the model class

$$f(\underline{x}) = \beta_0 \exp\Big(\sum_{i=1}^{p} \beta_i x_i \Big) = \beta_0 \exp(\underline{\beta} \cdot \underline{x}), \tag{3.6.9}$$

where obvious transformations of the stressors have been made. Similarly, (3.6.6) and (3.6.7) may be written on the form

$$f(\underline{x}) = \beta_0 \, x_1 \exp(\underline{\beta} \cdot \underline{x}). \tag{3.6.10}$$

Note that (3.6.9) is equivalent to

$$f(\underline{x}) = \beta_0 \, y_1^{\beta_1} \, y_2^{\beta_2} \ldots y_p^{\beta_p}, \tag{3.6.11}$$

where

$$y_i = \log(x_i).$$

Thus, (3.6.8) is a special case of (3.6.9), with $\beta_i = 1$ for $i \geq 1$.

4. STOCHASTIC DETERIORATION MODELS

4.1 INTRODUCTION

So far, little has been said about the stochastic modelling of the deterioration process $\underline{D}(t)$. From now on, $\underline{D}(t)$ will be considered as a stochastic process. Probability models for stochastic processes may, generally, be rather complex. Such a model must not only describe the probability distribution of $\underline{D}(t)$ for all separate $t \geq 0$, but also joint distributions for times t_1, t_2, ... For example, a model must be able to describe the probability distribution of $\underline{D}(t)$, given the history up to some point in time $u \leq t$. This is the conditional probability distribution

$$P(\underline{D}(t) \leq \underline{d} \mid \underline{D}(s) = \underline{d}(s),\ 0 \leq s \leq u),\quad t > u \tag{4.1.1}$$

We shall use the notation $\underline{D}(t) \leq \underline{d}$ in the meaning that each component of the vector $\underline{D}(t)$ is less than or equal to the corresponding component of the vector $\underline{d}$, that is,

$$\{ \underline{D}(t) \leq \underline{d} \} \overset{\text{def}}{=} \{ \bigcap_{i=1}^{h} D_i(t) \leq d_i \} . \tag{4.1.2}$$

Illustrating this in the one-dimensional case, two possible histories both leading to the value $D_1(u)=d_1$ at time u, are shown in the upper part of Figure 4.1.1. In the general case, the probability distribution of D(t) for $t > u$, given these two histories, may be different. For example, in the upper part of Figure 4.1.1, it seems natural to expect case (a) to deteriorate more slowly than case (b) from time u on.

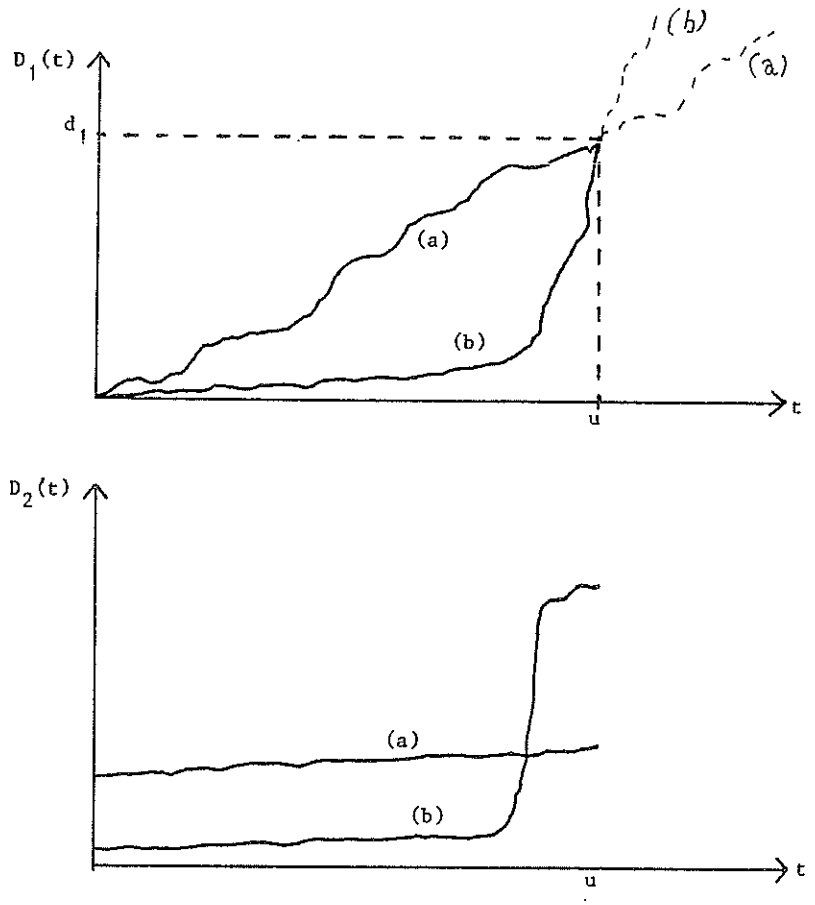

Figure 4.1.1. Two possible histories for a stochastic process $\underline{D}(\cdot)$, both leading to the value d of $D_1(u)$ at time u. For example, $D_1(\cdot)$ may represent the wear depth of an automobile tyre, and $D_2(\cdot)$ may represent the degree at which the wheel is out of balance.

The theory of martingales has been applied to describe the stochastic nature of $\underline{D}(t)$. For a survey, see e.g. Andersen and Borgan (1984). Further, deterministic models of deterioration mechanisms are frequently given in terms of differential equations. Hence, the theory of stochastic differential equations could be used here. For an introduction to this theory, see e.g. Øksendal (1985). We shall, however, use an approach based on the more basic theory of stochastic processes.

Modelling is significantly easier within the Markov class of stochastic processes. A stochastic process is said to be a Markov process, or have the Markov property, if, given the history up to time u, the distribution at time $t > u$ depends only on $\underline{D}(u)$, and not on $\underline{D}(s)$ for $s < u$. That is, if we know the state at time u, the history up to time u gives no extra information about future behaviour.

In a Markov process, the conditional distribution (4.1.1) depends on the history up to time u through the state at time u omly. That is, there exists some function $G(t,u,\underline{d},\underline{e})$ for $u \leq t$ such that

$$G(t,u,\underline{d},\underline{e}) = P(\ \underline{D}(t) \leq \underline{d} \mid \underline{D}(u) = \underline{e}\ )$$

$$= P(\ \underline{D}(t) \leq \underline{d} \mid \{\underline{D}(u) = \underline{e} \cap \underline{D}(s) = \underline{d}(s),\ 0 \leq s \leq u\ \})$$

$$\text{for all } \underline{D}(s),\ t \geq u \geq 0. \quad (4.1.3)$$

The Markov property gives considerable convenience in modelling and estimation. It should be noted, however, that the Markov property is not an acceptable approximation to assume for all physical deterioration processes. We shall mention two important reasons occurring in practical applications.

The first reason that Markov models may be inadequate, is illustrated by the process $D_1(t)$ in Figure 4.1.1: It seems like item (a) has undergone a gradual, steady deterioration, while the history of item (b) indicates that it may have received some kind of "shock" prior to time u, causing the deterioration to speed up. One would expect item (b) to deteriorate faster that item (a), also after time u. This example rises an interesting issue. Clearly, in this situation, the deteriority state $D_1(u)=d$ does not tell us everything about the item state at time u. It is possible, at least theoretically, that the deterioration process may have the Markov property if one or more extra deteriorities are measured in addition to the one shown in the upper part of Figure 4.1.1. For example, let $D_1(\cdot)$ represent the wear depth of an automobile tyre, and let $D_2(\cdot)$ represent the degree at which the wheel is out of balance. If $D_2(t)$ is "large", $D_1(\cdot)$ will tend to increase more rapidly. This example is illustrated in Figure 4.1.1. In this example, it may be sensible to use a

Markov model for $\underline{D}(t) = (D_1(t), D_2(t))$, even though $D_1(t)$ is clearly not a Markov process.

Another reason that Markov models sometimes are inadequate, may be illustrated by the data set from Part II of this thesis. Figure 4.1.2 shows the leakage development for 5 control valves, from Part II. The leakage as function of time follows an approximately linear trend for each valve, but the coefficients for this lines is significantly different between the valves. A satisfactory explanation is obtained by considering the coefficients of the straight line as an unobservable quantity for each valve, as discussed in detail in Part II of this thesis. Hence, the leakage development is not a Markov process: If a certain point $(t; d_1(t))$ was reached from a rather low initial value d(0), the deterioration from this point on is expected to continue at a rather high rate. On the other side, if this point was reached from a rather high initial value and through a low rate, the deterioration is expected to continue at a low rate. Hence, the expected future does not only depend on the point $(t, d_1(t))$, but on the history up to that point. This implies that the process is not Markov.

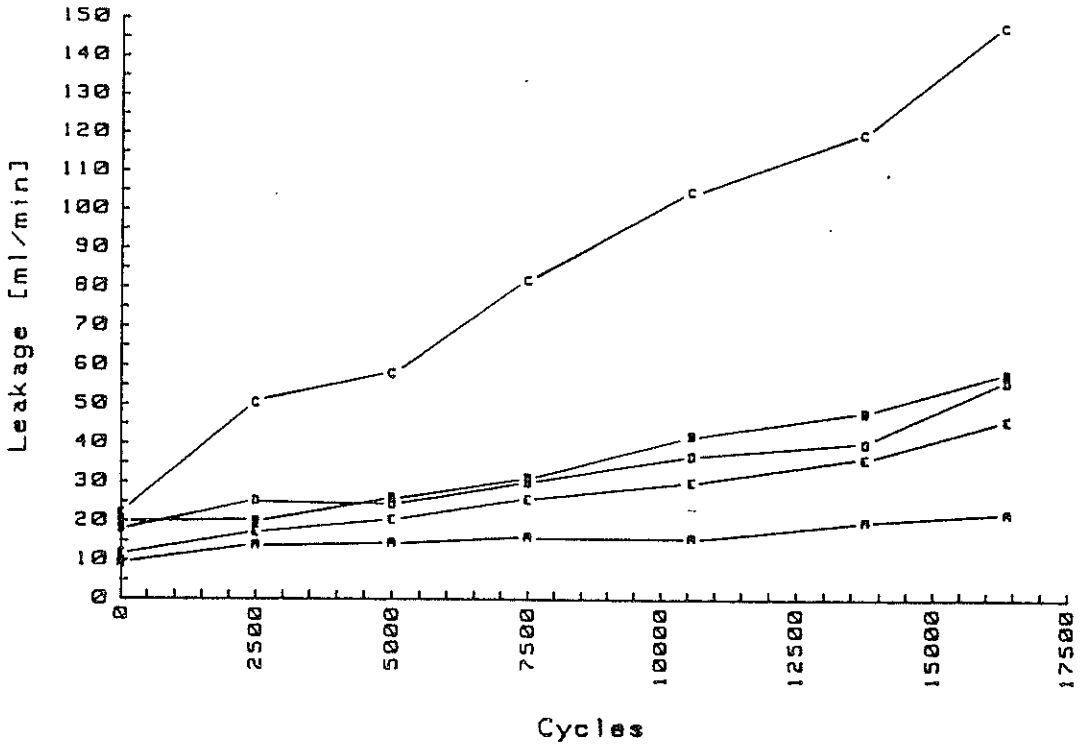

Figure 4.1.2: Leakage through in closed position for 5 control valves, as function of time (number of cycles operated). From Part II of this thesis.

Similar phenomena as for these valves seem to be present for other physical deterioration mechanisms, on several types of components. Especially, this seems to be so for fatigue crack growth in metals. According to Paris' law, the fatigue crack growth rate da/dN is given by

$$\log(da/dN) = \log(C) + m \cdot \Delta K, \qquad (4.1.4)$$

where ΔK is the stress intensity factor, and C and m are material constants. Both theory end empirical results establish equation (4.1.4) as a good approximation to reality, as long as ΔK is within specified limits. Paris' law is also treated in Section 3.3.

Virkler & al (1979) report crack growth measuremnts on 68 specimens of 2024-T3 aluminum alloy. On each specimen, an initial crack length of 9.0 mm was produced. The number of stress cycles needed to rach crack lengths of a = 9, 9.2, 9.4, ..., 36.2, 36.6, ..., 44.2, 45.0, ..., 49.8 mm were measured. This gave 163 increment values per specimen. The original data are depicted in Figure 4.1.3. This seems to have become a "classical" data set on fatigue crack growth, and has subsequently been studied by several authors. Virkler & al (1979), Bogdanoff and Kozin (1985), Oritz (1986), and Ditlevsen and Olesen (1986) all use different stochastic models based on (4.1.4). It seems that Ditlevsen and Olesen (1986) were the first to find a model giving a satisfactory description of the scatter between the specimens. Their basic model was a stochastic extension of (4.1.4), where the set of parameter in the models was considered a stochastic vector with one (not direct observable) value per specimen.

Hudak & al (1978) report data set similar to the Virkler data. The Hudak data have also been studied by several authors, e.g. Bogdanoff and Kozin (1985). However, a satisfactory model does not seem to have been applied. Probably, the type of model proposed by Ditlevsen and Olesen (1986) would also provide a satisfactory fit to the Hudak data.

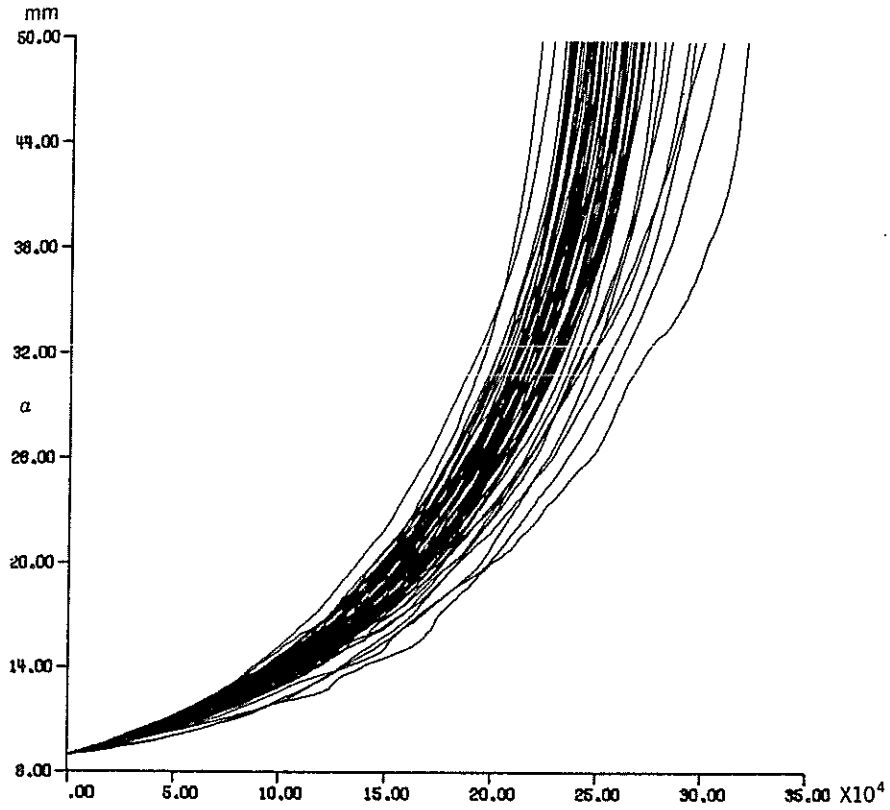

Figure 4.1.3: The Virkler & al (1979) fatigue crack length measurements. Crack length (a) as function of number of cycles (n). (Figure from Bodganoff and Kozin, 1985.)

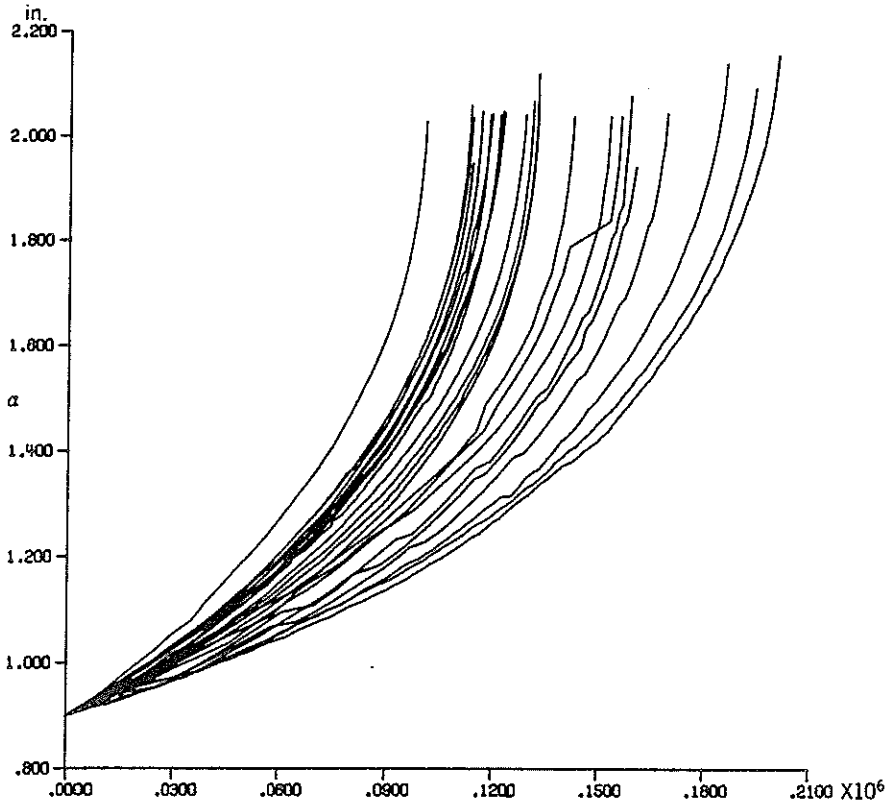

Figure 4.1.4: The Hudak & al (1978) fatigue crack length measurements. Crack length (a) as function of number of cycles (n). (Figure from Bodganoff and Kozin, 1985.)

Ørjasæter & al (1985) report crack growth rate measurements on 16 specimens from one steel plate, with 4 specimens tested at each of 4 different laboratories. Narbuvoll (1987) treat these data using the theory of stochastic regression coefficients. The coefficients (C, m) in equation (4.1.4) were found to differ significantly between the specimens, even for specimens tested within the same laboratory.

Iuculano and Zanini (1986) report testing of metallic layer resistors. They use the Arrhenius model, but with an individual value of B for each specimen. The Arrhenius model is defined in Section 3.5.

The preceding examples reveal one weakness of the Markov models: They do not incorporate the individual ability to withstand deterioration, which may vary from specimen to specimen. For example, the expected deterioration of metallic parts may depend on physical properties such as:

- material composition
- pores or inclusions
- surface treatment
- lubrication
- etc.

Cox and Miller (1975) divide stochastic processes into four cases:

i) discrete time, discrete state space
ii) discrete time, continuous state space
iii) continuous time, discrete state space
iv) continuous time, continuous state space

In practically all applications, it seems natural to view the deterioration as continuous both in time and state on the macroscopic level. However, the cases i) to iii) may prove useful both as approximations to the continuous case, and may also provide a basis for developing a continuous model as a limiting case. Such cases are discussed from this point of view in Sections 4.2. Two special cases of iv) will be discussed in sections 4.3 and 4.5, namely Wiener processes and Wiener processes with random starting point and drift. Section 4.5 treats linear regression with random coefficients, which also seems useful in deteriora-

tion data analysis. Finally, Section 4.6 covers the Bernstein life distribution and related models.

4.2 CUMULATIVE STOCHASTIC PROCESSES

This section concerns a number of model classes for stochastic processes with one property in common: They all non-decreasing in time. That is, if $t_1 < t_2$, then $D(t_1) \leq D(t_2)$. Further, all these models are discrete in time or state space. The section is divided into 4 subsections, each covering one model class. Not all of these model classes are disjoint.

4.2.1 Bivariate Renewal Processes

Pieper and Tiedge (1983) define a class of cumulative stochastic processes in the following way: Let

$$\{(X_n, Y_n);\ n = 1, 2, \ldots\} \tag{4.2.1}$$

be a bivariate renewal process, that is, a sequence of non-negative, independent, identically distributed bivariate random variables. Further, define the counting process N(t) as

$$N(t) = \max\left(n: \sum_{i=1}^{n} X_i < t\right) \tag{4.2.2}$$

Assume that an item is set into service at time $t = 0$, and that the initial value of the deterioration is $D(0) = Y_0$. The distribution of Y_0 is not (necessarily) the same as the distribution of Y_i, $i \geq 1$. At the points in time X_1, $X_1 + X_2$, ..., the item is exposed to a "shock" causing the deterioration to increase with the quantity Y_1, Y_2, ..., respectively. The state of deterioration at time t is thus

$$D(t) = \sum_{i=0}^{N(t)} Y_i. \tag{4.2.3}$$

The model is illustrated in Figure 4.2.1. The time interval between "shocks" number i-1 and i is X_i, and "shock" number i causes the deterioration increment Y_i.

Consider, for example an item exposed to working cycles of varying length X_i, and let Y_i be the deterioration increment during working cycle number i. In this case, the deterioration increment may tend to be higher during longer working cycles. Hence, it is natural to allow for dependence between X_i and Y_i.

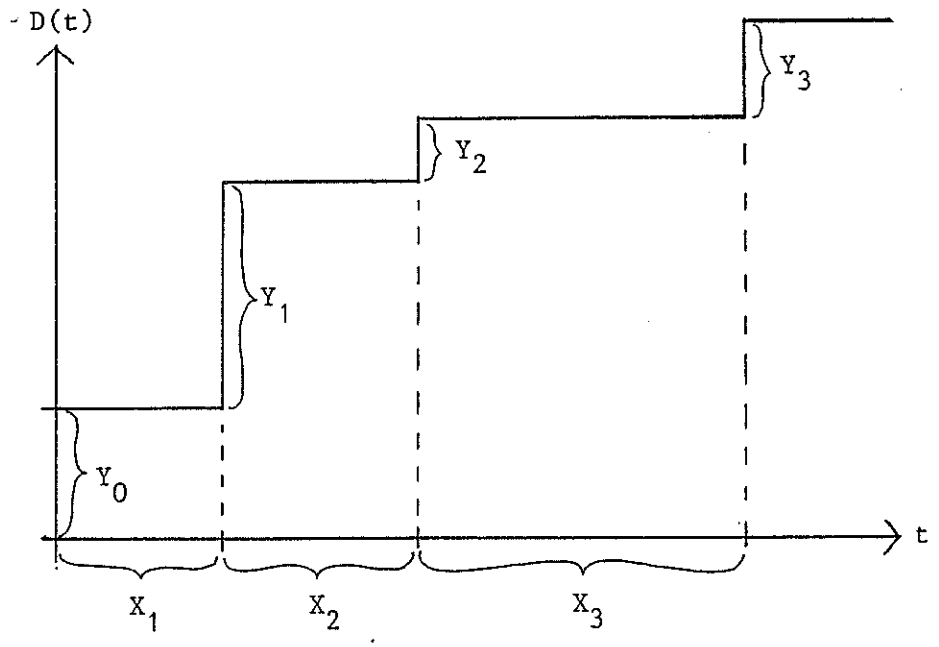

Figure 4.2.1: A class of cumulative stochastic processes suggested by Pieper and Tiedge (1983)

In general, the distribution of (X_i, Y_i) is given by

$$P((X_i \leq x) \cap (Y_i \leq y)) = G(x,y). \qquad (4.2.4)$$

Note that the Poisson process with constant intensity λ evolves as a special case by setting

$$G(x,y) = (1 - e^{-\lambda x})\ I(y \geq 1) \tag{4.2.5}$$

where

$$I(y \geq 1) = \begin{cases} 1 & \text{if } y \geq 1 \\ 0 & \text{if } y < 1 \end{cases} \tag{4.2.6}$$

is the indicator function. One of the elementary model classes for fatigue crack also turns out as a special case: In these model classes, the crack increments in each stress cycle are assumed independent, identically distributed. Let t_0 be the duration of each cycle, and let $F_Y(y)$ be the probability distribution of one crack increment. Then,

$$G(x,y) = I(x \geq t_0)\ F_Y(y). \tag{4.2.7}$$

Some results for the general model (4.2.1) - (4.2.4) are given in Pieper and Tiedge (1983) and in references therein. These include general results, asymptotic results, and results for a few special cases.

4.2.2 Poisson processes

Consider the following random shock model: Assume that the unit receives "shocks" according to a Poisson process with intensity λ, and that failure occurs after exactly r shocks. The lifetime of such a unit equals the sum of r independent, identically exponentially distributed variables. It follows that the lifetime is gamma distributed with parameters λ and r, that is, the probability density is

$$f(t) = \frac{\lambda}{\Gamma(r)} (\lambda r)^{r-1}\ e^{-\lambda t}\ . \tag{4.2.8}$$

The expected time to failure is

$$E(T) = \lambda r, \tag{4.2.9}$$

and the variance is

$$Var(T) = \lambda^2 r. \tag{4.2.10}$$

The critical deterioration is d_c, that is, failure occurs at the instant when D(t) reaches the value d_c. Each shock causes D(t) to increase with the quantity d_c/r. This is illustrated in Figure 4.2.2.

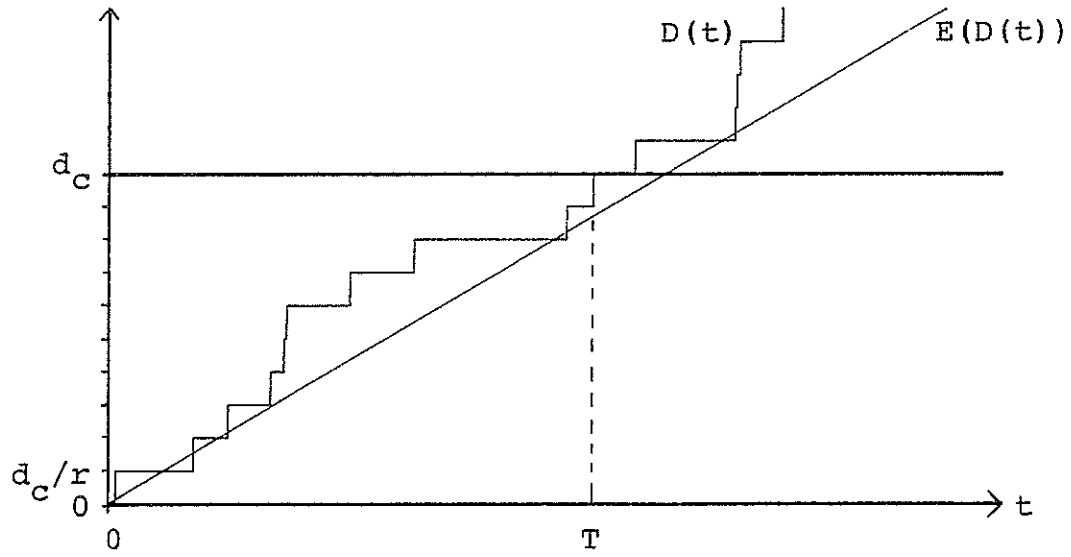

Figure 4.2.2. A random shock model for the deterioration process.

The coefficient of variation for a variable T is defined as

$$c_T = \frac{SD(T)}{E(T)} = \frac{\sqrt{Var(T)}}{E(T)}. \tag{4.2.11}$$

In the gamma distribution (4.2.8), the coefficient of variation is

$$C_T = \frac{\sqrt{\text{Var}(T)}}{E(T)} = \frac{\sqrt{r\lambda^2}}{r\lambda} = \sqrt{1/r}, \tag{4.2.12}$$

which implies that

$$r = (1/C_T)^2. \tag{4.2.13}$$

If the Poisson process model should be used an approximation to continuous deterioration, it would require a rather "large" value of r. However, experience shows that lifetime distributions usually have a coefficient of variation in the size of order 1. In many practical situations, $C_T > 1$, and C_T is seldom much less than about 0.5. Since $r \in \{1,2,3,\ldots\}$, the model cannot be used when $C_T > 1$. Further, $C_T \gtrsim 0.5$ implies $r \lesssim 4$, making the path of D(t) very far from a continuous path. Hence, the above model is hardly suitable as an approximation to continuously increasing deterioration.

4.2.3 B-models

In their book "Probabilistic Models of Cumulative Damage", Bogdanoff and Kozin (1985) discuss what they call B-models of cumulative damage. A basic version of the B-model is based on these assumptions (Bogdanoff and Kozin, 1985, pp 72 - 74):

1. There is a repetitive constant severity duty cycle (DC).

2. Damage states are discrete and labelled 1, 2, ..., b. State b is the state of failure.

3. Damage in a DC depends only on that DC and on the state of damage at the start of that DC. That is, the damage process possesses the Markov property.

4. Damage can only increase in a DC from the state occupied at the start of that DC to the state of one unit higher.

5. The state at time 0 may vary between specimens, due to manufacturing standards, quality control, and so on. This is described in terms of a probability distribution over the states 1, 2, ..., b-1.

The initial probability distribution is given by the 1xb row vector

$$p_0 = (\pi_1, \pi_2, \ldots, \pi_{b-1}, 0). \tag{4.2.14}$$

The probability that the state after a DC is higher than at the start of the DC, may, generally, depend on the state at the start of the DC. These probabilities are denoted

$$p_j = P(\text{Remain in state } j \mid \text{Initially in state } j) \tag{4.2.15}$$

and

$$q_j = 1 - p_j = P(\text{Go to state } j+1 \mid \text{Initially in state } j). \tag{4.2.16}$$

The transition matrix for the Markov process is

$$P = \begin{bmatrix} p_1 & q_1 & 0 & 0 & \ldots & 0 & 0 \\ 0 & p_2 & q_2 & 0 & \ldots & 0 & 0 \\ 0 & 0 & p_3 & q_3 & \ldots & 0 & 0 \\ \vdots & & & & & & \\ 0 & 0 & 0 & 0 & \ldots & p_{b-1} & q_{b-1} \\ 0 & 0 & 0 & 0 & \ldots & 0 & 1 \end{bmatrix}. \tag{4.2.17}$$

Using one of the elementary results from Markov processes (see e.g. Cox and Miller, 1965), the state at time t, that is, after t duty cycles, is seen to have probability distribution

$$p_t = p_0 P^x. \tag{4.2.18}$$

A number of extensions of the basic B-model (assumptions 1 - 5) are given by Bogdanoff and Kozin (1985). These extensions include:

- Periodic inspections with replacement or repair, possibly with imperfect inspection.

- Positive probability for jumps of size more than 1 (multiple jump models).

- B-models in continuous time.

- Non-stationarity in time, i.e. the transition matrix P or related quantities depend on time.

All the extensions studied by Bogdanoff and Kozin (1985) have two properties in common:

i) The Markov property.

ii) Zero probability of negative jumps, except upon repair or replacement.

The B-models suggested by Bogdanoff and Kozin (1985) have been discussed and compared to alternative models by a number of authors, see i.e. Sobczyk (1986), Newby (1987a), and Newby (1987b). These authors consider the models primarily in connection with fatigue crack growth.

4.3 WIENER PROCESSES

The Wiener process represents a model class which may prove useful in modelling D(t). The process D(t) is said to be a Wiener process with drift parameter μ and variance parameter σ^2 if

$$D(t_2) - D(t_1) \sim N(\mu(t_2-t_1), \sigma^2(t_2-t_1)) \qquad (4.3.1)$$

for all $t_1<t_2$, and increments in D(t) over disjoint intervals are independent (See e.g. Cox and Miller, 1965). In the literature, many authors use the term Brownian motion in the same meaning as Wiener process.

Simulated realizations of Wiener process for some values of μ and σ are shown in Figures 4.3.1 to 4.3.3. The Wiener process has one feature which, at least theoretically, does not agree with a model for deterioration: The increment in D(t), given by (4.3.1), has a positive probability of obtaining negative values. This is clearly seen in Figure 4.3.1, and to some extent in Figure 4.3.2. The processes D(t) given in these figures are seen to be decreasing over some intervals. For the simulated Wiener processes in Figure 4.3.3, the negative increments are "fewer" and smaller than in the two preceding figures. On the other hand, the coefficient of variation for the lifetime distribution in this figure seems too small for almost all practical lifetime distributions. (See the discussion at the end of Section 4.2.2.)

However, the existence of negative increments does not necessarily exclude the Wiener process as an acceptable approximation for a number of deterioration processes. Also, there exist examples where a temporary improvement (decrase in D(t)) seems plausible. For example, see the discussion on the valve leakage data in Part II of this thesis.

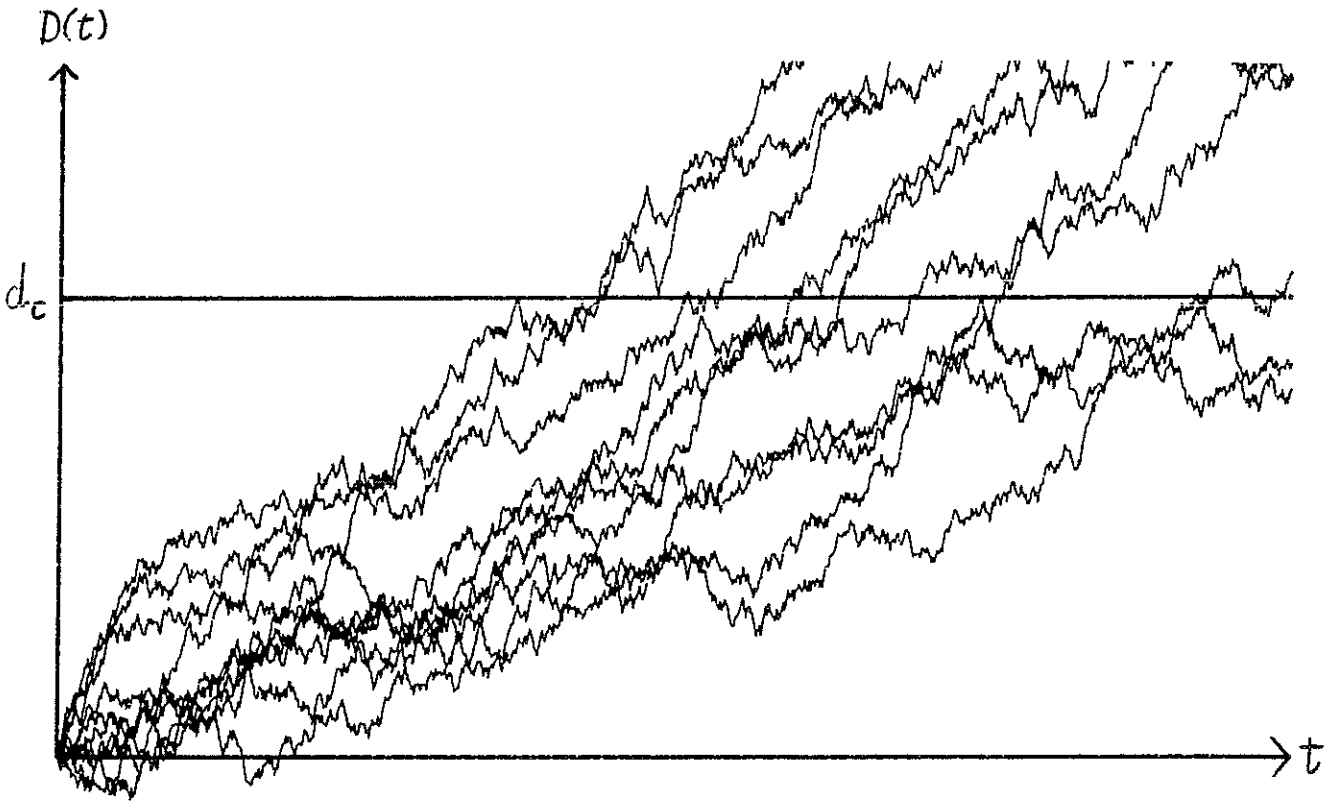

Figure 4.3.1. Simulated Wiener processes with $\sigma = 0.3\mu$.

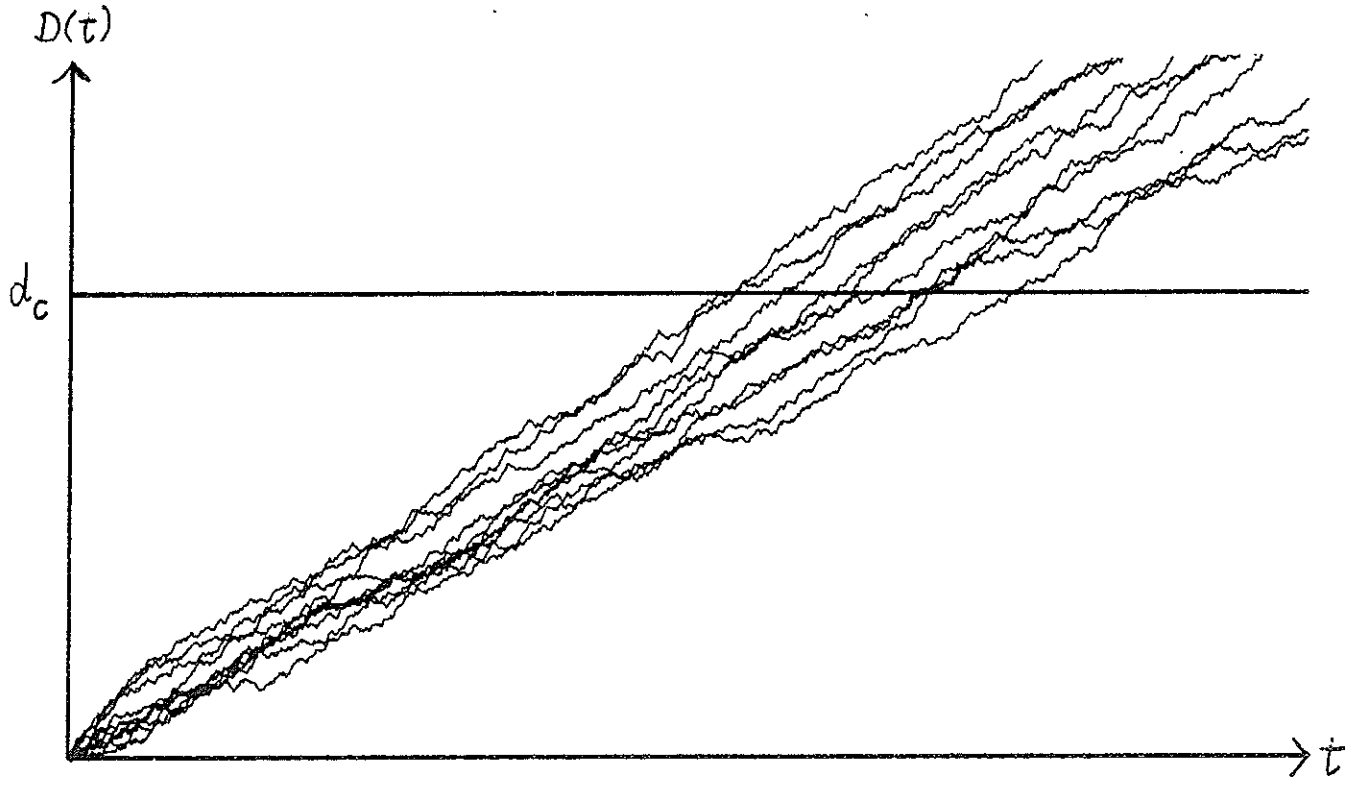

Figure 4.3.2. Simulated Wiener processes with $\sigma = 0.1\mu$.

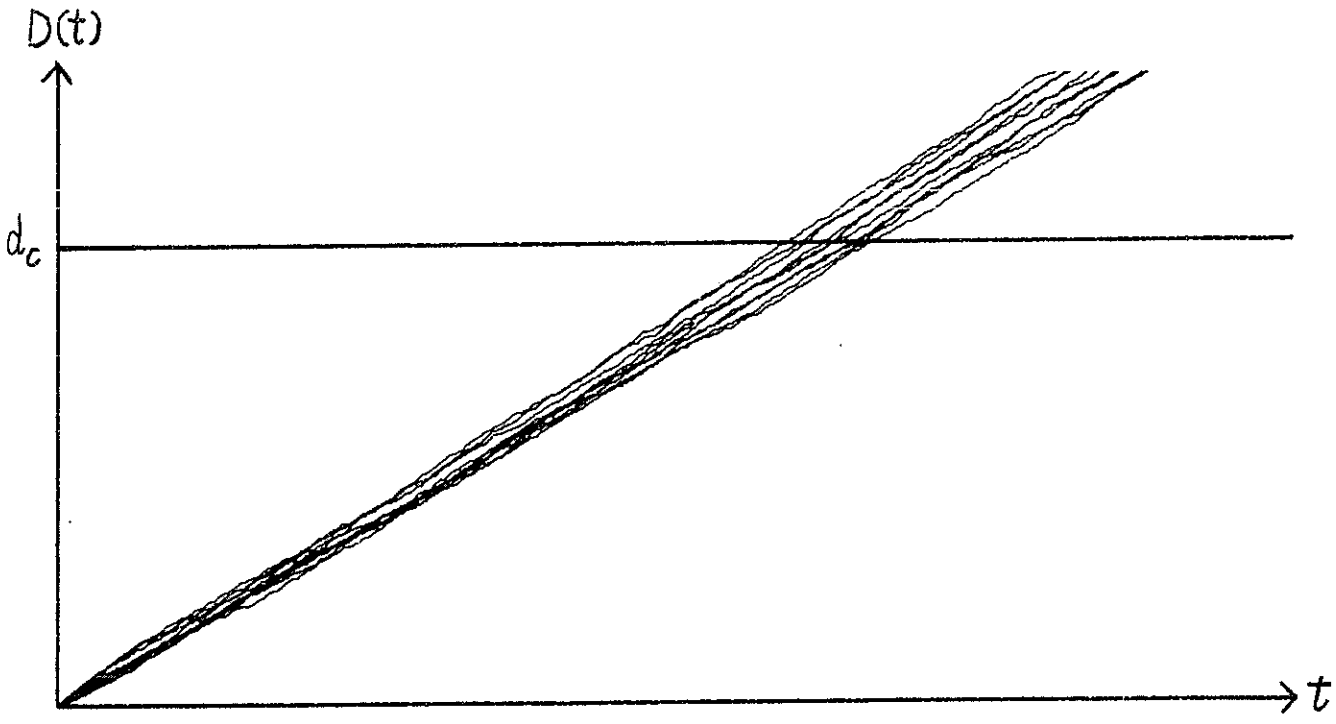

Figure 4.3.3. Simulated Wiener processes with $\sigma = 0.03\mu$.

If failure occurs when D(t) first reaches the value d_c, the failure time equals

$$T = \inf \{ t : D(t) \geq d_c \}. \qquad (4.3.2)$$

It can be shown (see e.g. Cox and Miller, 1965) that T has the inverse Gaussian distribution (IG), and has probability density

$$g(t) = \frac{d_c}{\sigma\sqrt{2\pi}} \frac{1}{t^{3/2}} \exp\left[- \frac{(d_c-\mu t)^2}{2\sigma^2 t} \right]. \qquad (4.3.3)$$

Birnbaum-Saunders fatigue-life distribution is obtained simply by setting $F_T(t) = P(D(t) \leq t)$. That is, one sets

$$P(T \leq t) = P(\, D(t) \geq d_c \,)$$

$$= 1 - \Phi \left[\frac{d_c - \mu t}{\sigma\sqrt{t}} \right]$$

$$= \Phi \left[\frac{1}{\sigma} \left(\mu\sqrt{t} - \frac{d_c}{\sqrt{t}} \right) \right] \qquad (4.3.4)$$

Equation (4.3.4) is the cumulative distribution function in Birnbaum-Saunders distribution, which is better known in the form

$$P(T \leq t) = \Phi \left[\frac{1}{\alpha} \left(\sqrt{\frac{t}{\beta}} - \sqrt{\frac{\beta}{t}} \right) \right] \qquad (4.3.5)$$

where

$$\alpha = \sigma / \sqrt{\mu d_c}$$
$$\beta = d_c / \mu .$$

The expectation and variance in Birnbaum-Saunders distribution are

$$E(T) = \beta(1 + \frac{\alpha^2}{2})$$

and

$$Var(T) = \alpha^2\beta^2(1 + \frac{5}{4}\alpha^2) .$$

In terms of the parametrization in (4.3.4), the mean and variance are

$$E(T) = \frac{d_c}{\mu} \left[1 + \frac{1}{2} \frac{\sigma^2}{\mu d_c} \right]$$

and

$$\mathrm{Var}(T) = \frac{\sigma^2 d_c}{\mu^3}\left[1 + \frac{5}{4}\frac{\sigma^2}{\mu d_c}\right].$$

Birnbaum-Saunders distribution (BS) is widely used in analysis of fatigue failure data. The BS model can be viewed as an approximation to the IG model. Although the difference between the models is negligible when $\mu >> \sigma$, there is no need to make this approximation, since the IG distribution is even simpler to work with than the BS distribution (Bhattacharyya and Fries, 1982). For a thorogh comparison between these distributions from a cumulative damage point of view, see Desmond (1987), who also gives an extensive list of references. Barry & al (1986) and Barry & al (1987) compare the IG and lognormal time to failure distributions for integrated circuit devices. In the Ditlevsen and Olesen (1986) analysis of the Virkler & al (1979) fatigue life data, the IG life distribution fits well to the measured data, within a total model similar to the Wiener process. The first passage problem for the Wiener process is also studied by Ditlevsen (1986).

The inverse Gaussian distribution is sometimes referred to in the probability density form

$$g(t) = \frac{1}{\sqrt{2\pi\nu}\ t^{3/2}} \exp\left[-\frac{(1-\delta t)^2}{2\nu t}\right], \qquad (4.3.6)$$

and denoted IG(δ,ν). The correspondence between the parametrizations in (4.3.3) and (4.3.6) are given by

$$\nu = \sigma^2/d_c^2$$

and

$$\delta = \mu/d_c.$$

In the notation of (4.3.6), the cumulative probability distribution is given by (Shuster, 1968)

$$G(t) = \Phi\left(\frac{\delta t - 1}{\sqrt{\nu t}}\right) + \exp\left(\frac{2\delta}{\nu}\right)\Phi\left(-\frac{\delta t + 1}{\sqrt{\nu t}}\right), \qquad (4.3.7)$$

where $\Phi(\cdot)$ denotes the standard normal distribution function. The mean and variance are $1/\delta$ and ν/δ^3, respectively. In terms of the parametrization in (4.3.3), the mean and variance is thus

$$E(T) = d_c/\mu^3 \tag{4.3.8}$$

and

$$Var(T) = \sigma^2 d_c/\mu. \tag{4.3.9}$$

In the case of Wiener-processes in more than one dimension, the first passage problem is much more complex (Iyengar, 1985). Assume that

$$\underline{D}(t) = (D_1(t), \ldots, D_h(t))'$$

is a h-dimensional Wiener process. (See i.e. Iyengar, 1985, for a definition.) Let

$$\underline{d}_c = (d_{c,1}, d_{c,2}, \ldots, d_{c,h})'$$

be the critical deteriority values for occurrence of failure (see Chapter 2). That is, the item fails as soon as $D_i(t)$ reaches $d_{c,i}$ for at least one $i = 1, 2, \ldots, h$. The time of failure may be written as

$$T = \min\{T_1, T_2, \ldots, T_h\}, \tag{4.3.10}$$

where

$$T_i = \inf\{\, t : D_i(t) \geq d_{c,i} \,\}, \quad i = 1, 2, \ldots, h. \tag{4.3.11}$$

For the two dimensional case, the joint probability distribution of (T_1, T_2) has been studied by Iyengar (1985), including Wiener process with drift. The article also includes some further references on the subject.

Below, two generalizations of the one-dimensional Wiener process (4.3.1) are included for the sake of completeness. The first generalization is

found in Lemoine and Wenocur (1985), and the second in Barndorff-Nielsen & al (1978).

Generalization 1

Let $g(\cdot)$ be an arbitrary strictly increasing function on $[0,\infty)$ with continuous second derivative and with $g(0)=0$. Set $D(t)=g[\sigma U(t) - \mu t]$, where $\mu>0$ and $\sigma>0$, and $U(\cdot)$ is a standard Wiener process, that is, a Wiener process having drift parameter 0 and variance parameter 1. Now, set

$$\sigma(d) = \sigma g'[g^{-1}(d)], \tag{4.3.12}$$

$$\theta(d) = \int_0^d \frac{1}{\sigma(s)} ds, \tag{4.3.13}$$

$$\mu(d) = \sigma(d) \left[-\frac{\mu}{\sigma} + \frac{1}{2}\sigma'(d) \right]. \tag{4.3.14}$$

Consider the diffusion process on $[0,\infty)$ with infinitesimal drift and variance parameters $\mu(d)$ and $\sigma(d)$ so defined. Let d_0 be the starting point of the process. Then the first hitting time to level 0 has the $IG(\delta,\nu)$ distribution with parameters $\delta=\mu/[\sigma\theta(d_0)]$ and $\nu=1/[\theta(d_0)]^2$ (Lemoine and Wenocur, 1985).

Generalization 2.

The generalized inverse Gaussian distribution is defined by the probability density

$$f(t) = \frac{(c/b)^{a/2}}{2K_a(\sqrt{bc})} t^{a-1} \exp\left[-\frac{bt^{-1} + ct}{2} \right]. \tag{4.3.15}$$

Here, $K_a(\ )$ is the modified Bessel function of the third kind and with index a (Abramowitz and Stegun, 1965). The domain of variation for the parameters (a,b,c) is

$$\begin{aligned} &a > 0, \quad b \geq 0, \quad c > 0; \\ &a = 0, \quad b > 0, \quad c > 0; \\ &a \leq 0, \quad b > 0, \quad c \geq 0. \end{aligned}$$

This class of distributions includes the inverse Gaussian distribution. It is readily shown that the generalized inverse Gaussian distribution with parameters (-1/2,b,c) is identical to the IG(δ,ν) with $\nu=1/b$ and $\delta=\sqrt{c/b}$.

Following Barndorff-Nielsen & al (1978), the first hitting time distribution for a rather general class of diffusion processes may be derived as follows:

Let α be a positive and differentiable function defined on the interval $(0,\infty)$. Set

$$\theta(x) = \int_0^x \sqrt{1/[\alpha(u)]}\, du, \tag{4.3.16}$$

and suppose that θ satisfies the conditions

$$\theta(x) < \infty, \quad 0 < x < \infty \tag{4.3.17}$$

and

$$\theta(\infty) = \infty. \tag{4.3.18}$$

Furthermore, let β be defined on $(0,\infty)$ by

$$\beta(x) = -\sqrt{\alpha(x)} \left[\frac{2\lambda - 1}{2\theta(x)} + \frac{\sqrt{\Psi} K_{\lambda-1}(\theta(x)\sqrt{\Psi})}{K_\lambda(\theta(x)\sqrt{\Psi})} \right] + \frac{1}{4} \frac{d}{dx}\alpha(x) \tag{4.3.19}$$

for $\Psi > 0$ and $\lambda \leq 0$, and by the limiting value of this expression, i.e.

$$\beta(x) = \sqrt{\alpha(x)}\,\frac{2\lambda + 1}{2\theta(x)} + \frac{1}{4}\frac{d}{dx}\alpha(x), \tag{4.3.20}$$

for $\Psi = 0$ and $\lambda < 0$. In the special case of $\lambda = -1/2$, the expressions (4.3.19) and (4.3.20) for β take the particularly simple form

$$\beta(x) = -\sqrt{\Psi a(x)} + \frac{1}{4}\frac{d}{dx}\alpha(x) \tag{4.3.21}$$

Consider a time-homogeneous diffusion process $x(t)$ with state space $[0,\infty)$ and such that the process has infinitesimal variance $\alpha(x)$ and infinitesimal mean $\beta(x)$, specified as above. Let $x_0 > 0$ be the initial position of the process. Then, the first hitting time of 0 follows the generalized inverse Gaussian distribution with parameters $(\lambda, \theta^2(x_0), \Psi)$. Here, $\lambda \leq 0$, and $\theta(x_0)$ is given by (4.3.16).

4.4 REGRESSION WITH RANDOM COEFFICIENTS

In terms of a simple linear model, the expected wear depth at time t may be $E(D(t)) = \mu_0 + \mu(\underline{x})t$, for a given stressor $\underline{x}$. As mentioned in Section 4.1, there are practical cases where it seems natural to let $(\mu_0, \mu(\underline{x}))$ have one value for each specimen. That is, consider $(\mu_0, \mu(\underline{x}))$ as a stochastic variable. For a given specimen, the value of $(\mu_0, \mu(\underline{x}))$ is unknown and cannot be direct observed. Such a model is also discussed and fitted to the valve leakage data in Part II of this thesis.

In this section, we shall confine ourselves to models where (the expectation of) μ is a linear function of $\underline{x}$. Not only do such linear models occur in many practical situations, but the results for simple models can hopefully also give indications on how non-linear models behave.

A review of random regression coefficients models is given e.g. by Spjøtvoll (1977). For the sake of completeness, some of these models are summarized below, adapted to our situation and with our terminology.

Consider first the general regression model

$$D(t_{ij}) = \beta_{0ij} + \beta_{1ij}u_{1ij} + \ldots + \beta_{pij}u_{pij} + e_{ij},$$
$$i = 1, \ldots, n_j, \qquad j = 1, \ldots, r. \tag{4.4.1}$$

Here, $D(t_{ij})$ is the result of the i'th deterioration measurement on specimen number j. The so-called independent variables u_{hij} are assumed to be fixed. They are known functions of the stressor $\underline{x}_i$ and the time t_{ij}, for example $u_{1ij} = x_i t_{ij}$ for a one-dimensional $\underline{x}$. The regression coefficients β_{hij} are random variables with

$$E(\beta_{hij}) = \theta_h \tag{4.4.2}$$

and

$$Cov(\beta_{hij}, \beta_{kij}) = \lambda_{hk}. \tag{4.4.3}$$

Two β_{hij} with different values of the pair (i,j) are independent. We denote the covariance matrix of $(\beta_{0ij}, \ldots, \beta_{pij})$ by Λ. The error terms e_{ij} are assumed to be independent with expectation 0 and variance σ^2. They are also assumed to be independent of the β_{hij}.

In the literature, several special cases of this type of model have been studied. In these special cases, one or more of these assumptions are made:

$$\beta_{0ij} = \beta_{0j}, \ \ldots, \ \beta_{pij} = \beta_{pj}$$
$$i = 1, \ldots, n_j, \qquad j = 1, \ldots, r. \tag{4.4.4}$$

$$u_{1ij} = u_1, \ \ldots, \ u_{pij} = u_p \tag{4.4.6}$$

Λ is diagonal. (4.4.7)

For a survey of these studies, see Spjøtvoll (1977), where the problem of estimating the mean regression coefficients (4.4.2) and the covariance matrix of these coefficients (4.4.3) is treated.

4.5 WIENER PROCESS WITH RANDOM DRIFT

This section discusses a Wiener process model where the drift parameter μ is a random variable with one value for each specimen. A similar, extended model of this kind is also discussed and fitted to data on valve leakage in Part II of this thesis.

Assume that μ has some distribution $F_\mu(\mu)$, and that given μ, then $D(t|\mu)$ is a Wiener process with drift parameter μ and variance parameter σ^2. This implies that

$$D(t) \mid \mu \sim N(\mu t, \sigma^2 t) \tag{4.5.1}$$

Note that $D(t) \mid \mu$ has the same distribution as

$$\mu t + \sigma\sqrt{t}U, \tag{4.5.2}$$

where $U \sim N(0,1)$.

This model is very convenient from a mathematical point of view if μ itself is assumed to have a normal distribution, say,

$$\mu \sim N(\theta,\lambda). \tag{4.5.3}$$

It follows from (4.5.2) and (4.5.3) that unconditionally, D(t) has the same distribution as

$$(\theta + \sqrt{\lambda}U_1)t + \sigma\sqrt{t}U_2, \tag{4.5.4}$$

where U_1, U_2 are independent and N(0,1). From (4.5.4) it is readily seen that

$$D(t) \sim N(\theta t, \lambda t^2 + \sigma^2 t). \tag{4.5.5}$$

To investigate this model further, we shall find the probability distribution of $D(t_2)$ given $D(t_1) = d_1$, where $t_2 > t_1 > 0$. For simplicity, we use the notation $D_1 = D(t_1)$ and $D_2 = D(t_2)$.

Conditionally given μ, then D_1 and $(D_2 - D_1)$ are independent with distributions

$$D_1|\mu \sim N(\mu t_1, \sigma^2 t_1)$$

$$(D_2 - D_1)|\mu \sim N(\mu(t_2 - t_1), \sigma^2(t_2 - t_1))$$

The conditional joint probability density of $(D_1, (D_2 - D_1))|\mu$ is thus

$$f(d_1,(d_2 - d_1)) = \frac{1}{2\pi\,\sigma^2\sqrt{t_1(t_2 - t_1)}} \cdot$$

$$\exp\left\{ -\frac{1}{2}\frac{(d_1 - \mu t_1)^2}{\sigma^2 t_1} - \frac{1}{2}\frac{[(d_2 - d_1) - \mu(t_2 - t_1)]^2}{\sigma^2(t_2 - t_1)} \right\}. \qquad (4.5.6)$$

The transformation

$$\begin{bmatrix} D_1 \\ D_2 \end{bmatrix} \rightarrow \begin{bmatrix} D_1 \\ D_2 - D_1 \end{bmatrix}$$

has a Jacobian matrix with determinant 1. It follows that the conditional joint distribution of $(D_1, D_2)|\mu$ is given by the same expression (4.5.6), and that it is a binormal distribution. A binormal distribution may be identified in terms of the five parameters $E(D_i|\mu)$, $Var(D_i|\mu)$, $i = 1,2$, and the correlation coefficient $\rho(D_1,D_2|\mu)$. The first four parameters are given by (4.5.1) as

$$E(D_i|\mu) = \mu t_i, \quad i = 1, 2, \qquad (4.5.7)$$

and

$$Var(D_i|\mu) = \sigma^2 t_i, \quad i = 1, 2. \qquad (4.5.8)$$

The correlation coefficient may be found by rearranging (4.5.6). However, it is more easily found from the general identity

$$Var(D_1 + D_2|\mu) = Var(D_1|\mu) + Var(D_2|\mu) + 2Cov(D_1,D_2|\mu).$$

This gives

$$\begin{aligned}\mathrm{Cov}(D_1,D_2|\mu) &= \tfrac{1}{2}[\mathrm{Var}((D_1 + D_2)|\mu) - \mathrm{Var}(D_1|\mu) - \mathrm{Var}(D_2|\mu)] \\ &= \tfrac{1}{2}[\mathrm{Var}([2D_1 + (D_2 - D_1)]|\mu) - \mathrm{Var}(D_1|\mu) - \mathrm{Var}(D_2|\mu)].\end{aligned}$$

Since D_1 and $D_2 - D_1$ are independent given μ, this becomes:

$$\begin{aligned}\mathrm{Cov}(D_1,D_2|\mu) &= \tfrac{1}{2}[4\mathrm{Var}(D_1|\mu) + \mathrm{Var}((D_2 - D_1)|\mu) \\ &\qquad - \mathrm{Var}(D_1|\mu) - \mathrm{Var}(D_2|\mu)] \\ &= \tfrac{1}{2}[3\mathrm{Var}(D_1|\mu) - \mathrm{Var}(D_2|\mu) + \mathrm{Var}((D_2 - D_1)|\mu)] \\ &= \tfrac{1}{2}[3\sigma^2 t_1 - \sigma^2 t_2 + \sigma^2(t_2 - t_1)] \\ &= \sigma^2 t_1.\end{aligned}$$

The correlation coefficient is

$$\rho(D_1,D_2|\mu) = \frac{\mathrm{Cov}(D_1,D_2|\mu)}{\sqrt{\mathrm{Var}(D_1|\mu)\ \mathrm{Var}(D_2|\mu)}} = \sqrt{t_1/t_2}\ . \tag{4.5.9}$$

Generally, the binormal probability density is given by

$$f_{X_1,X_2}(x_1,x_2) = \frac{1}{2\pi\sigma_1\sigma_2(1-\rho^2)^{1/2}}\cdot$$

$$\cdot\exp\left\{-\frac{1}{2(1-\rho^2)}\left[\frac{(x_1 - \mu_1)^2}{\sigma_1{}^2} - 2\rho\frac{(x_1 - \mu_1)(x_2 - \mu_2)}{\sigma_1\sigma_2} + \frac{(x_2 - \mu_2)^2}{\sigma_2{}^2}\right]\right\}, \tag{4.5.10}$$

where

$$E(X_i) = \mu_i, \quad \mathrm{Var}(X_i) = \sigma_i, \quad i = 1, 2,$$

and

$$\rho = \frac{\mathrm{Cov}(X_1, X_2)}{\sigma_1 \sigma_2}.$$

The conditional distribution for $(D_1, D_2) | \mu$ is found by entering (4.5.7), (4.5.8), and (4.5.9) into (4.5.10). The unconditional distribution of (D_1, D_2) may be found from

$$f(d_1, d_2) = \int_{-\infty}^{\infty} f(d_1, d_2 | \mu)\ f_\mu(\mu)\ d\mu. \tag{4.5.11}$$

By inserting the appropriate expressions into (4.5.11), it is readily seen that it is a binormal density. It is straightforward, but however rather cumbersome, to calculate the parameters in this distribution by working further on (4.5.11). It is easier, and more instructive, to use known results from Bayesian statistics to derive the distribution of D_2 given $D_1 = d_1$.

To summarize our model, μ is a stochastic variable with "prior" distribution given by (4.5.3):

$$\mu \sim N(\theta, \lambda).$$

Given $\mu = \mu$, then D(t) has the distribution given by (4.5.1):

$$D(t) \mid \mu \sim N(\mu t, \sigma^2 t),$$

or, equivalent, D(t)/t given μ has the distribution

$$D(t)/t \mid \mu \sim N(\mu, \sigma^2/t). \tag{4.5.12}$$

The unconditional distribution of D(t)/t is found direct from (4.5.5) as

$$D(t)/t \sim N(\theta, \lambda + \sigma^2/t). \tag{4.5.13}$$

Now, let the observation $D(t_1) = d_1$, or equivalent, $D(t_1)/t_1 = d_1/t_1$, be given. The posterior distribution of μ is found by direct application of

the results Bayesian estimation in the normal distribution with a normal prior on the mean (See e.g. Lehmann, 1983, example 4.1.3):

$$\mu \mid d_1 \sim N(\theta_1, \lambda_1) \tag{4.5.14}$$

where

$$\begin{aligned}\theta_1 &= \frac{(d_1/t_1)/\mathrm{Var}(D_1/t_1) + E(\mu)/\mathrm{Var}(\mu)}{1/\mathrm{Var}(D_1/t_1) + 1/\mathrm{Var}(\mu)} \\ &= \frac{(d_1/t_1)/(\sigma^2/t_1) + \theta/\lambda}{1/(\sigma^2/t_1) + 1/\lambda} \\ &= \frac{1/(\sigma^2/t_1)}{1/(\sigma^2/t_1) + 1/\lambda}\, d_1/t_1 + \frac{1/\lambda}{1/(\sigma^2/t_1) + 1/\lambda}\, \theta \end{aligned} \tag{4.5.15}$$

and

$$\begin{aligned}\lambda_1 &= [1/\mathrm{Var}(D_1/t_1) + 1/\mathrm{Var}(\mu)]^{-1} \\ &= [1/(\sigma^2/t_1) + 1/\lambda]^{-1} \end{aligned} \tag{4.5.16}$$

We shall make two observations at this point:

i) The posterior mean θ_1 is a weighted average between the prior mean θ and the "empirical" mean d_1/t_1.

ii) The posterior variance λ_1 is less than the prior variance λ.

It follows from the basic property (4.3.1) of the Wiener process that given μ, then the distribution of $D(t_2) - D(t_1)$ given $D(t_1) = d_1$ is

$$D(t_2) - d_1 \mid \mu \sim N(\mu(t_2-t_1), \sigma^2(t_2-t_1)) \tag{4.5.17}$$

The posterior distribution of μ given d_1 may now be used as an adjusted prior on $\mu|d_1$:

$$\mu|d_1 \sim N(\theta_1, \lambda_1) \tag{4.5.18}$$

Using (4.5.17) and (4.5.18), it follows from (4.5.5) that given d_1 and unconditionally on μ, then

$$D(t_2) - d_1 \sim N(\theta_1(t_2 - t_1), \lambda_1(t_2 - t_1)^2 + \sigma^2(t_2 - t_1)). \tag{4.5.19}$$

The distribution of D(t), and the distribution of $D(t)|D(t_1)=d_1$ for $t>t_1$, are illustrated in Figure 4.5.1.

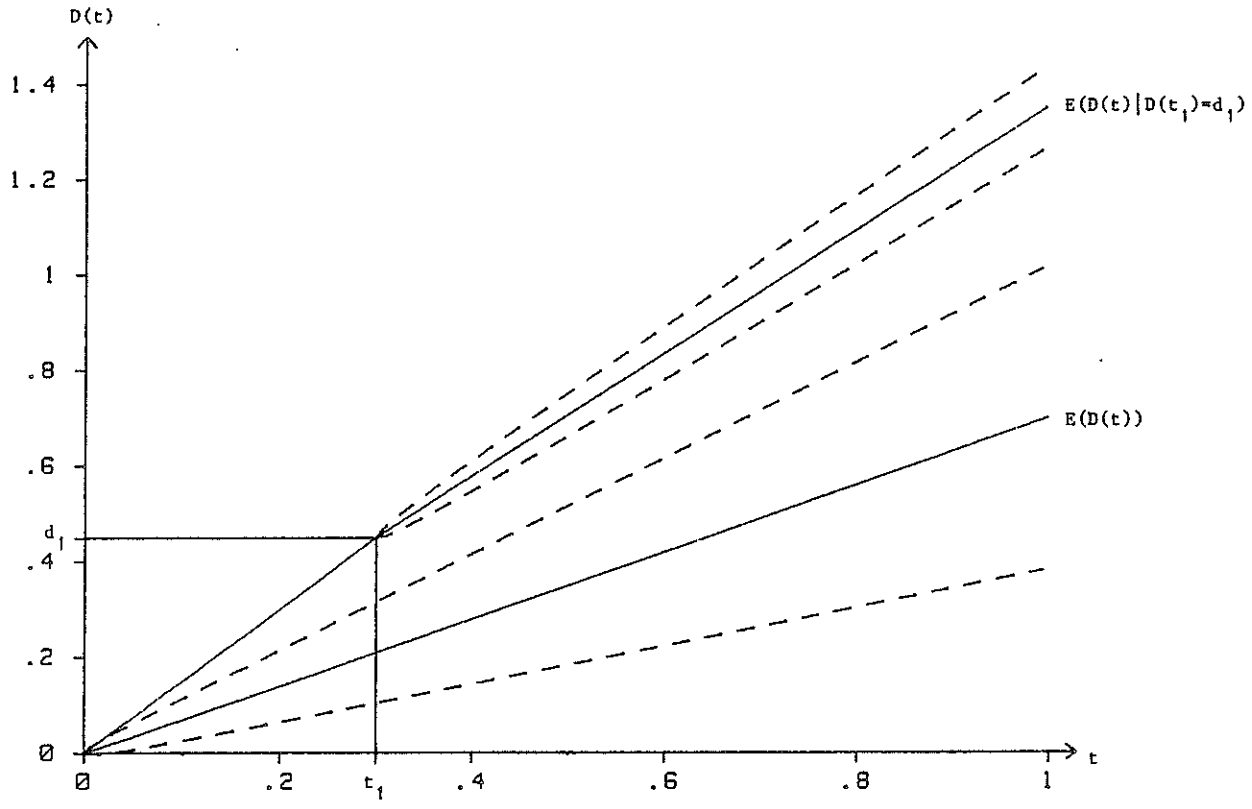

Figure 4.5.1: The distributions for D(t) and $D(t)|D(t_1)=d_1$, illustrated in terms of their expectation (solid line) and expectation ± standard deviation (dotted lines). The illustration is an example with the values θ=0.7, $\sqrt{\lambda}$=0.3, σ=0.1, t_1=0.3, d_1=0.45.

4.6 THE BERNSTEIN DISTRIBUTION AND RELATED MODELS

A general class of wear models discussed by Pieper and Tiedge (1983) and references therein, may be written on the form

$$D(t) = \mu_0 + \mu_1 t^a. \tag{4.6.1}$$

In this expression, $D(t)$ is wear depth at time t, μ_0 is initial wear depth, i.e. $D(0)$, μ_1 is a quantity characterizing wear rate, and $a > 0$ is a parameter. The vector $\underline{\mu} = (\mu_0, \mu_1)'$ is a stochastic vector with one realization per specimen. Conditionally given $\underline{\mu}$, the wear process is assumed to follow the deterministic equation (4.6.1). Failure occurs when $D(t)$ reaches the critical limit d_c. The lifetime distribution is given by

$$\begin{aligned} F_T(t) &= P(T \leq t) \\ &= P(D(t) \geq d_c) \\ &= P(\mu_0 + \mu_1 t^a \geq t) \end{aligned} \tag{4.6.2}$$

Assume, now, that μ_0 and μ_1 are independent and normally distributed. Under these assumptions, Gertsbakh and Kordonsky (1969) have shown that the distribution function is given by

$$F_T(t) = \Phi\left(\frac{\theta_0 + \theta_1 t^a - d_c}{\sqrt{\lambda_0 + \lambda_1 t^{2a}}} \right), \quad -\infty < t < \infty, \tag{4.6.3}$$

where

$$\begin{aligned} \theta_0 &= E(\mu_0), \quad & \lambda_0 &= \mathrm{Var}(\mu_0), \\ \theta_1 &= E(\mu_1), \quad & \lambda_1 &= \mathrm{Var}(\mu_1). \end{aligned}$$

If $a = 1$, the distribution is known as the Bernstein distribution. The Bernstein distribution function is usually referred to in the form (see e.g. Sheikh, Ahmad and Mirza, 1983)

$$F_T(t) = \Phi\left(\frac{t - c}{\sqrt{\alpha t^2 + \beta}} \right), \quad -\infty < t < \infty, \tag{4.6.4}$$

with obvious parameter changes from (4.6.3). When the initial value is zero (i.e. $D(0) = \mu_0 \equiv 0$), the distribution reduces to a two-parameter Bernstein distribution, also known as the alpha distribution. Usually the alpha distribution is truncated at zero, and the distribution function is referred to in the form

$$F_T(t) = \frac{1}{\Phi(1/\sqrt{\alpha})} \Phi\left(\frac{1}{\sqrt{\alpha}} - \frac{c}{\sqrt{\alpha} t} \right), \quad t > 0. \tag{4.6.5}$$

Now, consider a normal distribution with mean θ_1 and variance λ_1 truncated at 0. That is, let U be distributed according to

$$F_U(u) = \frac{1}{\Phi(\theta_1/\sqrt{\lambda_1})} \Phi\left(\frac{t - \theta_1}{\lambda_1} \right), \quad t > 0. \tag{4.6.6}$$

Then, $T = 1/U$ is alpha distributed according to (4.6.5), with $\alpha = \mathrm{Var}(U)/[E(U)^2]$ and $c = 1/E(U)$. Ahmad and Sheikh (1985) refer to (4.6.5) as the "inverted normal distribution". This name can be somewhat misleading, since the alpha distribution does not coincide with the Inverse Gaussian distribution (see equation 4.3.4 in Section 4.3).

If $\sqrt{\alpha} < 0.35$, then $1/\Phi(\theta_1/\sqrt{\lambda_1}) \approx 1$, and the factor $1/\Phi(\theta_1/\sqrt{\lambda_1})$ is often omitted in the distribution function and the probability density.

Estimation methods for the parameters in the alpha distribution are given by Johnson and Kotz (1970), Ahmad and Sheikh (1984), and Salvia (1985). Renewal analysis with the distribution is discussed by Sheikh, Ahmad and Mizra (1983).

The model seems usatisfactory when D(t) is measured for several t values per specimen, since it assumes the behaviour of D(t) given $\underline{\mu}$ to be deterministic. In these cases, the model classes discussed in Sections 4.4 and 4.5 are more adequate. However, the failure probability for the valves treated in part III of this thesis turns out to be similar to (4.6.2) in one of the models discussed (Part II, Section 5.2).

5. ESTIMATION METHODS

5.1 INTRODUCTION

In this chapter, estimation methods within two of the established models are given, the Wiener process/IG model, and the Wiener process with random drift. Methods for regression in the IG model will not be given here, but some results are given by Whitmore (1980, 1983).

The observations are assumed to be of the following type: For each observed specimen, only the failure time, or a censored lifetime with corresponding deteriority d_i, is recorded. A failure time is the (first) time the deteriority reaches the critical value d_c. In the case of a censored lifetime, the lifetime t_i at censoring, and the deteriority d_i at that time, $d_i = D(t_i)$, are recorded.

The probability density functions for the lifetime T and the deteriority D(t) at time t are denoted

$$f_T(t;d_c,\underline{\theta}) = \frac{\partial}{\partial t}P(T \leq t;\underline{\theta}) \tag{5.1.1}$$

and

$$f_D(d;t,\underline{\theta}) = \frac{\partial}{\partial d}P(D(t) \leq d;t,\underline{\theta}), \tag{5.1.2}$$

respectively. Let the observations be labeled such that $t_1, \ldots, t_f$ are failure times, and $(t_{f+1}, d_{f+1}), \ldots, (t_n, d_n)$ are censored lifetimes with corresponding deteriority. Assuming independence between the observations, and given that failure times are recorded for f of the specimens, the joint probability density for the observed outcome may be written

$$f(t_1, \ldots, t_f, t_{f+1}, d_{f+1}, \ldots, t_n, d_n;d_c,\underline{\theta})$$

$$= \left[\prod_{i=1}^{f} f_T(t_i;d_c,\underline{\theta}) \right] \cdot \left[\prod_{i=f+1}^{n} f_D(d_i;t_i,\underline{\theta}) \right]. \tag{5.1.3}$$

In Section 5.2 and 5.3, the likelihood will be based on (5.1.3).

In Part II of the thesis, some estimation methods for the Wiener process with random starting point and drift are studied. This is done using the theory of regression with random coefficients. Further, in Part II, the observations of another type. The deteriority is measured at several points in time on each specimen, also above the critical value d_c which defines failure in the relevant application.

5.2 ESTIMATION IN THE WIENER PROCESS/IG MODEL

Here, we shall consider the situation where a total of n items are tested under identical conditions. For each failed item, the failure time is observed. This is the time when D(t) first reaches d_c, and is assumed to be IG distributed according to (4.3.3). For censored lifetimes, the value of D(t) at the censoring time are observed. According to the definition of the Wiener process in Section 4.3, D(t) is assumed to be normally distributed with mean μt and variance $\sigma^2 t$. The joint probability density for the observations is given by

$$f(t_1, \ldots, t_f, t_{f+1}, d_{f+1}, \ldots, t_n, d_n; \mu, \sigma, d_c)$$

$$= \prod_{i=1}^{f} \frac{d_c}{\sigma\sqrt{2\pi}\, t_i^{3/2}} \exp\left[- \frac{(d_c-\mu t_i)^2}{2\sigma^2 t_i} \right] \cdot$$

$$\prod_{i=f+1}^{n} \frac{1}{\sigma\sqrt{2\pi}} \exp\left[- \frac{(d_i-\mu t_i)^2}{2\sigma^2 t_i} \right] \qquad (5.2.1)$$

where the observations are labelled such that $t_1,\ldots,t_f$ represent failure times, and $t_{f+1},\ldots,t_n$ represent censored lifetimes. The observed values of D(t) at the censoring times are denoted $d_{f+1},\ldots,d_n$, respectively. The probability density (5.2.1) may be written as

$$f(t_1, \ldots, t_f, t_{f+1}, d_{f+1}, \ldots, t_n, d_n; \mu, \sigma, d_c)$$

$$= \frac{{d_c}^f}{(2\pi)^{n/2}\,\sigma^n} \prod_{i=1}^{f} t_i^{-3/2} \cdot$$

$$\exp\left\{ -\left[\frac{1}{2\sigma^2} \sum_{i=1}^{f} \frac{(d_c-\mu t_i)^2}{t_i} + \sum_{i=f+1}^{n} \frac{(d_i-\mu t_i)^2}{t_i} \right]\right\} \qquad (5.2.2)$$

We shall distinguish between two cases:

i) d_c is a known constant.

ii) d_c is a parameter to be estimated.

In both cases, μ and σ are parameters to be estimated.

A parametric family of distributions is said to form an exponential family if the density may be written on the form

$$f(\underline{t};\underline{\theta}) = h(\underline{t}) \exp\left[\sum_{i=1}^{s} \eta_i(\underline{\theta}) \cdot S_i(\underline{t}) - B(\underline{\theta}) \right] \qquad (5.2.3)$$

The statistic $\underline{S} = (S_1, \ldots, S_s)$ is sufficient for estimating the parameters $\underline{\theta}$, see e.g. Lehmann (1983). The density (5.2.2) is easily seen to be an exponential family by writing the exponential function part of it on the form

$$\exp\left\{ -\frac{1}{2\sigma^2} \left[{d_c}^2 \sum_{i=1}^{f} \frac{1}{t_i} + \sum_{i=f+1}^{n} \frac{{d_i}^2}{t_i} - 2f\mu d_c - 2\mu \sum_{i=f+1}^{n} d_i + \mu^2 \sum_{i=1}^{n} t_i \right]\right\}. \qquad (5.2.4)$$

Sufficient statistics are:

Case i):

$$\left(\sum_{i=1}^{n} \frac{d_i^2}{t_i} , \sum_{i=1}^{n} d_i , \sum_{i=1}^{n} t_i \right) \tag{5.2.5}$$

Case ii):

$$\left(\sum_{i=1}^{f} \frac{1}{t_i} , \sum_{i=1}^{n} \frac{d_i^2}{t_i} , \sum_{i=1}^{n} d_i , \sum_{i=1}^{n} t_i \right) \tag{5.2.6}$$

In (5.2.5), the notation $d_i=d_c$ has been used for $i=1,\ldots,f$.

In the following, we shall confine to case i), that is, assume d_c to be a known constant. The log likelihood based on (5.2.2) is readily seen to be

$$L = C - \frac{n}{2} \log(\sigma^2) - \frac{1}{2\sigma^2} \sum_{i=1}^{n} \frac{(d_i-\mu t_i)^2}{t_i} \tag{5.2.7}$$

where the constant C is not a function of the parameters μ and σ. Maximum likelihood estimates (MLE) are found by straightforward calculations, to be

$$\hat{\mu} = \frac{\sum d_i}{\sum t_i} \tag{5.2.8}$$

and

$$\hat{\sigma}^2 = \frac{1}{n} \sum \frac{(d_i-\hat{\mu}t_i)^2}{t_i}$$

$$= \frac{1}{n} \sum \frac{d_i^2}{t_i} - 2\hat{\mu} \frac{1}{n} \sum d_i + \hat{\mu}^2 \frac{1}{n} \sum t_i , \tag{5.2.9}$$

where all sums are taken over $i=1,\ldots,n$.

5.3 ESTIMATION IN THE WIENER PROCESS WITH RANDOM DRIFT

Consider a Wiener process with random drift, that is, the drift parameter μ is a stochastic variable with one realization per specimen. Given μ, then D(t) is a Wiener process with drift μ and infinitesimal variance σ^2. Especially, given μ, then

$$D(t)|\mu \sim N(\mu t, \sigma^2 t). \tag{5.3.1}$$

Let T be the time until D(t) first reaches d_c. As mentioned in Section 4.3, given $\mu > 0$, then T is IG distributed with probability density

$$g(t|\mu) = \frac{d_c}{\sigma\sqrt{2\pi}} \frac{1}{t^{3/2}} \exp\left[- \frac{(d_c-\mu t)^2}{2\sigma^2 t} \right], \quad t > 0. \tag{5.3.2}$$

A mathematically convenient prior distribution for μ is the normal distribution. However, there are cases where estimated parameters in the normal distribution give a non-negligible probability for the impossible event $\mu < 0$ (Part II of the thesis). Here, we shall remedy this problem by using a normal distribution truncated at 0, that is, μ is assumed to have the probability density

$$f_\mu(\mu) = \frac{1}{\Phi(\theta/\sqrt{\lambda})} \frac{1}{\sqrt{2\pi}\sqrt{\lambda}} \exp\left[-\frac{1}{2} \frac{(\mu-\theta)^2}{\lambda} \right], \quad \mu > 0. \tag{5.3.3}$$

The unconditional density of T is given by

$$f_T(t) = \int_0^\infty g(t|\mu)\, f_\mu(\mu)\, d\mu \tag{5.3.4}$$

Inserting (5.3.2) and (5.3.3) into (5.3.4), carrying out the cumbersome, but straightforward integration, yields

$$f_T(t) = \frac{1}{\Phi(\theta/\sqrt{\lambda})} \frac{d_c}{\sqrt{2\pi}\, t^{3/2} \sqrt{\lambda t + \sigma^2}} \exp\left[- \frac{(d_c - \theta t)^2}{2t(\lambda t + \sigma^2)} \right]$$

$$\cdot \Phi\left[\frac{(\lambda d_c + \theta\sigma^2)}{\sqrt{(\lambda t + \sigma^2) 2\sigma^2 \lambda}} \right]. \qquad (5.3.5)$$

Given μ, then the distribution of D(t) is $N(\theta t, \sigma^2 t)$. The unconditional distribution of D(t) is

$$f_{D(t)}(d) = \int_0^\infty f_{D(t)|\mu}(d|\mu)\, f_\mu(\mu)\, d\mu \qquad (5.3.6)$$

Inserting the $N(\theta t, \sigma^2 t)$ probability density and (5.3.3) into (5.3.6) yields

$$f_{D(t)}(d) = \frac{1}{\Phi(\theta/\sqrt{\lambda})} \frac{1}{\sqrt{2\pi}\sqrt{t(\lambda t + \sigma^2)}} \exp\left[- \frac{(d - \theta t)^2}{2t(\lambda t + \sigma^2)} \right]$$

$$\cdot \Phi\left[\frac{(\lambda d + \theta\sigma^2)}{\sqrt{(\lambda t + \sigma^2) 2\sigma^2 \lambda}} \right]. \qquad (5.3.7)$$

The joint probability density for the observations is given by

$$f(t_1, \ldots, t_f, t_{f+1}, d_{f+1}, \ldots, t_n, d_n; \theta, \lambda, \sigma, d_c)$$

$$= \prod_{i=1}^{f} \frac{1}{\Phi(y_0)} \frac{d_c}{\sqrt{2\pi}\, t_i^{3/2} \sqrt{\lambda t_i + \sigma^2}} \exp\left[- \frac{(d_c - \theta t_i)^2}{2\sigma^2 t_i} \right] \Phi(y_i)$$

$$\cdot \prod_{i=f+1}^{n} \frac{1}{\Phi(y_0)} \frac{d_c}{\sqrt{2\pi}\, \sqrt{t_i(\lambda t_i + \sigma^2)}} \exp\left[- \frac{(d_c - \theta t_i)^2}{2\sigma^2 t_i} \right] \Phi(y_i)$$

$$= \Phi(y_0)^{-n} d_c^{f} (2\pi)^{-n/2} \left[\prod_{i=1}^{f} \frac{1}{t_i} \right]$$

$$\cdot \prod_{i=f+1}^{n} \frac{1}{\sqrt{t_i(\lambda t_i + \sigma^2)}} \exp\left[- \frac{(d_c - \theta t_i)^2}{2\sigma^2 t_i} \right] \Phi(y_i), \qquad (5.3.8)$$

where

$$y_0 = \theta/\sqrt{\lambda}, \qquad (5.3.9)$$

and

$$y_i = \frac{\lambda d_i + \theta\sigma^2}{(\lambda t_i + \sigma^2) 2\sigma^2 \lambda}, \quad i = 1, 2, \ldots, n. \qquad (5.3.10)$$

As in Section 5.2, the observations are labelled such that $t_1, \ldots, t_f$ represent failure times, and $t_{f+1}, \ldots, t_n$ represent censored lifetimes. The observed values of D(t) at the censor times are denoted $d_{f+1}, \ldots, d_n$, respectively, and the notation $d_c = d_i$ for $i = f+1, \ldots, n$ has been used.

As is the preceding section, we shall confine to the case where d_c is assumed to be a known constant. The log likelihood based on (5.3.8) is readily seen to be

$$L = C - \frac{1}{2}\Sigma \log(\lambda t_i + \sigma^2) - \frac{1}{2}\Sigma \frac{(d_i - \theta t_i)^2}{t_i(\lambda t_i + \sigma^2)} - n \log \Phi(\theta/\sqrt{\lambda}) + \Sigma \log \Phi(y_i) \tag{5.3.11}$$

where the constant C is not a function of the parameters θ, λ, and σ^2, y_i is given by (5.3.10), and all the sums are taken over $i = 1, 2, \ldots, n$.

If $y_0 = \theta/\sqrt{\lambda}$ is large enough, then $\Phi(y_0)$ is close enough to 1 to be neglected. For example, $y_0 \geq 3$ implies

$$0.9987 \leq \Phi(y_0) < 1.$$

In these cases, the values of y_i are usually also large enough to make $\Phi(y_i)$ near enough 1 to be neglected. Note, however, that if t_i is large and d_i is small, this needs not be the case. Hence, care must be taken if at least one of the pairs (t_i, d_i) contains relatively large and small values, respectively. We shall find approximate equations for the MLE by setting these Φ-functions equal to 1. In practice, the estimates obtained this way should be inserted in the appropriate expressions to check whether they really are approximately 1. The approximate log likelihood obtained by setting these Φ-functions equal to 1, is

$$L = C - \frac{1}{2}\Sigma \log(\lambda t_i + \sigma^2) - \frac{1}{2}\Sigma \frac{(d_i - \theta t_i)^2}{t_i(\lambda t_i + \sigma^2)}. \tag{5.3.12}$$

The derivatives of L in (5.3.12) with respect to the parameters are:

$$\frac{\partial L}{\partial \theta} = \Sigma \frac{d_i}{\lambda t_i + \sigma^2} - \theta \Sigma \frac{t_i}{\lambda t_i + \sigma^2}, \tag{5.3.13}$$

$$\frac{\partial L}{\partial \lambda} = -\frac{1}{2} \Sigma \frac{t_i}{\lambda t_i + \sigma^2} + \frac{1}{2} \Sigma \frac{(d_i - \theta t_i)^2}{(\lambda t_i + \sigma^2)^2}, \tag{5.3.14}$$

$$\frac{\partial L}{\partial (\sigma^2)} = -\frac{1}{2} \Sigma \frac{1}{\lambda t_i + \sigma^2} + \frac{1}{2} \Sigma \frac{(d_i - \theta t_i)^2}{t_i (\lambda t_i + \sigma^2)^2}. \tag{5.3.15}$$

The MLE may be found by setting (5.3.13), (5.3.14), and (5.3.15) equal to 0. However, these equations cannot be solved analytically for any of the parameters. Numerical methods must used to find the MLE if a data set is given. We shall not go any further on this matter here, except for noting that the first equation yields

$$\hat{\theta} = \frac{\Sigma \dfrac{d_i}{\hat{\lambda} t_i + \hat{\sigma}^2}}{\Sigma \dfrac{t_i}{\hat{\lambda} t_i + \hat{\sigma}^2}}, \tag{5.3.16}$$

where $\hat{\lambda}$ and $\hat{\sigma}^2$ are the MLE for λ and σ^2, respectively. The estimator for θ may, thus, be written as a weighted average of the "empirical slopes" d_i/t_i per specimen:

$$\hat{\theta} = \frac{\Sigma v_i (d_i/t_i)}{\Sigma v_i} \tag{5.3.17}$$

where

$$v_i = \frac{t_i}{\hat{\lambda} t_i + \hat{\sigma}^2}, \quad i = 1, 2, \ldots, n.$$

For the limiting case when $\sigma^2 \to 0$, all the weights v_i are equal, and the expression (5.3.17) reduces to

$$\hat{\theta} = \frac{1}{n}\Sigma(d_i/t_i). \tag{5.3.18}$$

In the limiting case when $\lambda \to 0$, or if all t_i's are equal, the expression (5.3.17) reduces to

$$\hat{\theta} = \frac{\Sigma d_i}{\Sigma t_i}, \tag{5.3.19}$$

which is identical to the MLE for μ in the Wiener process/IG model (Section 5.2, equation 5.2.8). This is natural, since the model reduces to the Wiener process/IG model if $\lambda \to 0$.

If the t_i's are not equal, which they need to be if it shall be possible to estimate both λ and $\sigma 2$, most weight in (5.3.17) is assigned to the data with highest t_i. This is natural, since the data with higher t_i contain more information on the unobservable μ_i than the data with shorter t_i.

REFERENCES

Abramowitz, M. & Stegun, I. A.: (1965) "Handbook of Mathematical Functions". Dover Publications, New York.

Ahmad, M. & Sheikh, A. K.: "Bernstein Reliability Model: Derivation and Estimation of Parameters". Reliability Engineering, Vol 8, 1984, pp 131-138.

Ahmad, M. & Sheikh, A. K.: (1985) "Accelerated Life Testing". Res Mechanica, Vol 15, 1985, pp 155 - 175.

Amster, S. J. & Hooper, J. H.: (1986) "Statistical Methods for Reliability Improvement". AT & T Technical Journal, Vol 66, No 2, March/April 1986..

Andersen, P. K. & Borgan, Ø.: (1984) "Counting Process Models for Life History Data". Invited lecture at the 10th Nordic Conference on Mathematical Statistics, Bolkesjø, Norway, 17 - 21 June 1984.

Bardal, E.: (1985) "Korrosjon og Korrosjonsvern" (Corrosion and Corrosion Protection. In Norwegian). Tapir, Trondheim.

Barndorff-Nielsen, O., Blæsid, P., & Halgreen, C.: (1978) "First Hitting Time Models for the Generalized Inverse Gaussian Distribution". Stochastic Processes and their Applications, Vol 7, pp. 49 - 54.

Barry, D. M., Chrysanthou, C., & Weir, N. A.: (1986) "Failure Pattern Determination using Wet-Chemical Decapsulation and Statistical Reliability Modelling". Reliability Engineering, Vol 15, 1986, pp 283 - 298.

Barry, D. M., Meniconi, M., & Weir, M. A.: (1987) "Reliability Modelling of Dynamic Random Access Memory Devices Subjected to High Temperature Soak Tests". Reliability Engineering, Vol 17, 1987, pp 255 - 266.

Birnbaum, Z. W. & Saunders, S. C.: (1969) "A new Family of Life Distributions". Journal of Appl. Prob., Vol. 6, pp 319 - 327.

Bhattacharyya, G. K. & Fries, A.: (1982) "Fatigue Failure Models - Birnbaum-Saunders vs. Inverse Gaussian". IEEE Transactions on Reliability, Vol R-31, No 5, December 1982.

Bogdanoff, J. L. & Kozin, F.: (1985) "Probabilistic Models of Cumulative Damage". Wiley, New York.

Cox, D. R.: (1972) "Regression Models and Life-Tables (with discussion)". J. R. Stat. Soc. B. 34, pp 187 - 220.

Cox, D. R. & Miller, H. D.: (1965) "The Theory of Stochastic Processes". Chapman and Hall, London.

Cox, D. R. & Oakes, D.: (1984) "Analysis of Survival Data". Chapman and Hall, London.

Cohen, H. M., LuValle, M. J., Mitchell, P., & Sproles, E. S. Jr.: (1987) "Reliability Evaluation of Interconnection Products". AT&T Technical Journal, Vol 66, No 4, July/August 1987, pp 70 - 80.

Desmond, A. F.: (1987) "On the Relationship between two Fatigue-Life Models". IEEE Transaction on Reliability, Vol R-35, No 2, June 1986, pp 167 - 169.

Ditlevsen, O.: (1986) "Random Fatigue Crack Growth - a First Passage Problem". Engineering Fracture Mechanics, Vol 23, No 2, 1986, pp 467-477.

Ditlevsen, O. & Olesen, R.: (1986) "Statistical Analysis of the Virkler Data on Fatigue Crack Growth". Engineering Fracture Mechanics, Vol 25, No 2, 1986, pp 177 - 195.

Fontana, M. G. & Green, N. D.: (1967) "Corrosion Engineering", McGraw Hill.

Fuchs, H. O. & Stephens, R. I.: (1980) "Metal Fatigue in Engineering". Wiley, New York.

Gertsbakh, I. B. & Kordonsky, K. B.: (1969) "Models of Failure". Springer-Verlag, New York.

Giglmayr, J.: (1987) "An Age-Wear Dependent Model of Failure". IEEE Transactions on Reliability, Vol R-36, No 5, December 1987.

Hudak, S. J. Jr, Saxena, A., Bucci, R. J., & Malcolm, R. C.: (1978) "Development of Standard Methods of Testing and Analyzing Fatigue Crack Growth Rate Data". AFML-TR-78-40.

Haagensen, P. J.: (1973) "Kumulativ utmatting i metalliske materialer" (Fatigue Failure in Metallic Materials. In Norwegian). SINTEF Report, 1973.

Iuculano, G. & Zanini, A.: (1986) "Evaluation of Failure Models through Step-stress Tests". IEEE Transactions on Reliability, Vol R-35, No 4, October 1986, pp 409 - 413.

Iyengar, S.: (1985) "Hitting Lines with two-dimensional Brownian Motion". SIAM J. Appl. Math., Vol 45, No 6, December 1985, pp 983 - 989.

Johnson, N. L. & Kotz, S.: (1970) "Continuous Univariate Distributions-1". Houghton Mifflin, New York.

Kielland, G. G., Lydersen, S., Onsøyen, E., & Slind, T.: (1985) "Subsea Control Valves: Accelerated Life Testing. Phase I - Final Report". SINTEF Report STF18 F85507 (Restricted).

Knezevic, J.: (1987) "Condition Parameter Based Approach to Calculation of Reliability Characteristics". Reliability Engineering, Vol 19, 1987, pp 29 - 39.

Lehmann, E. L.: (1983) "Theory of Point Estimation". Wiley, New York.

Lemoine, A. J. & Wenocur, M. L.: (1985) "On Failure Modelling". Naval Research Logistics Quarterly, Vol 32, pp 497 - 508.

Lemoine, A. J. & Wenocur, M. L.: (1986) "A note on shot-noise and reliability modelling". Operations Research, 1986.

Lydersen, S.: (1986) "Accelerated Life Testing". SINTEF Report STF75 A86010.

Lydersen, S., Onsøyen, E., Renolen, P. & Slind, T.: (1986) "Subsea Control Valves. Accelerated Testing. Phase II." SINTEF Report STF18 F86036 (Restricted).

Lydersen, S., Sæther, F., & Ørjasæter, O.: (1987) "Accelerated Life Testing of Pilot Valves" SINTEF Report STF18 F87040 (Restricted).

Lydersen, S. & Rausand, M.: (1987) "A systematic Approach to Accelerated Life Testing". Reliability Engineering, Vol 18, 1987, pp 285 - 293.

Maskalick, H. J.: (1975) "Accelerated Life Testing of Lead-Acid Motive Power Cells". J. Electrochem. Soc., Vol 122, No 1, 1975, pp 19 - 25.

Narbuvoll, H.: (1987) "Regresjonsmodeller med stokastiske koeffisienter for analyse av sprekkvekst i stål" (Regression Models with Stochastic Coefficients for Analysis of Fatigue Crack Growth in Steel. In Norwegian). M.Sc. thesis at NTH, Department of Mathematical Statistics.

Nelson, W.: (1981) "Analysis of Performance-Degradation Data from Accelerated Tests". IEEE Transactions on Reliability, Vol R-30, No 2, June 1981, pp 149 - 155.

Newby, M. J.: (1987a) "Markov Models for Fatigue Crack Growth". Engineering Fracture Mechanics, Vol 27, No 4, 1987, pp 477 - 482.

Newby, M. J.: (1987b) "Comments on Fatigue Crack Growth Models". Reliability Engineering, Vol 18, 1987, pp 57 - 60.

Newby, M. J.: (1988) "Accelerated Failure Time Models for Reliability Data Analysis". Reliability Engineering and System Safety, Vol 20, 1988, pp 187-197.

Oritz, K.: (1986) "Time Series Analysis of Fatigue Crack Growth Data". Engineering Fracture Mechanics, Vol 24, No 5, 1986, pp 657 - 675.

Paris, P. C. & Erdogan, F.: (1963) "A Critical Analysis of Crack Propagation Laws". Trans. ASME, J. Basic Eng., Vol 85, No 4, 1963, p 528.

Peng, S. T. J.: (1985) "Constitutive Equations of Ageing Polymeric Materials". Journal of Materials Science, Vol 20, pp. 1920 - 1928.

Pieper, V. & Tiedge, J.: (1983) "Zuverlässigkeitsmodelle auf der Grundlage stochastischer Modelle von Verschleissprozessen" (Reliability Models Based on Stochastic Models for Wear Processes. In German). Math. Operationsforschung und Statistik, Ser. Statist., Berlin, Vol 14, No 3, pp 485 - 502.

Rausand, M., Lippe, J., Lydersen, S., Ulleberg, T., & Ørjasæter, O.: (1985) "Reliability of Subsea Gate Valves - Phase I". SINTEF Report STF18 F85506 (Restricted).

Renolen, P.: (1975) "Varmealdring av plastmaterialer" (Heat Ageing of Plastic Material. In Norwegian). SINTEF Report STF21 A75027.

Renolen, P.: (1979) "Varmealdring av byggfolie" (Heat Ageing of Building Foil. In Norwegian). SINTEF Report STF16 F79052 (Restricted).

Salvia, A. A.: "Reliability Application of the Alpha Distribution". IEEE Transactions on Reliability, Vol R-34, No 3, August 1985, pp 251 - 252.

Saunders, S. C.: (1975) "A Synthesis of Crack Growth Theories in Fatigue into some Statistical Distributions of Fatigue Life". Aerospace Research Laboratories (AFSC), Wright Patterson Air Force Base, Ohio, June 1975.

Sheikh, A. K., Ahmad, M., & Mirsa, T. S.: "Renewal Analysis Using Bernstein Distribution". Reliability Engineering, Vol 5, 1983, pp 1 - 19.

Shuster, J. J.: (1968) "On the Inverse Gaussian Distribution Function". J. Amer. Statist. Assoc., 63, 1514 - 1516.

Sobczyk, K.: (1986) "Modelling of Random Fatigue Crack Growth". Engineering Fracture Mechanics, Vol 24, No 4, 1986, pp 609 - 623.

Solomon, P. J.: (1984) "Effect of Misspecification of Regression Models in the Analysis of Survival Data". Biometrica, Vol 71, No 2, pp 291-298.

Spjøtvoll, E.: (1977) "Random Coefficients Regression Models". A Review. Math. Operationsforsch. Statist., Ser. Statistics, Vol 8 (1977), No 1, pp 69 - 93.

Treseder, R. S.: (1980) NACE Corrosion Engineer's Reference Book, National Association of Corrosion Engineers.

Valanis, K. C. & Peng, S.T.J.: (1982) "Deformation Kinetics of Ageing Materials". Polymer, Vol 24, pp. 1551 - 1557.

Virkler, D. A., Hillberry, B. M., & Goel, P. K.: (1979) "The Statistical Nature of Fatigue Crack Propagation". Transactions of the ASME, Vol 101, April 1979, pp 148 - 153.

Whitmore, G. A.: (1980) "An Exact Multiple Regression Method for Inverse Gaussian Data". Submitted for publication.

Whitmore, G. A.: (1983) "A Regression Method for Censored Inverse-Gaussian Data". The Canadian Journal of Statistics, Vol 11, No 4, pp. 305 - 315.

Øksendal, B.: "Stochastic Differential Equations. An Introduction with Applications." Springer-Verlag, Berlin Heidelberg, 1985.

Ørjasæter, O., Grøvlen, M., & Sæther, F.: (1985) "Scatter in Fatigue Crack Growth Data of C-MN Steel". SINTEF Report STF18 A85091.

Ørjasæter, O., Thuestad, L., Renolen, P., Grøvlen, M., Lydersen, S., & Holand, P.: (1986) "Reliability of Subsea Gate Valves. Phase II". SINTEF Report STF18 F86002 (Restricted).

Ørjasæter, O., Lydersen, S., Renolen, P., Bønå, L., Muri, T., & Edwards, J.: (1987) "Reliability of Subsea Gate Valves. Phase III". SINTEF Report STF18 F87031 (Restricted).

Ørjasæter, O., Lydersen, S., Renolen, P., & Rausand, M.: (1988) "Reliability of Subsea Gate Valves". SINTEF Report STF18 F88024 (Restricted).

STIAN LYDERSEN

RELIABILITY TESTING BASED ON DETERIORATION MEASUREMENTS
PART II: DETERIORATION OF HYDRAULIC CONTROL VALVES

DOKTOR INGENIØRAVHANDLING 1988:32
NTH, INSTITUTT FOR MATEMATISKE FAG
TRONDHEIM 1988

ABSTRACT

In an accelerated life testing (ALT) of solenoid operated, hydraulic control valves, leakage through the valves as function of operational cycles was measured. The results are analyzed in this report.

The expected leakage through valve number j at time t is modelled as $E(D_j(t)|\underline{\mu}) = \mu_0 + \mu_1 t$, *where* $\underline{\mu}$ *is considered as a stochastic vector with one realization per specimen. Two alternative models are applied, a linear regression model with random coefficients, and a Wiener process with random starting point and drift. Valve reliability has been estimated in terms of failure probability, and in terms of the probability distribution for* $D(t)$. *The two models are compared both in general, and with respect to the particular data on valve leakage.*

Acceptance testing of valves may be performed as follows: Measure the leakage through new valves, after they have gone through a number of cycles. Valves with good enough predicted future reliability are taken into use, the rest are discharged. A class of linear acceptance criteria for this situation has been derived, as well as a more general procedure for determining the approximately best among linear criteria.

Contents of Part II

SUMMARY AND CONCLUSIONS

Accelerated life testing (ALT) of solenoid operated, hydraulic control valves was carried out at SINTEF, Division of Machine Design in 1985-1986. This was performed as part of the NTNF-sponsored SERA project and two projects sponsored by industry. In one of the test series, leakage through the valves in closed position was measured as function of the number of operational cycles. This test series included 5 valves, using particle contamination level ISO 19/16 in the hydraulic fluid. This is just above working conditions for "coarse hydraulic equipment". The purpose of the test series was to study wear deterioration. A description of the test programme is given in Chapter 1.

The laboratory test results are given in Chapter 2. The measurements are shown graphically in Figure 1. Unfortunately, no repeated measurements were performed on the same valve at the same points in time. According to the laboratory personnel who carried out the measurements, the accuracy is of the size of order ± 1 ml/min.

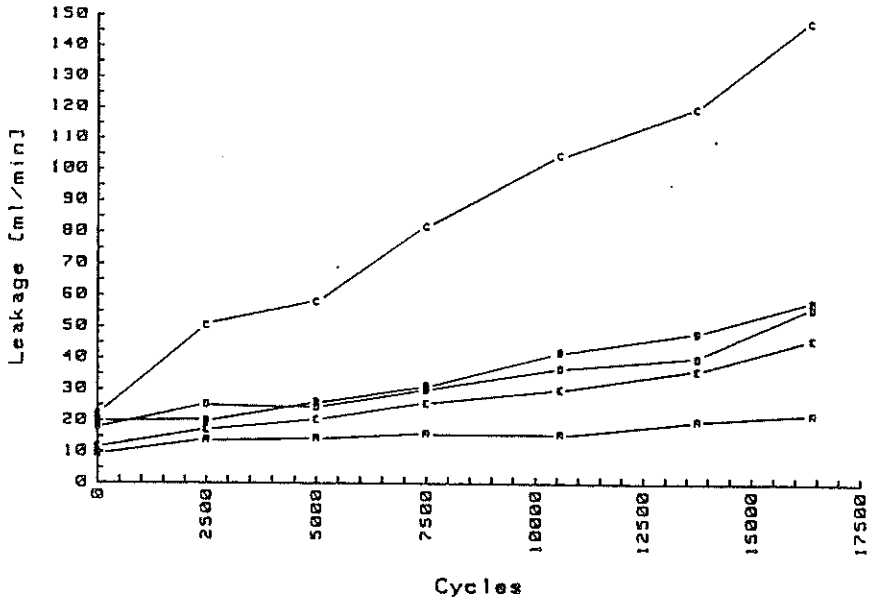

Figure 1: Leakage through the valves in closed positions for the 5 valves A - E, as function of time (number of valve cycles).

The measurements for each valve lie near a straight line. Let D_{ij} denote the i-th leakage measurement, on valve number j, taken at time t_{ij}. The following model was used for the expectation of D_{ij}:

$$E(D_{ij}) = \mu_{0j} + \mu_{1j}t_{ij}. \tag{1}$$

The coefficients $\underline{\mu}_j = (\mu_{0j}, \mu_{1j})'$ clearly seem to have different values for each valve. This has been confirmed by studying confidence regions for the parameters $\underline{\mu}_j$, j = 1, ..., 5. We consider these 5 sets of coefficients as realizations of a stochastic vector $\underline{\mu}$.

Two models have been fitted to the valve leakage measurements. Model 1 is a random coefficient regression model

$$D_{ij} = \mu_{0j} + \mu_{1j}t_{ij} + e_{ij}, \tag{2}$$

with the error terms e_{ij} independent, normally distributed with mean 0 and variance σ^2.

Model 2 is a Wiener process with random starting point μ_{0j}, and random drift μ_{1j}, and infinitesimal variance σ^2. This implies that, conditionally given $\underline{\mu}_j = (\mu_{0j}, \mu_{1j})$, the distribution of $D_{ij} - (\mu_{0j} + \mu_{1j}t_{ij})$ is assumed normal with mean 0 and variance $\sigma^2 t_{ij}$.

Both the "true leakages" and some measurement error contribute to the measured values D_{ij}:

$$D_{ij} = \text{"true leakage"} + \text{measurement error} \tag{3}$$

It would seem plausible to assume Model 2 for "true leakage", and assume the measurement errors as independent, identically distributed with mean 0. However, we have not entered the problem of splitting up the measured values D_{ij} into the two components (3). Model 1 or Model 2 are simply regarded as models of the measured values D_{ij}. Both models seem to agree with the data, Model 1 somewhat better than Model 2. The models are defined in more detail in Chapter 3.

In Chapter 4, estimators for the parameters are derived. In both models, the mean and variance-covariance matrix of $\underline{\mu} = (\mu_0, \mu_1)'$ are denoted

$$E(\underline{\mu}) = \underline{\theta} = \begin{bmatrix} \theta_0 \\ \theta_1 \end{bmatrix} \tag{4}$$

and

$$V(\underline{\mu}) = \Lambda = \begin{bmatrix} \lambda_{00} & \lambda_{01} \\ \lambda_{10} & \lambda_{11} \end{bmatrix} \tag{5}$$

where $\lambda_{10} = \lambda_{01}$. If $\underline{\mu}$ is assumed binormally distributed, uniformly minimum variance unbiased (UMVU) estimators $\hat{\underline{\theta}}$, $\hat{\Lambda}$, and $\hat{\sigma}^2$ are found in the literature (see e.g. Spjøtvoll, 1977). In Model 2, the data were transformed, in order to obtain the conditionally independent, homoscedastic observations required for these UMVU estimators. Parameters estimates obtained for the valve leakage data using these assumptions and estimators, gave a probability $P(\mu_{1j} < 0)$ too high to be negligible. The events $\mu_{0j} < 0$ and $\mu_{1j} < 0$ are considered as physically impossible. To obtain a model agreeing better with the physical processes taking place, $(\log(\mu_{0j}), \log(\mu_{1j}))$ was assumed to be binormally distributed with

$$E\begin{bmatrix} \log(\mu_0) \\ \log(\mu_1) \end{bmatrix} = \begin{bmatrix} \nu_0 \\ \nu_1 \end{bmatrix} \tag{6}$$

and

$$V\begin{bmatrix} \log(\mu_0) \\ \log(\mu_1) \end{bmatrix} = \begin{bmatrix} \tau_{00} & \tau_{01} \\ \tau_{01} & \tau_{11} \end{bmatrix}. \tag{7}$$

Under these assumptions, the entries in the expectation and variance-covariance matrix of $\underline{\mu}$ are:

$$\theta_i = E(\mu_i) = \exp(\nu_i + \frac{1}{2}\tau_{ii}), \qquad i = 0, 1, \tag{8}$$

$$\lambda_{ii} = \mathrm{Var}(\mu_i) = \exp(2\nu_i)[\exp(2\tau_{ii}) - \exp(\tau_{ii})],\ i = 0,\ 1, \qquad (9)$$

$$\lambda_{01} = \exp(\nu_0 + \nu_1 + \tfrac{1}{2}\tau_{00} + \tfrac{1}{2}\tau_{11})\ [\exp(\tau_{01}) - 1]. \qquad (10)$$

Estimators for the parameters in (6) and (7) were obtained by solving (8) to (10) for ν_0, ν_1, τ_{00}, τ_{11}, τ_{01} in terms of $\underline{\theta}$, Λ, and inserting the UMVU estimators $\hat{\underline{\theta}}$ and $\hat{\Lambda}$.

The reliability of this type of valve, with respect to the failure mode "leakage through the valve in closed position", has been estimated for the given conditions in Chapter 5. Reliability has been estimated in terms of two quantities:

- The time to failure distribution, where failure is defined to be the time when the leakage exceeds some critical value d_c. In this report, estimation has been carried out for $d_c = 100$ ml/min to illustrate the procedure. Actually, the tolerance limit d_c depends on the application of the valve.

- The leakage distribution at time t. In this report, the expectation and variance of this distribution has been studied as function of t. The most interesting point in time is when the valve is expected to be most worn. This is at the end of the planned working life of the valve, time t_{max}. The value of t_{max} depends on the application. The leakage distribution has been studied in more detail for the value $t_{max} = 13908$ cycles.

With the estimated parameter values, a very close approximation to the distribution of time to failure, T, was found for Model 1:

$$P(T \le t) \approx 1 - \Phi\left(\frac{\log(d_c) - [\log(a) - \frac{1}{2}\log(b^2/a^2 + 1)]}{\sqrt{\log(b^2/a^2 + 1)}}\right), \qquad (11)$$

where

$$a = E(D(t)) = \theta_0 + \theta_1 t$$

and

$$b^2 = \mathrm{Var}(D(t)) = \lambda_{00} + 2t\lambda_{01} + t^2\lambda_{11} + \sigma^2.$$

Similar approximations may be found for the time to failure distribution using Model 2. This has not been carried out in detail in this report.

In Chapter 6, the obtained results were used to study acceptance testing with respect to leakage deterioration. Such acceptance testing may be performed in alternative ways, such as:

i) Measure the leakage through the new valves, $D(0)$. Discharge the valves with initial leakage above a given limit.

ii) Measure the leakage through new valves, $D(0)$, and after a given number of cycles, $D(t_1)$. Discharge the valves with lowest predicted future reliability.

iii) As alternative ii), but in addition with measurements at one or more intermediate points in time between 0 and t_1.

In alternative i), the obvious acceptance criterion is $D(0) \leq k$, determined by the critical value k. For alternative ii) and iii), an acceptance criterion may be written on the form

$$f(D(0), \ldots, D(t_1)) \leq k, \tag{12}$$

and is determined by the function f and the critical value k. An acceptance criterion is said to be linear if the function f is linear in $D(0), \ldots, D(t_1)$. The class of linear acceptance criteria for alternative ii) is derived in Section 6.2, and may be written on the form

$$aD(0) + D(t_1) \leq k, \qquad -1 < a < 1. \tag{13}$$

The values of a and k determine the proportion of the valves that will be accepted, and the relative weight to put on $D(0)$ and $D(t_1)$.

In Section 6.3, a general procedure for determining the weights in linear acceptance criteria for case ii) and iii) has been developed. It is partly based on results from multivariate normal distribution theory.

This procedure has been investigated, using estimated parameters from Model 1. Comparisons with Monte Carlo simulated distribution of $\underline{D}$ in Model 1 indicated that the obtained acceptance criterion was very close to optimal, even though the distribution of $\underline{D}$ was far from multinormal.

One word of precaution is appropriate here: The observations D(t) at time $t = 0$ seem to agree slightly less with the models than D(t) for $t > 0$. This is quite plausible, since mechanical components often have a burn-in phase with different performance than the rest of their life. In general, one ought to use an acceptance criterion with less weight on D(0), than the weight obtained with the procedure based on the model.

1. INTRODUCTION

1.1 BACKGROUND

As part of the SERA project, accelerated life testing (ALT) of solenoid operated, hydraulic control valves was carried out at SINTEF, Division of Machine Design in 1986. More extensive ALT of the same type of valves was carried out later in 1986 and 1987 on a contract for an oil company. These tests, with results, are described in Kielland & al (1986) and Lydersen & al (1987).

In this report, the leakage measurements from one of the test series performed in the SERA project are analyzed according to the ideas presented in Part I of the thesis.

The rest of the introductory chapter describes the test specimen and the test programme.

1.2 OBJECTIVES OF THE TEST PROGRAMME

The main objective of the test programmes was to extend knowledge on ALT and modelling. There seemed to be a lack of knowledge both concerning modelling of failure mechanisms, and how to carry out the practical testing. To obtain data on ALT on mechanical components and to get a practical example, it was decided to perform a series of laboratory accelerated life tests on mechanical components.

Directional control valves are critical parts of all subsea control systems used with offshore petroleum exploration and production. As a consequence, ALT of such components seem to have increasing importance in the years to come.

Directional control valves especially made for subsea application are very expensive. It was decided to perform testing on ordinary directional control valves used in onshore industries. This choice of component was due to:

- The chosen valves are similar to the valves used in subsea oil and gas production sites.

- Limited knowledge was available on the complex and interacting deterioration mechanisms present in such components.

- The experience gained in this project would be useful in other on-going and future industry sponsored projects.

- Operational experience with such valves indicated that failures are anticipated to occur during a reasonable test time.

- The chosen component was cheap enough to allow a reasonable number of valves to be tested within limited budgets.

1.3 DESCRIPTION OF VALVES

This section gives a description of the selected hydraulic control valve. A general description of hydraulic control valves used in subsea control systems is also given.

The Tested Valve Type

A valve type was selected for testing according to these conditions:

- The valve type is similar to valves used in subsea control systems.

- The valve type is ordinary stock line.

- The valve is so cheap that a large number of valves may be tested.

- It is possible to test other types of valves without re-building the test rig.

The selected valve make/type was Parker D 1 VW. This is a solenoid operated, 4-way 2-position hydraulic directional control valve. Here, the valve is described as it was used in the test. There are also alternative applications of the valve.

Figure 1.3.1 shows the hydraulic symbol for a 4-way 2-position hydraulic directional control valve. Hydraulic component symbols may be studied in ISO standard 1219-1976 and in Norsk Standard 1422. The valve has 4 ports:

P = Pressure port
R = Return port
A and B = Function ports

During the test programme, port A was plugged.

The two rectangles of Figure 1.3.1 show the two possible positions of the valve. The right rectangle represents the "closed" position of the valve. In this position, there is a passage from P to A and from B to R.

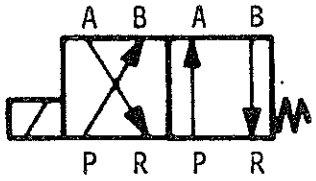

Figure 1.3.1. 4-way, 2-position directional solenoid valve

If hydraulic pressure is present on the B-port of the valve, the pressure will be bled off when the valve is in the "closed" position. Port A is plugged. This means that even though there is a passage from P

to A, the pressure port P is closed in this position. The function of the valve in "closed" position is illustrated in Figure 1.3.2.

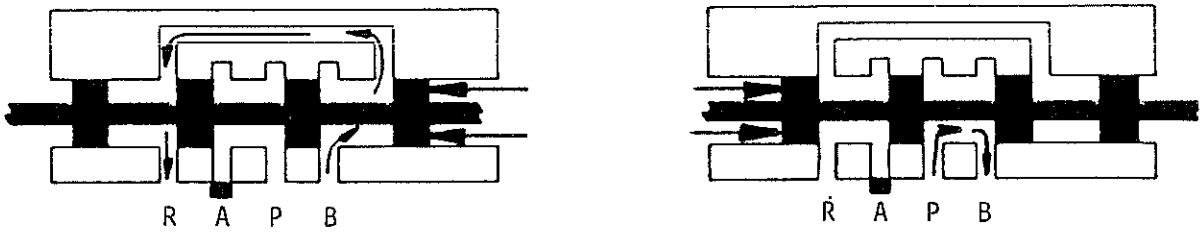

"closed" "open"

Figure 1.3.2. The valve in "closed" and "open" position.

In "open" position, represented by the left rectangle in Figure 1.3.1, the passage from P to B is open. The passage from A to R is also open, but since A is plugged, R is virtually closed. The function of the valve in "open" position is illustrated in Figure 1.3.2.

The valve is operated by electric signals. The sealing principle is a piston with O-rings. The piston is operated by the solenoid. The Parker D 1 VW valve is shown in Figure 1.3.3.

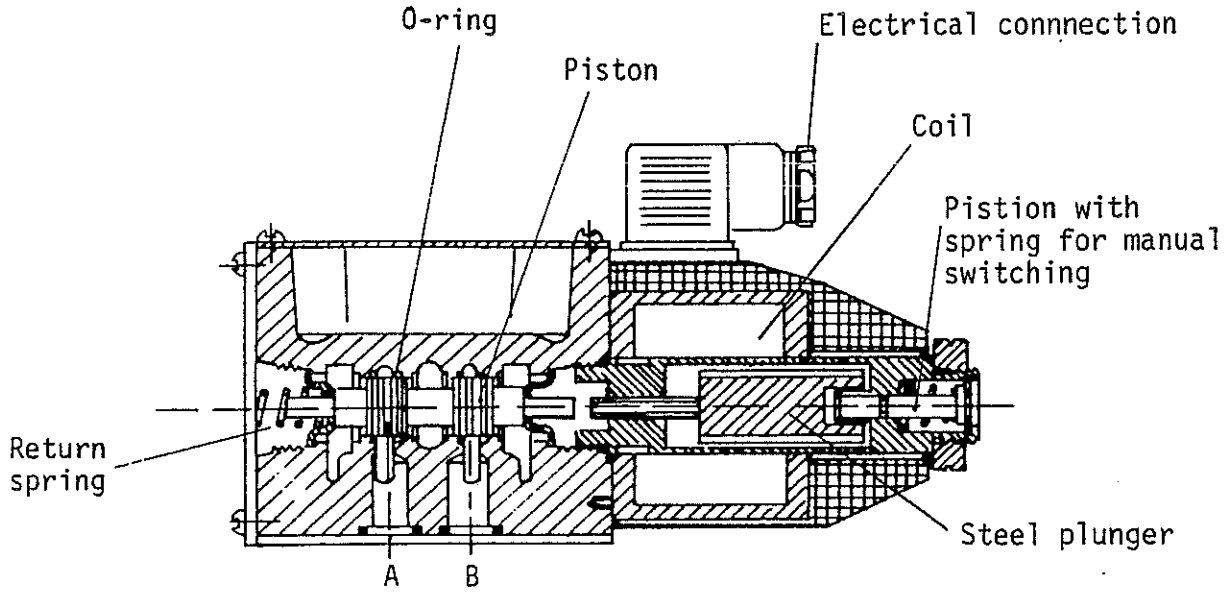

Figure 1.3.3. The Parker D 1 VW valve.

The valve is direct operated by a solenoid, which is also shown in Figure 1.3.3. The solenoid is an integrated part of the directional control valve. When current is applied to the coil, the steel plunger is moved towards the piston of the valve. The steel plunger will cause a movement of the piston. When the current is switched off, the magnetic field of the coil will be de-energized. The return spring in the other end of the piston will force the piston and the steel plunger back to their initial positions.

The valve may also be operated manually. This is done by means of the small piston and the return spring seen in Figure 1.3.3.

The electric parts of the solenoid are physically separated from the rest of the valve. The mechanical parts, on the other hand, are surrounded by oil. The purpose is lubrication, and to soften the movement of the steel plunger.

Subsea Control Valves

Different types of hydraulic control valves are used in subsea control systems. The principles of some of these valves are the same as for valves used onshore. Valves similar to the one tested in this project, also are found in subsea control systems. In 1985 - 1986, SINTEF performed ALT of subsea directional control and shuttle valves for an oil company (Kielland & al, 1985, Lydersen & al, 1986).

Subsea control valves are generally more expensive than control valves used onshore. This is mainly due to the high quality demands for equipment to be situated on the seabed without maintenance for several years.

The main differences between subsea and onshore applications, are the quality, the working conditions, and the environment.

In subsea control systems, the hydraulic control valves are normally located in an oil-filled "pod". The subsea control module will experience an outer pressure on the seabed. The pressure of the closed unit filled with oil is equalized to the sea water pressure. The temperature on the seabed is approximately 5°C.

1.4 VALVE TEST PROGRAMME

The Complete Test Programme

During the SERA project and the subsequent testing mentioned at the start of this chapter, a number of test series on this valve type were performed. Prior to these tests, the most important failure modes and stressors were identified (Kielland & al, 1986). It was decided to study the effect of these stressors during the tests:

- Contamination level in the hydraulic fluid
- Duration of idle periods between valve operations

- Valve age, that is, the performance of new valves versus used (somewhat worn) valves.

A total of 25 valves were tested, in 7 test series with different levels on these stressors. During some of the test series, one or more of these properties were measured:

- Leakage through the valve in closed position
- Current needed to operate the solenoid
- Voltage needed to operate the solenoid
- If the valve did not operate at first trial, the number of trials until success.

After testing, the valves were disassembled and inspected.

The Test Series Analyzed in the Present Report

Among the results from this test programme, the leakage measurements from one of the test series is particularly interesting in connection with the topic of this thesis. These measurements are subject of further analysis in the present report.

The test series in question was started with new valves. The contamination level was ISO 19/16, which is just above working conditions for "coarse hydraulic equipment". The valves were operated every 5 minutes, that is, performing one cycle per 5 minutes. The purpose of the test series was to study wear deterioration. The contamination level changed during the run, mainly due to crushing of larger particles into smaller ones. For this reason, the test was stopped every 2500 cycles, and the contamination was renewed, to ensure an approximately constant level. Valve leakage measurements are given in Chapter 2.

2. LABORATORY TEST RESULTS

2.1 LEAKAGE MEASUREMENTS

Table 2.1.1 shows leakage measurements from the test of 5 hydraulic control valves described in Chapter 1. The leakage through the valve in closed position was measured at certain points in time. Here, time is the number of cycles undertaken by the valve, and not clock time. Graphical displays of the data are given in Figure 2.1.1 to 2.1.3.

Table 2.1.1: Measured leakage through the valves in closed positions, ml/min. Contamination level ISO 19/16 (High contamination level).

Valve no.	Accumulated number of cycles						
	0	2500	5000	7500	10584	13756	16408
A	9.2	13.8	14.4	16.0	15.7	20	22
B	19.6	20.0	26.0	31.2	42	48	58
C	22.0	50.4	58.0	82.0	105	120	148
D	18.0	25.2	24.4	30.0	36.8	40	56
E	11.6	17.2	20.4	25.6	30	36	46

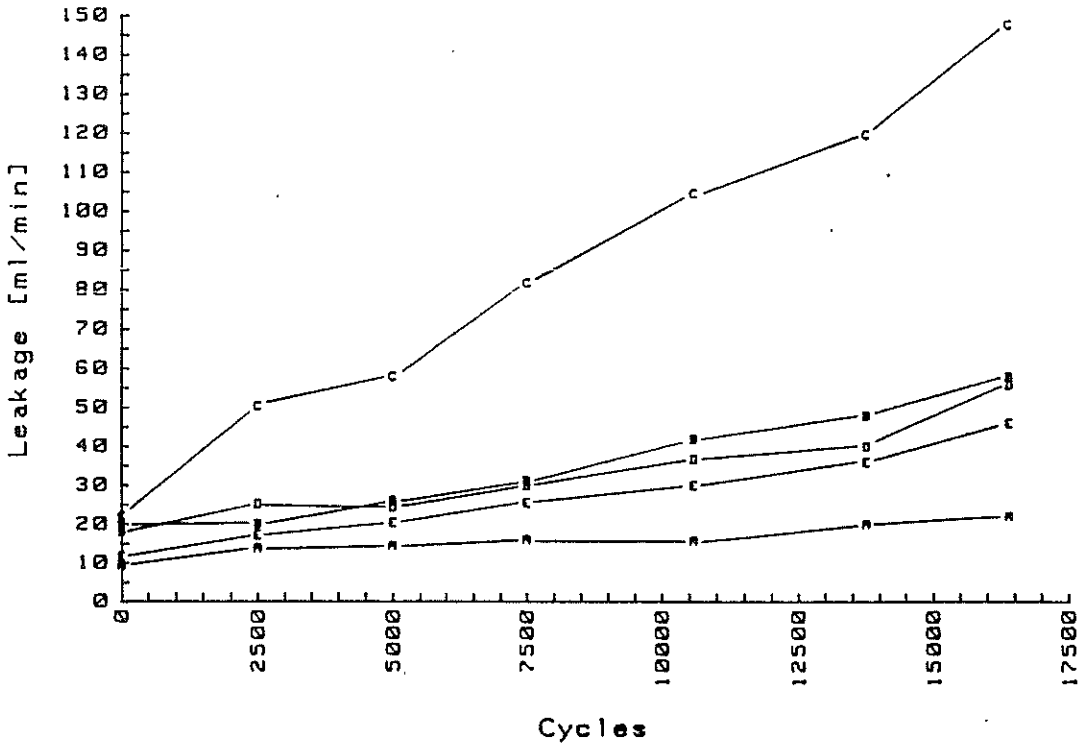

Figure 2.1.1: Leakage through the valves in closed positions for the 5 valves A - E, as function of time (number of valve cycles). Linear leakage scale.

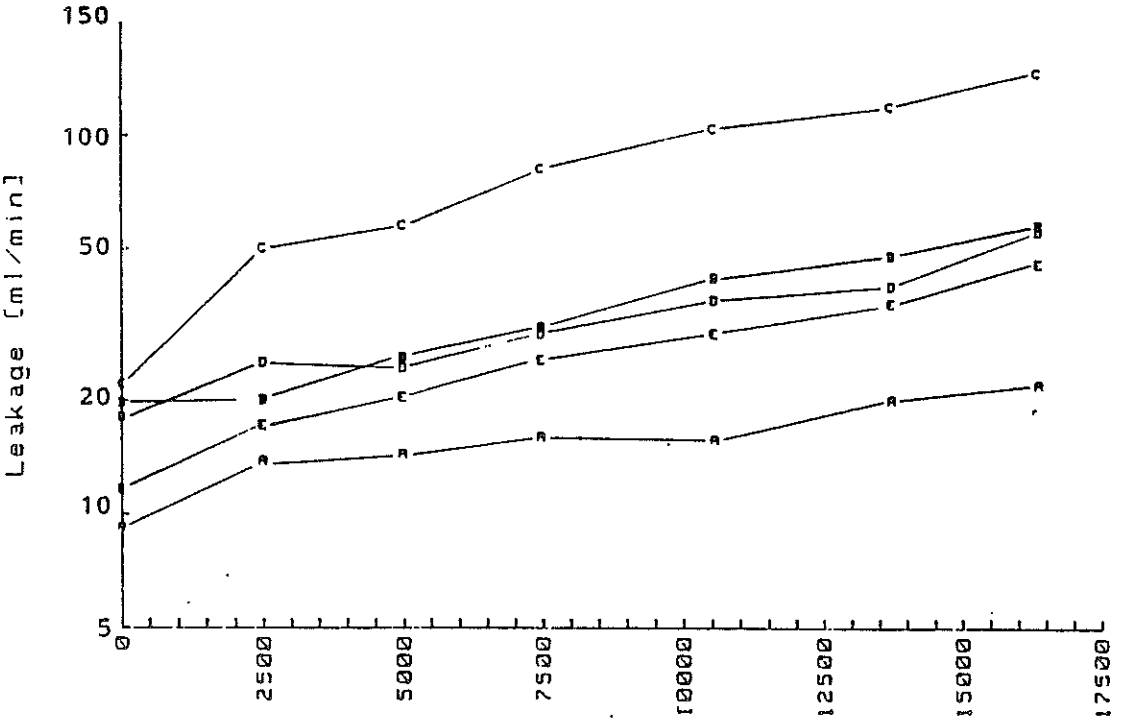

Figure 2.1.2: Leakage through the valves in closed positions for the 5 valves A - E, as function of time (number of valve cycles). Logarithmic leakage scale.

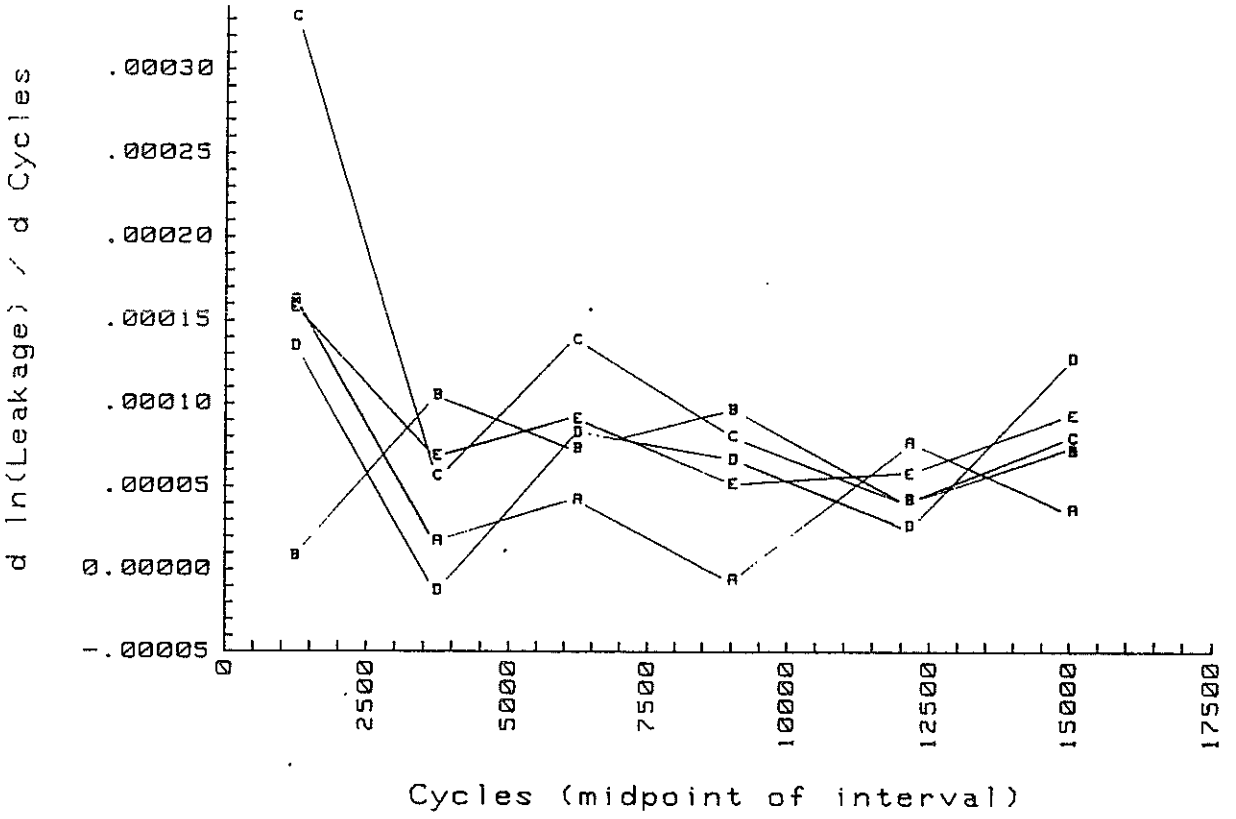

Figure 2.1.3: Logarithm of relative increment in leakage in closed positions, ml/min, for the 5 valves A - E. That is, each point in this figure gives the slope of the corresponding line segment in Figure 2.1.2.

2.2 SUPPLEMENTARY INFORMATION AND COMMENTS

Some additional remarks to the data set are appropriate:

i) No repeated measurements on the same valve at the same points in time were performed to assess the accuracy of the measuring method. However, according to the laboratory personnel who carried out the measurements, the accuracy is of the size of order ± 1 ml/min. That is, if the "true" leakage is d ml/min, then most measurements would be in the range d ± 1 ml/min if repeated measurements had been performed.

ii) The data set is a part of a valve test programme performed at SINTEF, Division of Machine Design, in 1987. After the test

mentioned here, valves A - E were cycled under other conditions. However, valve C broke down after a short time. The valves were disassembled. A small fabrication defect at the sealing area on valve C was detected. This defect seems to be the main cause of the rapid deterioration of valve C.

iii) The data set includes cases where the measured leakage decreases (valve A from 7500 to 10584 cycles, and valve D from 2500 to 5000 cycles). Other parts of the valve test programme also revealed cases with valve leakage temporarily decreasing significantly more than the measurement error. Hence, such a decrease may reflect a "true" decrease in leakage, even if it is within the measurement error.

A plausible explanation for this phenomenon is sand or other contamination temporarily blocking part of the leakage passage.

The plot of leakage on a linear scale (Figure 2.1.1) seems to indicate:

- The leakage of each individual valve seems to follow an approximately linear trend in time. That is, for each individual valve, the leakage measurements lie near a straight line. However, the axis intercept and the slope seems to vary from valve to valve.

The plot of leakage on a logarithmic scale (Figure 2.1.2) seems to indicate:

- The log leakage of each individual valve seems to follow an approximately linear trend in time, except for the first interval (0 - 2500 cycles), where there seems to be a significantly higher increase in log leakage. That is, for each individual valve, the log leakage measurements above 2500 cycles lie near a straight line. The axis intercept of these lines seems to vary from valve to valve, but the slopes need not have significant differences. The slopes of each line segment from Figure 2.1.2 are given in Figure 2.1.3.

3. STOCHASTIC DETERIORATION MODELS

3.1 INTRODUCTION

Figure 2.1.1 shows that the leakage of each individual valve seems to follow an approximately linear trend in time. A reasonable model for the expected leakage on valve number j seems to be

$$E(D_j(t)) = \mu_{0j} + \mu_{1j}t, \tag{3.1.1}$$

where $D_j(t)$ denotes the measured leakage at time t. The coefficients $\underline{\mu}_j = (\mu_{0j}, \mu_{1j})'$ clearly seem to have different values for each valve. We shall consider the $\underline{\mu}_j$'s as realizations of a stochastic vector $\underline{\mu}$. Note that the $\underline{\mu}_j$'s are not explicitly observed, but the measured values of D_{ij} give information about the $\underline{\mu}_j$'s. The different $\underline{\mu}_j$'s are assumed to be stochastically independent, with mean

$$E(\underline{\mu}) = \underline{\theta} \tag{3.1.2}$$

and variance-covariance matrix

$$V(\underline{\mu}) = \Lambda = \begin{bmatrix} \lambda_{00} & \lambda_{01} \\ \lambda_{10} & \lambda_{11} \end{bmatrix}. \tag{3.1.3}$$

Selecting a binormal distribution for $\underline{\mu}_j$ makes modelling and estimation convenient. However, the binormal distribution assigns positive probability density to all pairs of real values $\underline{\mu}_j$, including those with one or two negative values. This may cause two problems:

i) A negative value of $\mu_{0j}+\mu_{1j}t$ for some t implies that the expected leakage D(t) is negative, which is physically impossible. If D(t) is taken to represent log leakage instead of leakage, this is no problem, since exp(D(t)) is always positive.

ii) A negative value of μ_{1j} implies that the expected leakage decreases with time. It does not seem plausible that this should occur in practice. Even if the estimated probability of a negative μ_{1j} is negligible for some practical purposes, great care must be

taken: For example, if Model 2 below is assumed, any nonzero probability of negative μ_{1j} implies that the expected time to exceed any critical leakage d_c would be infinitely large.

Figure 2.1.2 shows that the log leakage of each individual valve seems to follow an approximately linear trend in time, except for the first period (0 - 2500 cycles). Hence, by letting $D_j(t)$ denote the logarithm of measured leakage, (3.1.1) may provide an alternative, reasonable model for the log leakage measurments, except those at t = 0 cycles. Excluding the measurements on uncycled valves from the linear model is not unreasonable: Many types of mechanical equipment experience a run-in phase with different performance from the most useful period.

Generally, fitting log leakage to the model may seem more attractive than fitting leakage: Choosing a normal distribution for leakage implies positive probabilities for negative leakages. This needs not be a practical problem if these probabilities are small enough to be negligible. On the other side, any probability distribution for log leakage will assign positive probability only to positive leakage.

The linear model on leakage states that for a given valve, the expected increment in leakage is the same over all time intervals with equal length. On the other side, the linear model on log leakage states that expected relative increment in leakage is the same for all time intervals with equal length. That is, the rate of increase in leakage is approximately proportional to the leakage at the beginning of the interval.

Two stochastic models will be fitted to the data set:

1) A random coefficient regression model (Model 1)

2) A Wiener process with random drift (Model 2).

Both models will be fitted to the leakage data. The two models are more accurately defined below, followed by a discussion concerning choice of model in Section 3.5.

3.2 NOTATION

First, let us summarize the structure of data set and introduce some common notation: Let D_{ij} denote the i-th leakage measurement, or log leakage measurement, on valve number j, at time t_{ij}. A total of r valves are included in the test. For each valve j, the measurements were taken at n points in time, $t_{1j}, \ldots, t_{nj}$.

In our data set, $r = 5$ and $n = 7$. When the model is fitted to D_{ij} = log leakage, the measurements at $t = 0$ cycles will be taken out, leaving $n = 6$.

Not only has the same number of measurements been taken for each valve, but the valves were measured at the the same points in time:

$$t_{1j} = t_1, \ldots, t_{nj} = t_n, \quad \text{for} \quad j = 1, \ldots, r.$$

This fact simplifies estimation significantly.

3.3 DEFINITION OF MODEL 1

This is a random coefficient regression model on the form

$$D_{ij} = \mu_{0j} + \mu_{1j} t_{ij} + e_{ij} \tag{3.3.1}$$

The error terms e_{ij} are assumed to be independent, identically distributed with mean 0. We shall further assume the error terms to be normally distributed,

$$e_{ij} \sim N(0,\sigma^2). \tag{3.3.2}$$

In the random coefficient regression model, we shall assume the observations to be conditionally independent within each valve: Given $\underline{\mu}_j = (\mu_{0j}, \mu_{1j})'$, then $D_{i_1 j}$ and $D_{i_2 j}$ are independent for all $i_1 \neq i_2$.

The e_{ij} are assumed independent of each other, and of the $\underline{\mu}_j = (\mu_{0j}, \mu_{1j})'$.

3.4 DEFINITION OF MODEL 2

In the Wiener process with random drift, we shall still assume (3.1.1) to hold. But the distribution is now assumed to be (see e.g. Cox and Miller, 1965)

$$D_{ij} = \mu_{0j} + \mu_{1j}t_{ij} + \sigma\sqrt{t_{ij}}U_{ij}, \qquad (3.4.1)$$

with the U_{ij}'s N(0,1). The increments in D within each valve are assumed conditionally independent: Given $\underline{\mu}_j = (\mu_{0j}, \mu_{1j})'$ and any four time points such that $t_{1j} \leq t_{2j} \leq t_{3j} \leq t_{4j}$, then $(D_{2j} - D_{1j})$ and $(D_{4j} - D_{3j})$ are independent. Actually, this is a Wiener process with random drift μ_{1j} and random starting point μ_{0j} (y-axis intercept). The U_{ij} are assumed independent of each other, and of the $\underline{\mu}_j = (\mu_{0j}, \mu_{1j})'$.

3.5 CHOICE OF MODEL

Generally, the choice of a stochastic model in this situation, and similar situation, may depend on one or more criteria. The model ought to:

i) agree with our prior knowledge of the physical phenomenon,
ii) agree with data set (fit to the data),
iii) have mathematical / computational convenience.

Some reflections concerning these criteria and our data set are given below.

Both the "true leakages" and some measurement error contribute to the measured values D_{ij}:

$$D_{ij} = \text{"true leakage"} + \text{measurement error} \qquad (3.5.1)$$

It seems plausible to consider the measurement errors as independent, identically distributed with mean 0 (no systematic errors). Unfortunately, the leakage measurements do not include repeated measurements at the same points in time, or close points in time. The time points (0, 2500, ...) lie at approximately equidistant intervals, and the assessment of measurement error would have to stem from other information sources. We shall not further enter the problem of splitting up the measured values D_{ij} into the two components (3.5.1), but note the following reflections:

True leakage is considered stochastic, even if $\mu_j = (\mu_{0j}, \mu_{1j})'$ is given. True leakage is assumed to follow a stochastic process with positive drift. That is, the valves will tend to deteriorate, and not stay at status quo or improve, in the long run. However, we assume a positive probability of negative increment in D(t) over a finite interval (cfr remark iii in Section 2.2). Both Model 1 and Model 2 assign positive probability to negative increment over finite intervals.

Both true leakage and measured leakage are always positive, since leakage from a high pressure to a low pressure side is measured. Both the proposed models allow positive probability for negative observation. Still, such a model can be a good approximation of reality if this probability is low.

The valves are constructed such that a small leakage through the valve in closed position should always be present. Erosive and abrasive wear will gradually remove sealing material, and increase the leakage. Sometimes, leakage may decrease temporarily due to sand deposits or other contamination. On a macroscopic level, it seems appropriate to consider the leakage development as a continuous process.

Based on these reflections, Model 2 may seem like the most attractive of the two for true leakage, being a continuous stochastic process. From a

theoretical point of view, the most attractive model would be a combined model: This combined model would include Model 2 for the true leakage, and assume the measurement errors to be independent, identically, normally distributed. In this way, the overall model for the measured leakage would include both Model 1 and Model 2 as limiting cases: Model 1 would be the limiting case if the variance of true leakage tends to zero, and Model 2 would be the limiting case if the measurement error tend to zero.

Model 1 may be more thought of as a model for the observations, than as a model for the underlying true leakage process. Still, Model 1 may be a good enough approximation to reality. In our case, the time points (0, 2500, ...) lie at approximately equidistant intervals. This fact reduces one of the distinctions between Model 1 and Model 2:

Consider the measured leakage increment from time t_{ij} to time $t_{(i+1),j}$ on valve number j. In Model 1, this difference is given by

$$\begin{aligned}\Delta D_{ij} &= (\mu_{0j} + \mu_{1j}t_{(i+1),j} + \sigma_1 U_{(i+1),j}) - (\mu_{0j} + \mu_{1j}t_{ij} + \sigma_1 U_{ij}) \\ &= \mu_{1j}\Delta t_{ij} + \sigma_1(U_{(i+1),j} - U_{ij}) \\ &= \mu_{1j}\Delta t_{ij} + \sigma_1\sqrt{2}V_{ij}, \end{aligned} \qquad (3.5.2)$$

where

$$\Delta D_{ij} = D_{(i+1),j} - D_{ij},$$
$$\Delta t_{ij} = t_{(i+1),j} - t_{ij},$$

$U_{(i+1),j}$ and U_{ij} are independent and standard normally distributed, $V_{ij} = (U_{(i+1),j} - U_{ij})/\sqrt{2}$ is standard normally distributed, and σ_1 is identical to σ in (3.3.2).

In Model 2, the difference is

$$\Delta D_{ij} = \mu_{1j}\Delta t_{ij} + \sigma_2\sqrt{\Delta t_{ij}}W_{ij}, \qquad (3.5.3)$$

where W_{ij} is standard normally distributed, and σ_2 is identical to σ in (3.4.1).

If all the time increments Δt_{ij} are equal, then the models (3.5.2) and (3.5.3) for the measured leakage increments are on the same form, with $\sigma_1\sqrt{2}$ corresponding to $\acute{U}_2\sqrt{\Delta t_{ij}}$. Still, there is a difference: Conditionally given μ, all measured leakage increments ΔD_{ij} are independent in Model 2. In Model 1, adjacent leakage increments are negatively correlated due to the negative correlation between V_{ij} and $V_{(i+1),j}$.

A more convenient, and better established, mathematical framework for estimation and inferences seems to be present for Model 1 than for Model 2. That is, Model 1 seems to have better mathematical / computational convenience than Model 2.

In this report, both models will be fitted to the leakage data.

3.6 APPLICATIONS TO OTHER FAILURE MECHANISMS

The rate of deterioration, with respect to leakage through the valve in closed position, clearly seems to differ between the individual specimens (valves). Similar phenomena are probably present for other physical deterioration mechanisms, on different types of components, as described below. This is more extensively treated in Part I of this thesis.

Regression with stochastic coefficients has recently been applied to fatigue crack growth in steel. According to Paris' law, the fatigue crack growth rate da/dN is given by

$$\log(da/dN) = \log(C) + m \cdot \Delta K, \qquad (3.6.1)$$

where ΔK is the stress intensity factor, and C and m are material constants. Both theory end empirical results establish equation (3.6.1) as a good approximation to reality, as long as ΔK is within specified limits.

Several independent authors have reported cases where (3.6.1) fits well to the measurements per specimen, while the parameter set (C, m) varies significantly between specimens. This is the case for the Ditlevsen and

Olesen (1986) analysis of the Virkler & al (1979) data from an aluminum alloy, and the Narbuvoll (1987) analysis of the Ørjasæter & al (1985) data from steel. Probably, the same theory would explain the variations in the Hudak & al (1978) data.

Iuculano and Zanini (1986) report similar phenomena for chemical degradation in metallic layer resistors.

4. PARAMETER ESTIMATION

4.1 INTRODUCTION

Tentatively, both models (Model 1 and Model 2) could be fitted to both data sets (leakage and log leakage). There are of 4 combinations of model and data set:

	Leakage	Log leakage
Model 1	I	III
Model 2	II	IV

In the present section, initial estimates for model parameters will be found for combinations I and III. Section 4.2 and 4.3 cover estimation of parameters for the leakage data using Model 1 and Model 2 (i.e. combinations I and II), respectively. Detailed estimation for the log leakage data will not be performed in this report. The procedure would be quite similar to the presentations in Section 4.2 and 4.3.

Whichever of these models is chosen, initial estimates for the parameters may be found by linear regression on the data for each valve separately. Least squares estimators for μ_j are given by

$$\tilde{\mu}_{1j} = \frac{\Sigma(t_i - \bar{t})D_{ij}}{\Sigma(t_i - \bar{t})^2} \tag{4.1.1}$$

and

$$\tilde{\mu}_{0j} = \frac{1}{n}\Sigma D_{ij} - \tilde{\mu}_{1j}\bar{t}, \tag{4.1.2}$$

where $\bar{t} = \frac{1}{n}\Sigma t_i$, and all sums are taken over i=1,2,...,n. The variance around the regression line for valve number j may be estimated by

$$\tilde{\sigma}_j^2 = \frac{1}{n-2}\sum_{i=1}^{n}[D_{ij} - (\tilde{\mu}_{0j} + \tilde{\mu}_{1j}t)]^2, \tag{4.1.3}$$

The above estimators are unbiased if μ_j is considered as a fixed parameter set (not a stochastic vector) for each valve j. Further, 100(1-ϵ)% confidence intervals for μ_{1j}, μ_{0j}, and σ_j^2 are given by

$$\tilde{\mu}_{1j} \mp t_{\epsilon/2,n-2} \frac{1}{\sqrt{\Sigma(t_i - \bar{t})^2}} \tilde{\sigma}_j, \tag{4.1.4}$$

$$\tilde{\mu}_{0j} \mp t_{\epsilon/2,n-2} \left[\frac{\Sigma t_i^2}{n \Sigma(t_i - \bar{t})^2} \right]^{1/2} \tilde{\sigma}_j, \tag{4.1.5}$$

and

$$\left[\frac{n-2}{z_{\epsilon/2,n-2}} \tilde{\sigma}_j^2, \quad \frac{n-2}{z_{1-\epsilon/2,n-2}} \tilde{\sigma}_j^2 \right], \tag{4.1.6}$$

respectively, where $t_{\epsilon,\nu}$ is the upper ϵ percentile of the Student t distribution with ν degrees of freedom, and $z_{\epsilon,\nu}$ is the upper ϵ percentile of the chi square distribution with ν degrees of freedom. A 100(1-ϵ)% confidence region for (μ_{0j}, μ_{1j}) is bounded by the ellipse

$$n(\tilde{\mu}_{0j}-\mu_{0j})^2 + 2(\tilde{\mu}_{0j}-\mu_{0j})(\tilde{\mu}_{1j}-\mu_{1j}) \sum_{i=1}^{n} t_i + (\tilde{\mu}_{0j}-\mu_{0j}) \sum_{i=1}^{n} t_i^2$$

$$= 2 \tilde{\sigma}_j^2 f_{\epsilon,2,n-2}, \tag{4.1.7}$$

where f_{ϵ,ν_1,ν_2} is the upper ϵ percentile of the Fisher distribution with ν_1 and ν_2 degrees of freedom.

Estimates and 90% confidence intervals computed using (4.1.1) - (4.1.6) are given in Tables 4.1.1 and 4.1.2. Scatter diagrams of the estimates are given in Figures 4.1.1 and 4.1.2. Figures 4.1.3 and 4.1.4 show 90% confidence regions (4.1.7) for regression on leakage and log leakage, respectively.

Figures 4.1.3 and 4.1.4 show that there are significant differences between the valves, since several of the confidence regions far from overlap each other. Even if the valve with seemingly most individual

behaviour, valve C, is disregarded, some of the remaining valves have confidence regions quite far apart. The distances from the confidence region for valve A to the confidence regions for valves B, D, and E are about 3 - 4 times the "width" of the confidence regions. This is the case both for the leakage data (Figure 4.1.3), and the log leakage data (Figure 4.1.4). The distances between the confidence regions are so large compared to the size of the regions, that it is unnecessary to carry out a formal overall significance test.

There are no significant differences between the variances σ_j^2. Actually, all of the one at a time 90% confidence intervals for σ_j^2 in Table 4.1.1 and 4.1.2, respectively, overlap each other.

In the remaining parts of this report, only leakage data (combinations I and II) will be studied further.

Table 4.1.1: Linear regression on leakage for each valve. Estimates obtained by least squares estimation.

Valve	Estimates and 90% confidence intervals for parameters		
j	μ_{0j}	μ_{1j}	σ_j^2
A	10.51 (8.90, 12.12)	0.00067 (0.00051, 0.00084)	1.324^2 (0.890^2, 2.760^2)
B	15.58 (12.29, 18.88)	0.00243 (0.00209, 0.00277)	2.708^2 (1.820^2, 5.646^2)
C	25.60 (19.57, 31.63)	0.00729 (0.00666, 0.00791)	4.959^2 (3.333^2, 10.339^2)
D	16.77 (11.84, 21.71)	0.00203 (0.00152, 0.00254)	4.058^2 (2.727^2, 8.461^2)
E	11.17 (8.92, 13.42)	0.00195 (0.00172, 0.00218)	1.850^2 (1.243^2, 3.857^2)

Table 4.1.2: Linear regression on log leakage for each valve. Estimates obtained by least squares estimation.

Valve	Estimates and 90% confidence intervals for parameters		
j	μ_{0j}	μ_{1j}	σ_j^2
A	2.506 (2.401, 2.610)	$3.354 \cdot 10^{-5}$ ($2.355 \cdot 10^{-5}$, $4.352 \cdot 10^{-5}$)	0.06125^2 (0.03977^2, 0.14529^2)
B	2.862 (2.769, 2.955)	$7.516 \cdot 10^{-5}$ ($6.630 \cdot 10^{-5}$, $8.402 \cdot 10^{-5}$)	0.05434^2 (0.03528^2, 0.12888^2)
C	3.740 (3.618, 3.862)	$7.867 \cdot 10^{-5}$ ($6.702 \cdot 10^{-5}$, $9.032 \cdot 10^{-5}$)	0.07145^2 (0.04639^2, 0.16947^2)
D	2.989 (2.834, 3.144)	$5.758 \cdot 10^{-5}$ ($4.279 \cdot 10^{-5}$, $7.237 \cdot 10^{-5}$)	0.09071^2 (0.05889^2, 0.21516^2)
E	2.684 (2.626, 2.742)	$6.838 \cdot 10^{-5}$ ($6.288 \cdot 10^{-5}$, $7.388 \cdot 10^{-5}$)	0.03372^2 (0.02189^2, 0.07997^2)

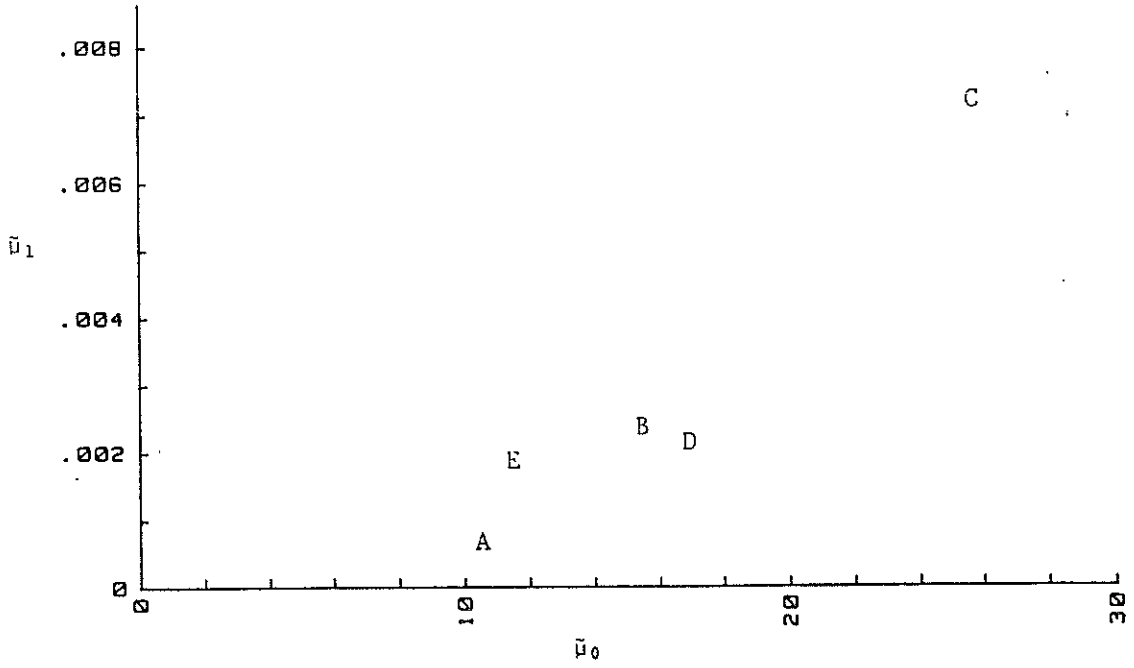

Figure 4.1.1: Scatter diagram of the estimates from Table 4.1.1.

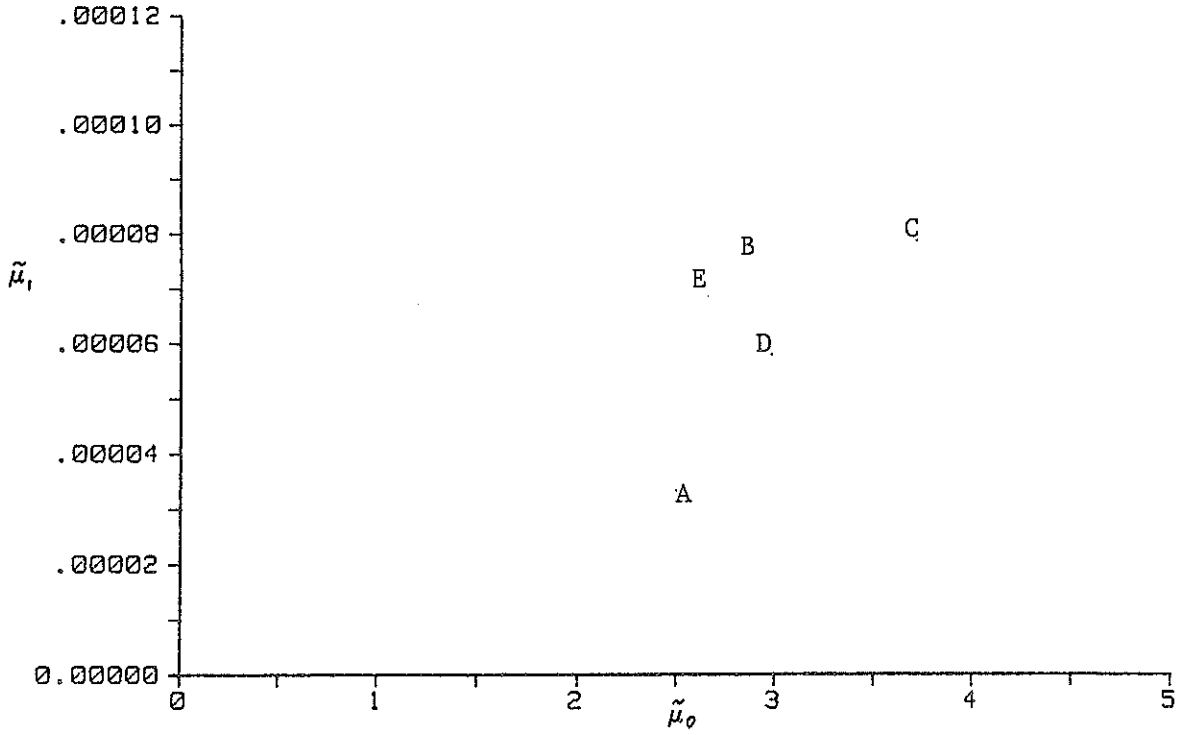

Figure 4.1.2: Scatter diagram of the estimates from Table 4.1.2.

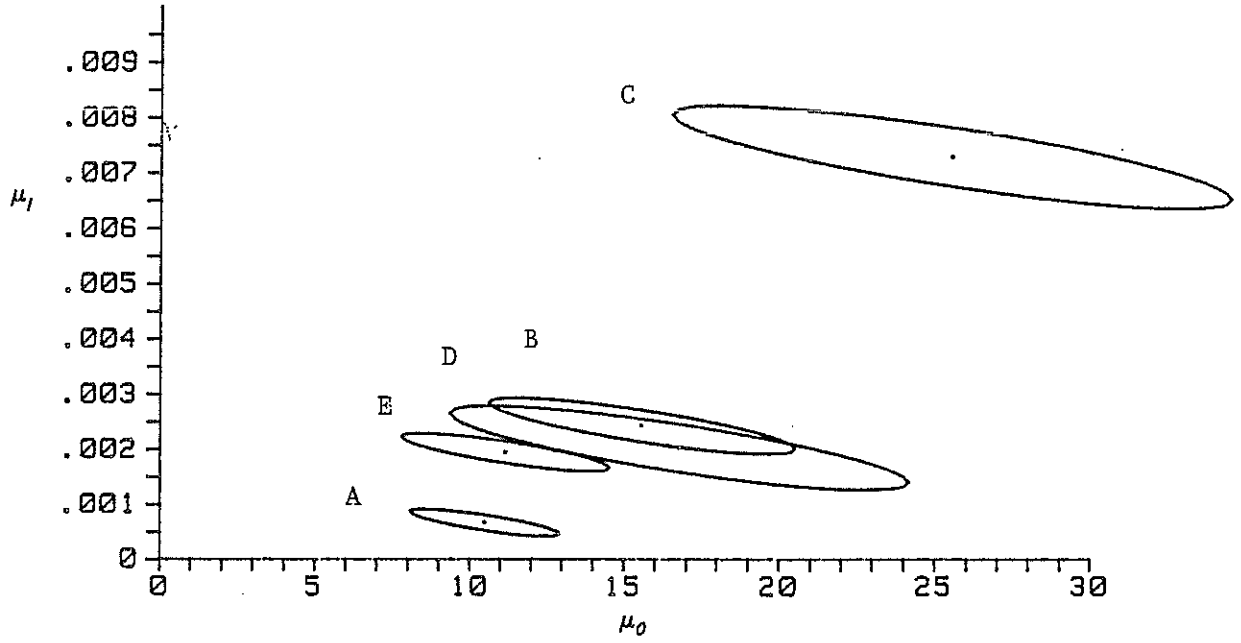

Figure 4.1.3: 90% confidence regions for the parameters, leakage.

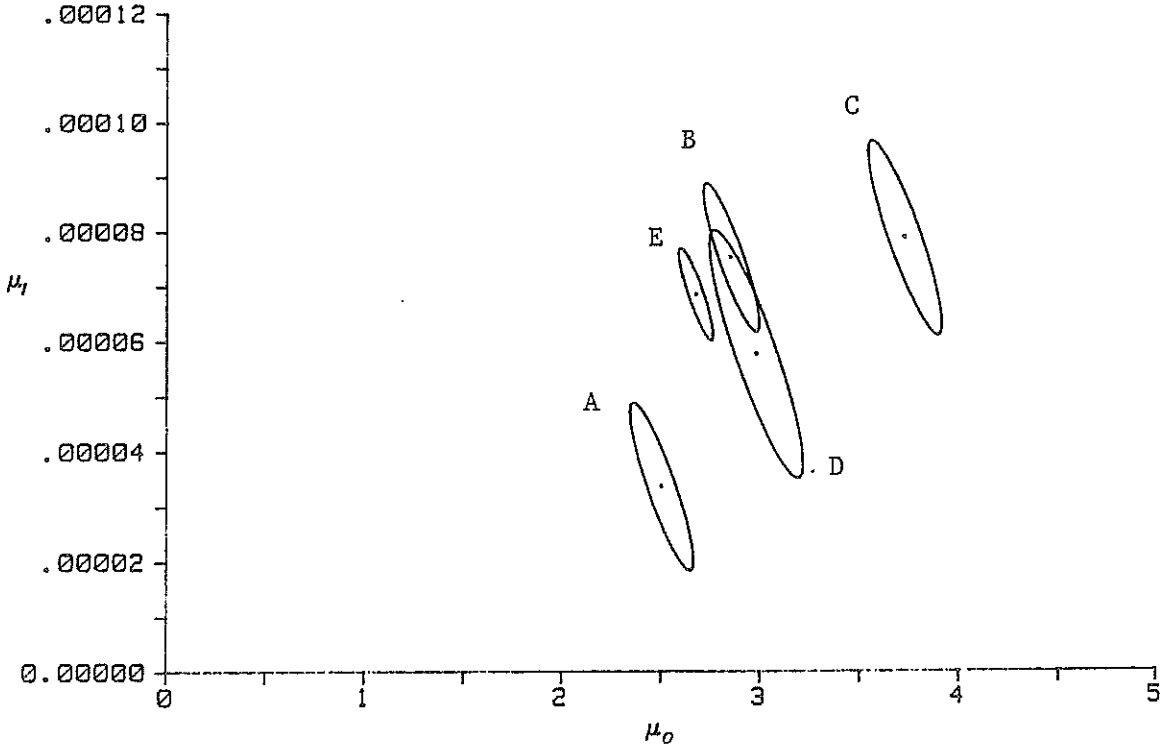

Figure 4.1.4: 90% confidence regions for the parameters, log leakage.

4.2 ESTIMATION IN MODEL 1

We shall assume $\underline{\mu} = (\mu_0, \mu_1)'$ to be binormally distributed. Under these assumptions, Model 1 has a total of 6 parameters:

$$E(\mu_0) = \theta_0$$
$$E(\mu_1) = \theta_1$$
$$Var(\mu_0) = \lambda_{00}$$
$$Var(\mu_1) = \lambda_{11}$$
$$Cov(\mu_0, \mu_1) = \lambda_{01}$$
$$Var(e_{ij}) = Var(D_{ij}|\underline{\mu}) = \sigma^2$$

If $\tilde{\mu}_{0j}$, $\tilde{\mu}_{1j}$, $j=1,\ldots,r$, given by (4.1.1) and (4.1.2) had been observations, rather than estimators, the natural estimators for the first 5 parameters above would have been

$$\hat{E}(\mu_0) = \frac{1}{r} \sum_{j=1}^{r} \tilde{\mu}_{0j} \tag{4.2.1}$$

$$\hat{E}(\mu_1) = \frac{1}{r} \sum_{j=1}^{r} \tilde{\mu}_{1j} \tag{4.2.2}$$

$$\hat{Var}(\mu_0) = \frac{1}{r-1} \sum_{j=1}^{r} (\tilde{\mu}_{0j} - \hat{E}(\mu_0))^2 \tag{4.2.3}$$

$$\hat{Var}(\mu_1) = \frac{1}{r-1} \sum_{j=1}^{r} (\tilde{\mu}_{1j} - \hat{E}(\mu_1))^2 \tag{4.2.4}$$

$$\hat{Cov}(\mu_0,\mu_1) = \frac{1}{r-1} \sum_{j=1}^{r} (\tilde{\mu}_{0j} - \hat{E}(\mu_0))(\tilde{\mu}_{1j} - \hat{E}(\mu_1)). \tag{4.2.5}$$

Since $\tilde{\mu}_{0j}$, $\tilde{\mu}_{1j}$, $j=1,\ldots,r$ are estimators, we can not use (4.2.1)-(4.2.5) direct, except possibly to obtain initial estimates.

Estimation methods for Model 1 are given, e.g., by Spjøtvoll (1977). A short survey of some random coefficients regression models is also given

in Part I of this thesis. In our case, leakage was measured at the same times for all valves, that is,

$$t_{1j} = t_1, \quad \ldots, \quad t_{nj} = t_n, \quad \text{for} \quad j = 1, \ldots, r.$$

In this situation, uniformly minimum variance unbiased (UMVU) estimators are given by (Spjøtvoll, 1977, Section 2.1). Actually, the estimators (4.2.1) and (4.2.2) for $\underline{\theta}$ are UMVU. The UMVU estimator for σ^2 is given by

$$\hat{\sigma}^2 = \frac{1}{r} \sum_{j=1}^{r} \tilde{\sigma}_j^2, \tag{4.2.6}$$

where $\tilde{\sigma}_j^2$ is given by (4.1.3).

The estimator for the variance-covariance matrix given by (4.2.3) to (4.2.5) is, however, biased. The UMVU estimators are obtained from (4.2.3) to (4.2.5) if the matrix

$$\hat{\sigma}^2 \, (\mathbf{X}'\mathbf{X})^{-1} \tag{4.2.7}$$

where

$$\mathbf{X} = \begin{bmatrix} 1 & t_1 \\ 1 & t_2 \\ \vdots & \vdots \\ 1 & t_n \end{bmatrix} \tag{4.2.8}$$

is subtracted from

$$\begin{bmatrix} \hat{\mathrm{Var}}(\mu_0) & \hat{\mathrm{Cov}}(\mu_0,\mu_1) \\ \hat{\mathrm{Cov}}(\mu_0,\mu_1) & \hat{\mathrm{Var}}(\mu_1) \end{bmatrix}.$$

The matrix $(X'X)^{-1}$ is found to be

$$(X'X)^{-1} = \frac{1}{\Sigma(t_i - \bar{t})^2} \begin{bmatrix} \frac{1}{n}\Sigma t_i^2 & -\bar{t} \\ -\bar{t} & 1 \end{bmatrix}, \qquad (4.2.9)$$

where all sums are taken over $i = 1, \ldots, n$, and $\bar{t} = \frac{1}{n}\Sigma t_i$. The UMVU estimator for the variance-covariance matrix of $\underline{\mu}$ thus gives:

$$\hat{\lambda}_{00} = \frac{1}{r-1} \sum_{j=1}^{r} (\tilde{\mu}_{0j} - \hat{E}(\mu_0))^2 - \hat{\sigma}^2 \frac{\Sigma t_i^2}{n\,\Sigma(t_i - \bar{t})^2} \qquad (4.2.10)$$

$$\hat{\lambda}_{11} = \frac{1}{r-1} \sum_{j=1}^{r} (\tilde{\mu}_{1j} - \hat{E}(\mu_1))^2 - \hat{\sigma}^2 \frac{1}{\Sigma(t_i - \bar{t})^2} \qquad (4.2.11)$$

$$\hat{\lambda}_{01} = \frac{1}{r-1} \sum_{j=1}^{r} (\tilde{\mu}_{0j} - \hat{E}(\mu_0))(\tilde{\mu}_{1j} - \hat{E}(\mu_1)) + \hat{\sigma}^2 \frac{\bar{t}}{\Sigma(t_i - \bar{t})^2} \qquad (4.2.12)$$

Numeric estimates

The data on valve leakage gives:

$$\hat{\theta}_0 = 15.93$$
$$\hat{\theta}_1 = 0.00287$$
$$\hat{\lambda}_{00} = 6.049^2 - 4.70 = 5.647^2$$
$$\hat{\lambda}_{11} = 0.00256^2 - 5.34 \cdot 10^{-7} = 0.00245^2$$
$$\hat{\lambda}_{01} = 0.0146 + 0.00040 = 0.0150$$
$$\hat{\sigma}^2 = 3.27^2$$

In the above expressions for $\hat{\lambda}_{00}$, $\hat{\lambda}_{11}$, and $\hat{\lambda}_{01}$, the last terms corresponds to the last terms in (4.2.7) - (4.2.9), i.e. the term due to the subtraction of the matrix $\hat{\sigma}^2(X'X)^{-1}$. The correlation coefficient between μ_0 and μ_1 may be estimated as

$$\hat{\rho} = \frac{\hat{\lambda}_{01}}{\sqrt{\hat{\lambda}_{00}\hat{\lambda}_{11}}} = 1.086.$$

Hence, the UMVU estimators lead to a correlation coefficient with absolute value greater than one. Equivalent, the estimated variance-covariance matrix $\hat{\Lambda}$ has a negative determinant, $\det(\hat{\Lambda}) < 0$. It should be noted, however, that calculations not included here gave an approximate 90% confidence interval for ρ including both 0 and 1.

As input to some calculations and Monte Carlo simulations performed later in this report, we need permissible estimates. In order to obtain a positive definite estimate for Λ, $\hat{\Lambda}$ ought to be adjusted some way. From a theoretical point of view, the "best" adjustment is perhaps to use the "closest" positive semidefinite matrix, according to some norm in the space of symmetrical 2x2 matrices. A simpler possibility is to set $\hat{\hat{\rho}}(\mu_0,\mu_1)$ equal to some value less than 1, and

$$\hat{\hat{\mathrm{Cov}}}(\mu_0,\mu_1) = \hat{\hat{\rho}}(\mu_0,\mu_1)\sqrt{\hat{\lambda}_{00}\,\hat{\lambda}_{11}}. \qquad (4.2.13)$$

As an ad hoc procedure, we shall simply choose the value $\hat{\hat{\rho}}(\mu_0,\mu_1)=0.99$ and

$$\hat{\hat{\mathrm{Cov}}}(\mu_0,\mu_1) = \hat{\hat{\rho}}(\mu_0,\mu_1)\sqrt{\hat{\lambda}_{00}\,\hat{\lambda}_{11}} = 0.0137. \qquad (4.2.14)$$

A correlation coefficient near 1 implies that the estimates $(\tilde{\mu}_{0j}, \tilde{\mu}_{1j})$ lie near some straight line

$$\tilde{\mu}_{1j} = \beta_0 + \beta_1\tilde{\mu}_{0j}, \quad \beta_1 > 0. \qquad (4.1.15)$$

This equation gives μ_{1j} as a monotonously increasing function of μ_{0j}. This is not unreasonable: The value of μ_{0j} is the initial leakage, and the value of μ_{1j} is the valve's susceptibility to deteriorate in terms of increase in leakage. An individual valve with inferior quality may be expected to have high values for both μ_{0j} and μ_{1j}.

Linear regression on the estimates $(\tilde{\mu}_{0j}, \tilde{\mu}_{1j})$, j=1, ..., r, gives

$$\mu_1 \approx -0.00349 + 0.00040\mu_0, \tag{4.2.16}$$

with μ_0 given in cycles^{-1}, and μ_1 given in ml/min. Using (4.2.16), the estimated expected wear depth becomes approximately

$$\begin{aligned} E(D(t)) &= \mu_0 + \mu_1 t \\ &\approx \mu_0 + (-0.00349 + 0.00040\mu_0)t \end{aligned} \tag{4.2.17}$$

The straight line (4.2.17) is shown in Figure 4.2.5, for several values of μ_0. The continuations of all the lines (4.2.17) pass through the point $(-1/\hat{\beta}_1, -\hat{\beta}_0/\hat{\beta}_1) = (-2502, 8.725)$. If $\mu_0 < -\beta_0/\beta_1$, then (4.1.11) implies $\mu_1 < 0$, such as the lowest of the straight lines in Figure 4.2.5. As already pointed out, $\mu_1 < 0$ does not harmonize with our understanding of the physical processes taking place. Still, the model may be useful if $P(\mu_1 < 0)$ is negligible for the practical purpose.

Assuming a bivariate normal distribution for (μ_0, μ_1), then

$$P(\mu_1 < 0) = \Phi\left(\frac{-E(\mu_1)}{\sqrt{Var(\mu_1)}} \right).$$

In our case, an estimate of this probability is

$$\hat{P}(\mu_1 < 0) = \Phi\left(\frac{-\hat{E}(\mu_1)}{\sqrt{\hat{Var}(\mu_1)}} \right) = \Phi\left(\frac{-0.00287}{0.00256} \right) = 0.131$$

which is far from negligible.

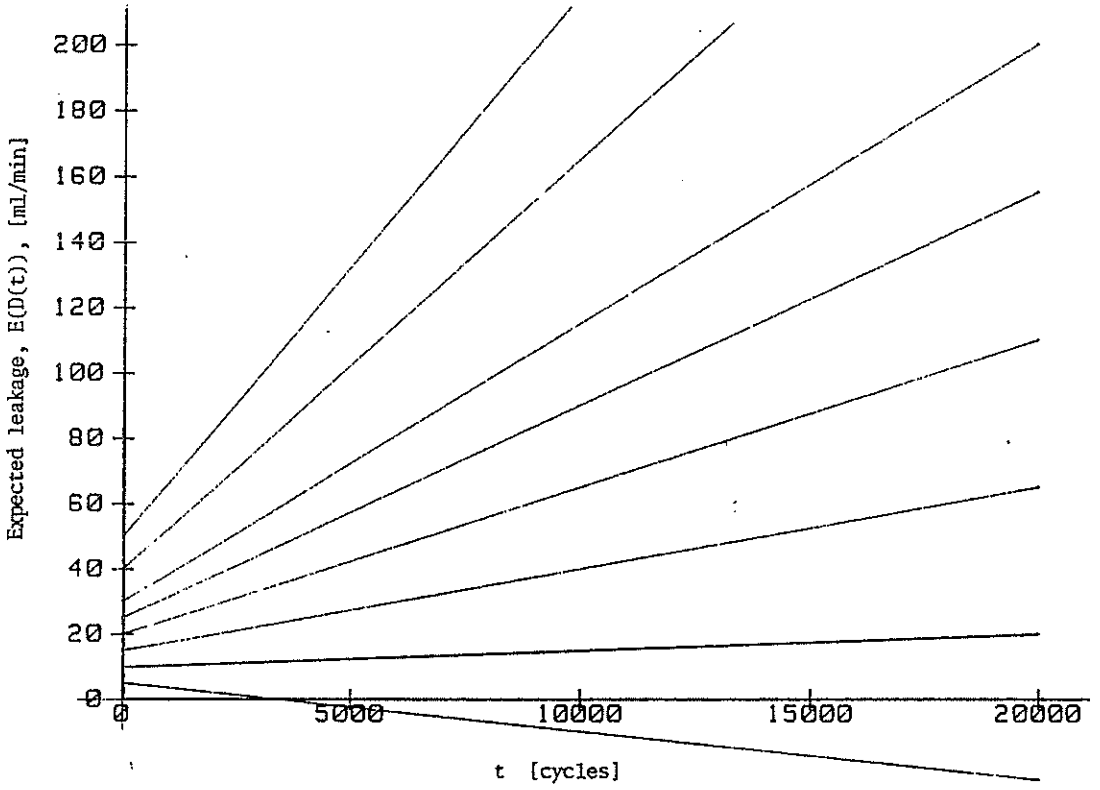

Figure 4.2.5. Estimated E(D(t)) according to (4.1.11), for several values of μ_0.

4.3 ESTIMATION IN MODEL 2

We shall assume $\underline{\mu} = (\mu_0, \mu_1)'$ to be binormally distributed. Under these assumptions, Model 1 has a total of 6 parameters:

$$E(\mu_0) = \theta_0$$
$$E(\mu_1) = \theta_1$$
$$\mathrm{Var}(\mu_0) = \lambda_{00}$$
$$\mathrm{Var}(\mu_1) = \lambda_{11}$$
$$\mathrm{Cov}(\mu_0, \mu_1) = \lambda_{01}$$
$$[\mathrm{Var}(D_{i_2 j} - D_{i_1 j} \mid \mu_{1j})]/(t_{i_2 j} - t_{i_1 j}) = \sigma^2$$

Note that in our data set, D_{1j} is the measured leakage through valve j after 0 cycles. Hence we have the observations

$$\mu_{0j} = D_{1j}, \quad j = 1, \ldots, r. \tag{4.3.1}$$

Unbiased estimators for the expectation and variance of μ_0 are given by

$$\hat{E}(\mu_0) = \frac{1}{r} \sum_{j=1}^{r} \mu_{0j} \tag{4.3.2}$$

and

$$\hat{Var}(\mu_0) = \frac{1}{r-1} \sum_{j=1}^{r} (\mu_{0j} - \hat{E}(\mu_0))^2. \tag{4.3.3}$$

Within each valve j, conditionally given μ_{1j}, then the n-1 leakage differences (increments) are independent, normally distributed:

$$D_{ij} - D_{i-1,j} \mid \mu_{1j} \sim N(\mu_{1j}(t_i - t_{i-1}), \sigma^2(t_i - t_{i-1})) \tag{4.3.4}$$

To make estimation easier, we transform these differences into variables with equal variances (given μ_{1j}):

$$\frac{D_{ij} - D_{i-1,j}}{\sqrt{(t_i - t_{i-1})}} \;\Big|\; \mu_{1j} \sim N(\mu_{1j}\sqrt{(t_i - t_{i-1})}, \sigma^2),$$

$$j=1,\ldots,r, \; i=2,\ldots,n \tag{4.3.5}$$

The model above may be written

$$Y_{ij} \mid \mu_{1j} \sim N(\mu_{1j}x_i, \sigma^2), \quad j=1,\ldots,r; \; i=2,\ldots,n, \tag{4.3.6}$$

where

$$Y_{ij} = \frac{D_{ij} - D_{i-1,j}}{\sqrt{(t_i - t_{i-1})}} \tag{4.3.7}$$

and

$$x_i = \sqrt{(t_i - t_{i-1})}. \tag{4.3.8}$$

If each valve is considered separately, linear regression using the model (4.3.6) give a set of estimators for $\mu_{11}, \ldots, \mu_{1r}$. The formulae obtained by least squares estimation in model (4.3.6) are given by

$$\tilde{\mu}_{1j} = \frac{\sum_{i=2}^{n} x_i Y_{ij}}{\sum_{i=2}^{n} x_i^2} \tag{4.3.9}$$

$$\tilde{\sigma}_j^2 = \frac{1}{n-2} \sum_{i=2}^{n} (Y_{ij} - \hat{\mu}_{1j} x_i)^2. \tag{4.3.10}$$

Further, $100(1-\epsilon)\%$ confidence intervals for μ_{1j} and σ_j^2 are given by

$$\tilde{\mu}_{1j} \mp t_{\epsilon/2,n-2} \frac{1}{\sqrt{\Sigma x_i^2}} \tilde{\sigma}_j \tag{4.3.11}$$

and

$$\left(\frac{n-2}{z_{\epsilon/2,n-2}} \tilde{\sigma}_j^2, \quad \frac{n-2}{z_{1-\epsilon/2,n-2}} \tilde{\sigma}_j^2 \right), \tag{4.3.12}$$

respectively, where $t_{\epsilon,\nu}$ is the upper ϵ percentile of the Student t distribution with ν degrees of freedom, and $z_{\epsilon,\nu}$ is the upper ϵ percentile of the chi square distribution with ν degrees of freedom.

Results from least squares estimation is given in Table 4.3.1. A scatter diagram of the points $(\mu_{0j}, \tilde{\mu}_{1j})$ is shown in Figure 4.3.1. Note that this scatter diagram resembles the scatter diagram in Figure 3.1.1, as we ought to expect from the similarities between Model 1 and 2.

Table 4.3.1: Linear regression on each valve using (4.3.6). Estimates obtained by least squares estimation. The observed values of $\mu_{0j} = D_{1j}$ are also included.

Valve	Initial leakage	Estimates and 90% confidence intervals for parameters	
j	$\mu_{0j} = D_{1j}$	$\tilde{\mu}_{1j}$	$\tilde{\sigma}_j^2$
A	9.2	0.00078 (0.00019, 0.00136)	0.03745^2 $(0.0252^2, 0.0773^2)$
B	19.6	0.00234 (0.00129, 0.00339)	0.06677^2 $(0.0449^2, 0.1379^2)$
C	22.0	0.00768 (0.00499, 0.01037)	0.17125^2 $(0.1151^2, 0.3536^2)$
D	18.0	0.00232 (0.00059, 0.00404)	0.10980^2 $(0.0738^2, 0.2267^2)$
E	11.6	0.00210 (0.00137, 0.00282)	0.04619^2 $(0.0310^2, 0.0954^2)$

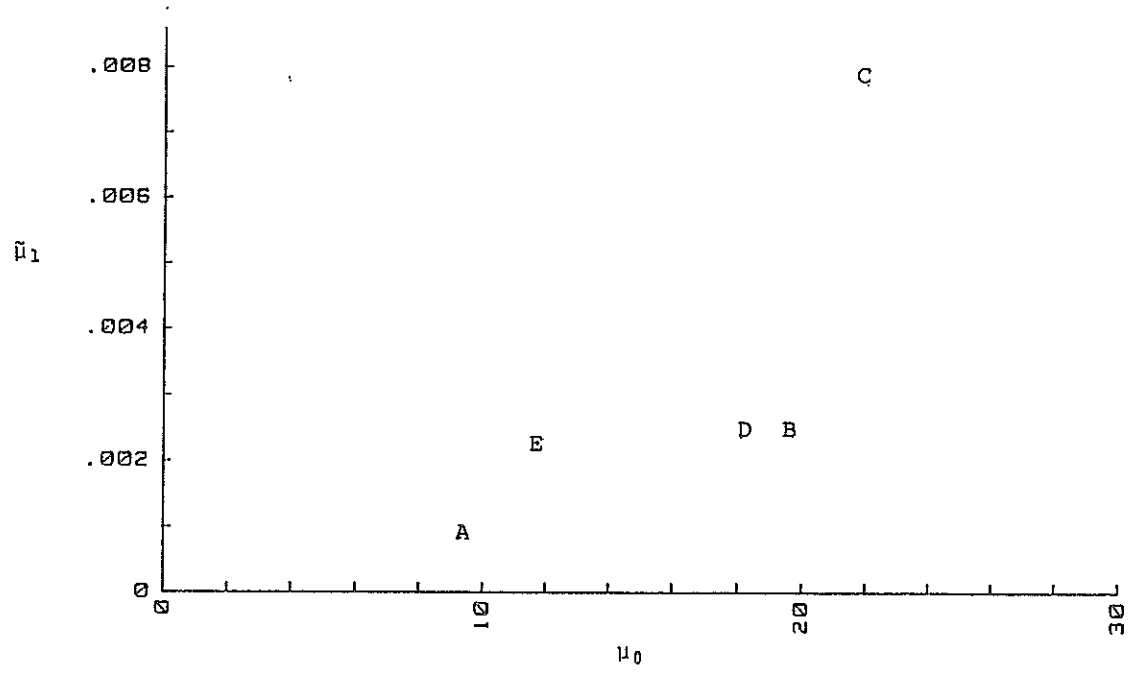

Figure 4.3.1: Scatter diagram of the points $(\mu_{0j}, \tilde{\mu}_{1j})$ from Table 4.3.1.

If $\tilde{\mu}_{1j}$, j=1,...,n, had been observations, rather than estimators, the natural estimators for $E(\mu_1)$, $Var(\mu_1)$, and $Cov(\mu_0,\mu_1)$ would have been

$$\hat{E}(\mu_1) = \frac{1}{r} \sum_{j=1}^{r} \tilde{\mu}_{1j} \tag{4.3.13}$$

$$\hat{Var}(\mu_1) = \frac{1}{r-1} \sum_{j=1}^{r} (\tilde{\mu}_{1j} - \hat{E}(\mu_1))^2 \tag{4.3.14}$$

$$\hat{Cov}(\mu_0,\mu_1) = \frac{1}{r-1} \sum_{j=1}^{r} (\mu_{0j} - \hat{E}(\mu_0))(\tilde{\mu}_{1j} - \hat{E}(\mu_1)). \tag{4.3.15}$$

Again, UMVU estimators are given by, e.g., (Spjøtvoll, 1977, Section 2.1). To obtain unbiased estimators for $Var(\mu_1)$ and $Cov(\mu_0,\mu_1)$, a term corresponding to (4.2.7) in the Model 1 has to be subtracted. To find this bias correcting term, we proceed as follows:

The model may be written in matrix form as

$$(Y_{1j}, \ldots, Y_{nj}) | \underline{\mu}_j \sim N_n(X \underline{\mu}_j , \sigma^2 A) \tag{4.3.17}$$

where

$$X = \begin{bmatrix} 1 & 0 \\ 0 & x_2 \\ \vdots & \vdots \\ 0 & x_n \end{bmatrix} \tag{4.3.18}$$

$$\underline{\mu}_j = (\mu_0, \mu_1)' \tag{4.3.19}$$

$$\mathbf{A} = \begin{bmatrix} 0 & 0 & 0 & \dots & 0 \\ 0 & 1 & 0 & & 0 \\ 0 & 0 & 1 & & 0 \\ \vdots & & & \ddots & \vdots \\ 0 & 0 & 0 & \dots & 1 \end{bmatrix} \tag{4.3.20}$$

and $Y_{1j} = D_{1j}$, $j = 1, \dots, r$. It follows that the variance-covariance matrix of $\underline{Y}_j = (Y_{1j}, \dots, Y_{nj})'$ is given by

$$\begin{aligned} V(\underline{Y}_j) &= V(X\underline{\mu}_j + \sigma^2 A) \\ &= V(X\underline{\mu}_j) + V(\sigma^2 A) \\ &= X \Lambda X' + \sigma^2 A. \end{aligned} \tag{4.3.21}$$

Least squares estimators $\hat{\underline{\mu}}_j$ for $\underline{\mu}_j$ are given as

$$\hat{\underline{\mu}}_j = (X'X)^{-1} X'Y_j \tag{4.3.22}$$

Inserting (4.3.18) into (4.3.22) yields

$$\hat{\underline{\mu}}_j = \begin{bmatrix} 1 & 0 \\ 0 & 1/\Sigma x_i^2 \end{bmatrix} \begin{bmatrix} Y_{1j} \\ \Sigma\, x_i Y_{ij} \end{bmatrix}, \tag{4.3.23}$$

which are the observations and least squares estimates already given in (4.3.1) and (4.3.9). It follows from (4.3.22) and (4.3.21) that the variance-covariance matrix of $\hat{\underline{\mu}}_j$ is

$$\begin{aligned} V(\hat{\underline{\mu}}_j) &= (X'X)^{-1} X'(X \Lambda X' + \sigma^2 A) X (X'X)^{-1} \\ &= \Lambda + \sigma^2 (X'X)^{-1} X'A X (X'X)^{-1}. \end{aligned} \tag{4.3.24}$$

Hence, the variable

$$V = \sum_{j=1}^{r} (\hat{\underline{\mu}}_j - \bar{\underline{\mu}})(\hat{\underline{\mu}}_j - \bar{\underline{\mu}})', \tag{4.3.25}$$

where

$$\bar{\underline{\mu}} = \frac{1}{r}\sum_{j=1}^{r} \hat{\underline{\mu}}_j,$$

has a 2-dimensional Wishart distribution with r-1 degrees of freedom and variance-covariance matrix (4.3.24). It follows that an unbiased estimatior for Λ is given by

$$V = \frac{1}{r}\sum_{j=1}^{r} (\hat{\underline{\mu}}_j - \bar{\underline{\mu}})(\hat{\underline{\mu}}_j - \bar{\underline{\mu}})' - \hat{\sigma}^2 (X'X)^{-1} X'A X (X'X)^{-1}. \qquad (4.3.26)$$

Above,

$$\hat{\sigma}^2 = \frac{1}{r}\sum_{j=1}^{r} \tilde{\sigma}_j^2 \qquad (4.3.27)$$

is an unbiased estimator for σ^2, and $\tilde{\sigma}_j^2$ is given by (4.3.10). Inserting (4.3.18) and (4.3.20) into the last term in (4.3.26), reduces the term to

$$\hat{\sigma}^2 \begin{bmatrix} 0 & 0 \\ 0 & 1/(\sum_{i=2}^{n} x_i^2) \end{bmatrix}. \qquad (4.3.28)$$

Hence, the estimators (4.3.3) for λ_{00} and (4.3.15) for λ_{01} are unbiased. To obtain an ubiased estimator for λ_{11}, we simply subtract $\hat{\sigma}^2/\Sigma x_i^2$ from (4.3.14). From (4.3.8) we see that

$$\sum_{i=2}^{n} x_i^2 = t_n - t_1. \qquad (4.3.29)$$

The complete set of estimators for Model 2 is, thus:

$$\hat{E}(\mu_0) = \frac{1}{r}\sum_{j=1}^{r} \mu_{0j} \qquad (4.3.30)$$

$$\hat{E}(\mu_1) = \frac{1}{r}\sum_{j=1}^{r} \tilde{\mu}_{1j} \tag{4.3.31}$$

$$\hat{Var}(\mu_0) = \frac{1}{r-1}\sum_{j=1}^{r} (\mu_{0j} - \hat{E}(\mu_0))^2. \tag{4.3.32}$$

$$\hat{Var}(\mu_1) = \frac{1}{r-1}\sum_{j=1}^{r} (\tilde{\mu}_{1j} - \hat{E}(\mu_1))^2 - \hat{\sigma}^2 \frac{1}{t_n - t_1} \tag{4.3.33}$$

$$\hat{Cov}(\mu_0,\mu_1) = \frac{1}{r-1}\sum_{j=1}^{r} (\mu_{0j} - \hat{E}(\mu_0))(\tilde{\mu}_{1j} - \hat{E}(\mu_1)) \tag{4.3.34}$$

$$\hat{\sigma}^2 = \frac{1}{r}\sum_{j=1}^{r} \tilde{\sigma}_j^2 \tag{4.3.35}$$

It can be shown that the above estimators are UMVU.

Numeric estimates

Using the above estimators, the data on valve leakage gives:

$$\hat{\theta}_0 = 16.08$$
$$\hat{\theta}_1 = 0.00304$$
$$\hat{\lambda}_{00} = 5.444^2$$
$$\hat{\lambda}_{11} = 0.00267^2 - 6.0180\cdot 10^{-7} = 0.00255^2$$
$$\hat{\lambda}_{01} = 0.00809$$
$$\hat{\sigma}^2 = 0.09937^2$$

In the expression for $\hat{\lambda}_{11}$, the last terms corresponds to $\hat{\sigma}^2/(t_n - t_1)$. The correlation coefficient between μ_0 and μ_1 may be estimated as

$$\hat{\rho} = \frac{\hat{\lambda}_{01}}{\sqrt{\hat{\lambda}_{00}\hat{\lambda}_{11}}} = 0.583.$$

A positive correlation tells us that the realizations of $\underline{\mu} = (\mu_0, \mu_1)$ tend to lie near some straight line

$$\mu_1 = \beta_0 + \beta_1 \mu_0.$$

Fitting the straight line

$$\tilde{\mu}_{1j} = \beta_0 + \beta_1 \tilde{\mu}_{0j}. \tag{4.3.9}$$

to the points $(\tilde{\mu}_{0j}, \tilde{\mu}_{1j})$, j=1, ..., r, using linear regression, gives the least squares estimates for the regression line

$$\mu_1 \approx -0.00284 + 0.00037\mu_0. \tag{4.3.10}$$

Above, μ_0 is given in cycles^{-1}, and μ_1 is given in ml/min. The estimated expectation of D(t) becomes approximately

$$\begin{aligned} E(D(t)) &= \mu_0 + \mu_1 t \\ &\approx \mu_0 + (-0.00284 + 0.00037\mu_0)t, \end{aligned} \tag{4.3.36}$$

which is similar to the straight line (4.2.17) obtained in the random coefficient regression model.

As already pointed out, $\mu_1 < 0$ does not harmonize with our understanding of the physical processes taking place, but the model may be useful if $P(\mu_1 < 0)$ is negligible for the practical purpose. Assuming a bivariate normal distribution for (μ_0, μ_1), then

$$P(\mu_1 < 0) = \Phi\left(\frac{-E(\mu_1)}{\sqrt{Var(\mu_1)}} \right).$$

In Model 2, an estimate of this probability is

$$\hat{P}(\mu_1 < 0) = \Phi\left(\frac{-\hat{E}(\mu_1)}{\sqrt{\hat{Var}(\mu_1)}} \right) = \Phi\left(\frac{-0.00304}{0.00255} \right) = 0.117,$$

which is far from negligible.

4.4 COMPARISON OF ESTIMATES IN MODEL 1 AND 2

The two models have already been compared with the prior knowledge of the physical processes taking place and measurement methods in Section 3.5. In the present section, the parameter estimates obtained in the two models are compared. These estimates are summarized in Table 4.4.1.

Table 4.4.1: Obtained estimates of the parameters.

Parameter	Model 1	Model 2
θ_0	15.93	16.08
θ_1	0.00287	0.00304
λ_{00}	5.647^2	5.444^2
λ_{11}	0.00245^2	0.00255^2
λ_{01}	0.01334	0.00809
σ^2	3.273^2	0.09937^2

Note that σ^2 represents the variance of the error term in Model 1, and the infinitesimal variance in Model 2. Hence, the two estimates at the bottom line in Table 4.4.1 are not comparable. The rest of the estimates are as about as near each other as could be expected, considering the similarities and differences between the models.

In both models, the variance terms σ^2 were tentatively estimated for each valve separately in a fixed parameter regression model. This gave the estimates $\tilde{\sigma}_j^2$, j=1,...,r shown in Table 4.2.1 and 4.3.1, respectively. Confidence intervals were also calculated and listed in the same tables. In Model 1 (Table 4.2.1), all the r 90% confidence intervals for σ_j^2 overlap each other. In Model 2, the 90% confidence interval for σ_j^2 for Valve C lies above the intervals for Valves A and E. This gives an indication that the transformed data (4.3.4) in Model 2 may not be homoscedastic. Still, the distance between these intervals is rather small compared to the length of the intervals. These confidence intervals indicate that Model 1 fits the data somewhat better than Model 2. However, we will not reject Model 2 for this reason.

If a model with estimated parameters shall harmonize with our understanding of the physical processes taking place, the probability $P(\mu_1 < 0)$ should be 0 or approximately 0 for practical purposes. Using the binormal distribution for $\underline{\mu} = (\mu_0, \mu_1)$ and the obtained parameter estimates, this probability has been estimated to 0.131 and 0.117 for the two models, respectively. These probabilities are not negligible in the applications treated in the remaining chapters. A bivariate log-normal model for $\underline{\mu}$ will be suggested in the next chapter and used throughout the report, in order to avoid these difficulties.

5. RELIABILITY ESTIMATION

The reliability of the component may be estimated for the given test conditions. Reliability may be measured in terms of several quantities, such as:

- The time to failure distribution, where failure is defined to be the time when the leakage exceeds some critical value d_c.

- The leakage distribution at time t_{max}, where t_{max} is the planned working life of the valve.

Section 5.1 suggests a revised probability model for the expectation of D(t). Estimators and estimates are obtained for the parameters in the revised model. In the remaining sections in this chapter, reliability in terms of the above quantities is estimated in Model 1 and Model 2, and the results are compared.

5.1 A REVISED MODEL FOR EXPECTED LEAKAGE

In both Model 1 and Model 2, the conditional distribution of D(t) given $\underline{\mu}$ is normal, and

$$E(D(t)|\underline{\mu}) = \mu_0 + \mu_1 t.$$

For mathematical and computational convenience, it would be desirable to assume $\underline{\mu}$ to be binormally distributed. However, in practical cases this may lead to estimated probability of $P(\mu_1 < 0)$ that are too high to be negligible, as the values 0.131 and 0.117 obtained in Chapter 4. Hence, the binormal distribution model is not always a good enough approximation to reality, and another model must be sought for these cases. A possible alternative is to assume $(\log(\mu_0),\log(\mu_1))'$ to be binormally distributed, with

$$E\begin{bmatrix} \log(\mu_0) \\ \log(\mu_1) \end{bmatrix} = \begin{bmatrix} \nu_0 \\ \nu_1 \end{bmatrix} \tag{5.1.1}$$

and

$$V\begin{bmatrix} \log(\mu_0) \\ \log(\mu_1) \end{bmatrix} = \begin{bmatrix} \tau_{00} & \tau_{01} \\ \tau_{01} & \tau_{11} \end{bmatrix}. \tag{5.1.2}$$

If $(\log(\mu_0),\log(\mu_1))'$ is binormally distributed with expectation and variance-covariance matrix as given above, then μ_0 and μ_1 are log-normally distributed with expectation and variance

$$\theta_i = E(\mu_i) = \exp(\nu_i + \tfrac{1}{2}\tau_{ii}), \qquad i = 0, 1, \tag{5.1.3}$$

and

$$\lambda_{ii} = \mathrm{Var}(\mu_i) = \exp(2\nu_i)\,[\exp(2\tau_{ii}) - \exp(\tau_{ii})], \; i = 0, 1. \tag{5.1.4}$$

To express $\mathrm{Cov}(\mu_0,\mu_1)$ in terms of the parameters in (5.1.1) and (5.1.2), we use the general identity

$$\mathrm{Cov}(\mu_0,\mu_1) = E(\mu_0\mu_1) - E(\mu_0)E(\mu_1). \tag{5.1.5}$$

Note that $\log(\mu_0) + \log(\mu_1)$ is normally distributed with

$$E(\log(\mu_0) + \log(\mu_1)) = \nu_0 + \nu_1 \tag{5.1.6}$$

and

$$\mathrm{Var}(\log(\mu_0) + \log(\mu_1)) = \tau_{00} + \tau_{11} + 2\tau_{01}. \tag{5.1.7}$$

It follows that $\mu_0\mu_1 = \exp(\log(\mu_0) + \log(\mu_1))$ is lognormally distributed, and

$$E(\mu_0\mu_1) = E\{\exp[\log(\mu_0) + \log(\mu_1)]\}$$

$$= \exp[\nu_0 + \nu_1 + \tfrac{1}{2}(\tau_{00} + \tau_{11} + 2\tau_{01})]. \qquad (5.1.8)$$

Inserting (5.1.3) and (5.1.8) into (5.1.5) gives

$$\lambda_{01} = \mathrm{Cov}(\mu_0, \mu_1)$$

$$= \exp(\nu_0 + \nu_1 + \tfrac{1}{2}\tau_{00} + \tfrac{1}{2}\tau_{11})\ [\exp(\tau_{01}) - 1]. \qquad (5.1.9)$$

Solving equations (5.1.3), (5.1.4), and (5.1.9) for ν_0, ν_1, τ_{00}, τ_{11}, τ_{01} in terms of $\underline{\theta}$, Λ gives:

$$\tau_{ii} = \log\left(\frac{\lambda_{ii}}{\theta_i^2} + 1\right), \quad i = 1, 2, \qquad (5.1.10)$$

$$\nu_i = \log(\theta_i) - \tfrac{1}{2}\tau_{ii}, \quad i = 1, 2, \qquad (5.1.11)$$

$$\tau_{01} = \log(1 + \lambda_{01}\exp[-(\nu_0 + \nu_1 + \tfrac{1}{2}\tau_{00} + \tfrac{1}{2}\tau_{11})]). \qquad (5.1.12)$$

Numeric estimates

In Section 4.2, the following estimates were found for Model 1:

$$\begin{aligned} \hat{\theta}_0 &= 15.93 \\ \hat{\theta}_1 &= 0.00287 \\ \hat{\lambda}_{00} &= 5.647^2 \\ \hat{\lambda}_{11} &= 0.00245^2 \\ \hat{\lambda}_{01} &= 0.0137 \end{aligned} \qquad (5.1.13)$$

The value of $\hat{\lambda}_{01}$ given above has been adjusted to make $\det(\hat{\Lambda}) > 0$. Inserting these values in equations (5.1.10) to (5.1.12) gives

$$\begin{aligned} \hat{\nu}_0 &= 2.709 \\ \hat{\tau}_{00} &= 0.1184 = 0.3441^2 \\ \hat{\nu}_1 &= -6.127 \\ \hat{\tau}_{11} &= 0.5474 = 0.7399^2 \\ \hat{\tau}_{01} &= 0.2621 \end{aligned} \qquad (5.1.14)$$

With the values (5.1.13), the correlation coefficient for (μ_0, μ_1) is $0.0137/(5.647 \cdot 0.00245) = 0.99$. The values (5.1.14) give as correlation coefficient for $(\log(\mu_0), \log(\mu_1))$:

$$\hat{\rho}(\log(\mu_0), \log(\mu_1)) = 0.2621/(0.3441 \cdot 0.7399) = 1.030.$$

Hence, equations (5.1.10) to (5.1.12) do not always give permissible values for ν_0, ν_1, τ_{00}, τ_{11}, τ_{01}, and the equations need to be adjusted. This is quite plausible. Two variables X_1 and X_2 have correlation 1 if and only if there exist constants $a > 0$ and b such that $X_2 = aX_1 + b$ with probability 1. Let X_1 and X_2 be normally distributed with correlation 1. This implies that $X_2 = aX_1 + b$, where $a > 0$, with probability 1. Then, the lognormally distributed variables $Y_1 = \log(X_1)$ and $Y_2 = \log(X_2)$ will lie on the curve $Y_2 = Y_1^a e^b$, with probability 1. This is not a straight line unless $a=1$, and hence, the correlation between Y_1 and Y_2 will be less than 1, unless $a=1$.

As input to calculations performed later in this report, we need permissible parameter estimates. Using the same ad hoc procedure as in Section 4.2, we shall simply adjust $\hat{\tau}_{01}$ such that the correlation becomes 0.99. That is, we set

$$\hat{\tau}_{01} = \sqrt{\hat{\tau}_{00}\hat{\tau}_{11}} \cdot 0.99 = 0.2521.$$

Hence, the complete set of estimated parameters for the distribution of $(\log(\mu_0), \log(\mu_1))$ becomes

$$\begin{aligned} \hat{\nu}_0 &= 2.709 \\ \hat{\tau}_{00} &= 0.1184 = 0.3441^2 \\ \hat{\nu}_1 &= -6.127 \\ \hat{\tau}_{11} &= 0.5474 = 0.7399^2 \\ \hat{\tau}_{01} &= 0.2521 \end{aligned} \tag{5.1.18}$$

To obtain a value $\hat{\lambda}_{01}$ corresponding to (5.1.18), these values are inserted into (5.1.9), giving

$$\hat{\lambda}_{01} = 0.01311.$$

In Section 4.3, the following estimates were found for Model 2:

$$\begin{aligned} \hat{\theta}_0 &= 16.08 \\ \hat{\theta}_1 &= 0.00304 \\ \hat{\lambda}_{00} &= 5.444^2 \\ \hat{\lambda}_{11} &= 0.00255^2 \\ \hat{\lambda}_{01} &= 0.00809 \\ \hat{\sigma}^2 &= 0.09937^2 \end{aligned} \tag{5.1.19}$$

Inserting these values in equations (5.1.10) to (5.1.12) gives

$$\begin{aligned} \hat{\nu}_0 &= 2.723 \\ \hat{\tau}_{00} &= 0.3294^2 \\ \hat{\nu}_1 &= -5.796 \\ \hat{\tau}_{11} &= 0.7299^2 \\ \hat{\tau}_{01} &= 0.1194. \end{aligned} \tag{5.1.20}$$

The values (5.1.20) give as correlation coefficient for $(\log(\mu_0),\log(\mu_1))$:

$$\hat{\rho}(\log(\mu_0),\log(\mu_1)) = 0.1194/(0.3294 \cdot 0.7299) = 0.4965.$$

5.2 VALVE RELIABILITY IN MODEL 1

Probability Distribution of D(t)

First, we shall study the probability distribution of D(t) as a function of t, and, as an example, assess it more closely for t = 13908 cycles. In Model 1, D(t) may be written

$$D(t) = \mu_0 + \mu_1 t + \sigma U$$

$$= [\ 1 \quad t\ ] \begin{bmatrix} \mu_0 \\ \mu_1 \end{bmatrix} + \sigma U$$

$$= T\underline{\mu} + \sigma U, \tag{5.2.1}$$

where $U \sim N(0,1)$ and is independent of $\underline{\mu}$. Hence, the expectation and variance of D(t) are given by

$$\begin{aligned} E(D(t)) &= T\ E(\underline{\mu}) + \sigma\ E(U) \\ &= T\ \underline{\theta} \\ &= \theta_0 + \theta_1 t \end{aligned} \tag{5.2.2}$$

and

$$Var(D(t)) = T\ V(\underline{\mu})\ T' + \sigma^2\ Var(U)$$

$$= [\ 1 \quad t\ ] \begin{bmatrix} \lambda_{00} & \lambda_{01} \\ \lambda_{01} & \lambda_{11} \end{bmatrix} \begin{bmatrix} 1 \\ t \end{bmatrix} + \sigma^2\ Var(U)$$

$$= \lambda_{00} + 2t\lambda_{01} + t^2\lambda_{11} + \sigma^2 \tag{5.2.3}$$

For example, inserting t = 13908 and the estimated values into (5.2.2) and (5.2.3) gives

$$E(D(t)) = 15.93 + 13908 \cdot 0.00287 = 55.84 \tag{5.2.4}$$

and

$$\begin{aligned} \mathrm{Var}(D(t)) &= 5.647^2 + 2\cdot 13908\cdot 0.01334 + 13908^2\cdot 0.0245^2 + 3.27^2 \\ &= 31.89 + 371.07 + 1161.08 + 10.69 \\ &= 1574.73 = 39.68^2 \end{aligned} \qquad (5.2.5)$$

In many practical situations, other characteristics of the distribution are of more interest than the expectation and variance, such as the probability of exceeding some value d_c, or some percentile of the distribution. In our model, D(t) is a sum of one or two lognormally distributed variables, and a normally distributed variable. In the numerical example above, the lognormally distributed term $t\mu_1$ gives the main part of the variance of D(t) for t=13908. Hence, the distribution of D(t) in this example should be "closer to" lognormal than to normal. In fact, this is confirmed by normal and lognormal plots of Monte Carlo simulated data. These plots are not included here, but show a reasonable fit for the lognormal distribution. The lognormal distribution will be used as an approximation below.

The Gram-Charlier and Edgeworth expansions (See e.g. Johnson & Kotz, 1970) give possible methods for finding better approximations to the distributions of $D_(t)$. These expansions give approximations in terms of the normal distributions, with corrective terms including skewness and kurtosis of the approximated distributions. These expansions were attempted on the distribution of $D_(t)$ in the example above. The results, which are not included here, gave strange-behaving multimodal "cumulative distributions", not suited for approximating the distribution of $D_(t)$. This is probably due to the fact that the estimated distribution of $D_(t)$ has skewness and kurtosis far outside the positive definite regions for these expansions (Figure 2, Johnson and Kotz, 1970).

Using the lognormal distribution as an approximation, we may, for example, estimate the probability $P(\bar{D}(13908) > 100)$. If D(t) is assumed to be lognormally distributed with mean and variance (5.2.4) and (5.2.5), then (5.1.10) and (5.1.11) give

$$\mathrm{Var}(\log(D(t))) = \log\left(\frac{39.68^2}{55.84^2} + 1\right) = 0.4088 = 0.6393^2$$

and

$$E(\log(D(t))) = \log(55.84) - \frac{1}{2}\cdot 0.4088 = 3.8181.$$

Using the lognormal distribution as an approximation, we obtain

$$P(D(13908) > 100) \approx 1 - \Phi(\frac{\log(100) - 3.8181}{0.6393}) = 0.109.$$

Other approximate probabilities, and percentiles of the distribution, may be obtained in a similar way.

Valve Failure Probability

Actually, Model 1 is not a stochastic process giving continuous sample paths. Hence, the time at which D(t) passes the critical value d_c is not well defined. We shall define the failure probability for a valve by

$$\begin{aligned} F_T(t) &= P(D(t) \leq d_c) \\ &= P(\mu_0 + \mu_1 t + \sigma U \leq d_c). \end{aligned} \tag{5.2.6}$$

In (5.2.6) the notation $F_T(t)$ is used, even though (5.2.6) as defined is not a lifetime distribution. However, $F_T(t)$ has the same properties as a lifetime distribution. The random vector $(\log(\mu_0), \log(\mu_1))$ is bilognormally distributed according to the model, and $U \sim N(0,1)$ is independent of (μ_0, μ_1). Since $P(\mu_1 > 0) = 1$, $F_T(t)$ may be expressed as

$$F_T(t) = P((\mu_0 + \sigma U - d_c)/\mu_1 \leq t), \tag{5.2.7}$$

which is equal to the cumulative distribution function for

$$W = (\mu_0 + \sigma U - d_c)/\mu_1. \tag{5.2.8}$$

If $\sigma = 0$, and μ_0 and μ_1 were independent, normally distributed, W would have a Bernstein distribution (see Section 4.6 in Part I of this thesis, and references therein). However, neither of these is the case here, and the distribution of W is not obtainable in a closed form. The cumulative

distribution function for W, based on 2000 Monte Carlo simulated sets (μ_0, μ_1, U), is shown in Figure 5.2.1.

Alternatively, an approximation of the $F_T(t)$ may be derived from the distribution of D(t). As already mentioned, the distribution of D(t) is not obtainable in a closed form. However, with the estimated parameter values, as discussed above, D(t) was found to be approximately lognormal distributed at t = 13908 cycles, and the lognormal approximation will improve when t increases. We have already found that with $d_c = 100$, then $P(T > 13908) \approx 0.891$. That is, approximately 89.1% of the failures occur for t > 13908 cycles, where the lognormal approximation is even better than at t = 13908 cycles. Hence, it seems appropriate to use the lognormal approximation for D(t) in (5.2.6). This gives

$$P(T \le t) = P(D(t) > d_c)$$

$$\approx 1 - \Phi\left(\frac{\log(d_c) - E(\log(D(t)))}{\sqrt{Var(\log(D(t)))}} \right)$$

$$= 1 - \Phi\left(\frac{\log(d_c) - [\log(a) - \frac{1}{2}\log(b^2/a^2 + 1)]}{\sqrt{\log(b^2/a^2 + 1)}} \right), \quad (5.2.9)$$

where

$$a = E(D(t)) = \theta_0 + \theta_1 t$$

and

$$b^2 = Var(D(t)) = \lambda_{00} + 2t\lambda_{01} + t^2\lambda_{11} + \sigma^2.$$

The distribution (5.2.9) is shown in Figure 5.2.1 for the estimated parameter values. In fact, the distribution (5.2.9) agrees very well with the Monte Carlo simulation based exact distribution. The two functions are hardly distinguishable in the figure.

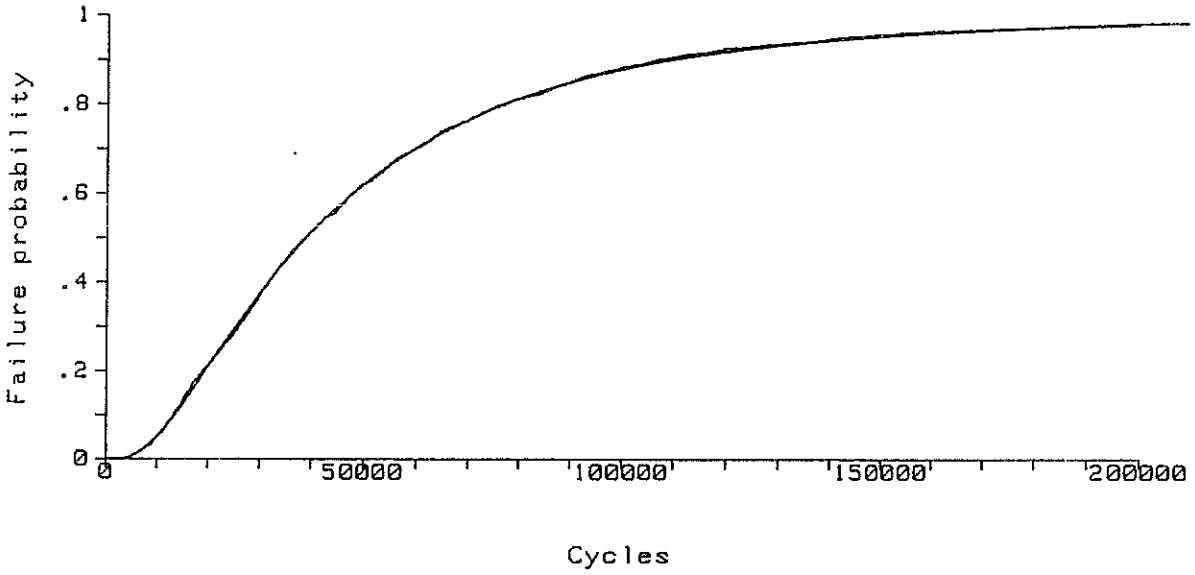

Figure 5.2.1. The failure probability $P(D(t) > d_c)$ for d_c = 100 ml/min, based on 2000 Monte Carlo simulations (step function), and the lognormal approximation (5.2.9) (smooth curve). The two curves are hardly distinguishable in the figure.

5.3 VALVE RELIABILITY IN MODEL 2

The methods and calculations used if model 2 is assumed, are quite similar to the preceding section.

Probability Distribution of D(t)

Again, we shall study the probability distribution of D(t) as a function of t, and, as an example, assess it more closely for t = 13908 cycles. In Model 2, D(t) may be written

$$D(t) = \mu_0 + \mu_1 t + \sigma\sqrt{t}\, U$$

$$= \begin{bmatrix} 1 & t \end{bmatrix} \begin{bmatrix} \mu_0 \\ \mu_1 \end{bmatrix} + \sigma\sqrt{t}\, U$$

$$= T\underline{\mu} + \sigma\sqrt{t}\, U, \qquad (5.3.1)$$

where $U \sim N(0,1)$ and is independent of $\underline{\mu}$. The expectation and variance of D(t) are given by

$$E(D(t)) = T\, E(\underline{\mu}) + \sigma\sqrt{t}\, E(U)$$
$$= T\, \underline{\theta}$$
$$= \theta_0 + \theta_1 t \qquad (5.3.2)$$

and

$$Var(D(t)) = T\, V(\underline{\mu})\, T' + \sigma^2 t\, Var(U)$$

$$= \begin{bmatrix} 1 & t \end{bmatrix} \begin{bmatrix} \lambda_{00} & \lambda_{01} \\ \lambda_{01} & \lambda_{11} \end{bmatrix} \begin{bmatrix} 1 \\ t \end{bmatrix} + \sigma^2 t\, Var(U)$$

$$= \lambda_{00} + 2t\lambda_{01} + t^2\lambda_{11} + \sigma^2 t. \qquad (5.3.3)$$

Inserting t = 13908 and the estimated values into (5.3.2) and (5.3.3) gives

$$E(D(t)) = 16.08 + 0.00304 \cdot 13908 = 58.36 \qquad (5.3.4)$$

and

$$\begin{aligned} Var(D(t)) &= 5.444^2 + 2 \cdot 13908 \cdot 0.00809 + 13908^2 \cdot 0.00255^2 \\ &\qquad + 0.09937^2 \cdot 13908 \\ &= 29.63 + 255.03 + 1257.79 + 137.33 \\ &= 1649.80 = 40.62^2. \end{aligned} \qquad (5.3.5)$$

Valve Failure Probability

The expressions for valve failure probability are somewhat different in Model 2, than was the case for Model 1. The sample paths D(t) in Model 2 are continuous functions. Hence, the lifetime of a valve is well defined in terms of the time T when D(t) first reaches the critical value d_c:

$$T = \inf \{ t : D(t) \geq d_c \}. \qquad (5.3.6)$$

Conditionally given $\underline{\mu} = (\mu_0, \mu_1)'$, then $D(t)|\underline{\mu}$ is a Wiener process with starting point μ_0 and drift μ_1. The time for this Wiener process to reach d_c has the same distribution as the time for a Wiener process with starting point 0 and the same drift to reach $d_c - \mu_0$. Hence, provided that $\mu_0 < d_c$, the conditional life distribution given $\underline{\mu}$ is inverse Gaussian with cumulative distribution function (See Section 4.4 in Part I of this thesis)

$$G(t|\underline{\mu}) = \Phi\left(\frac{\delta t - 1}{\sqrt{\nu t}} \right) + \exp\left(\frac{2\delta}{\nu} \right) \Phi\left(- \frac{\delta t + 1}{\sqrt{\nu t}} \right), \qquad (5.3.7)$$

where

$$\nu = \sigma^2/(d_c - \mu_0)^2,$$
$$\delta = \mu_1/(d_c - \mu_0).$$

On the other hand, the time to failure distribution may be defined analogous to Birnbaum-Saunders distribution by setting (See Section 4.4 in Part I of this thesis)

$$P(T \leq t) = P(\ D(t) \geq d_c\ ) \tag{5.3.8}$$

This is also analogous to the definition of valve failure probability given for Model 1 (Equation 5.2.6). In this case, provided that $\mu_0 < d_c$, the conditional life distribution is Birnbaum-Saunders with cumulative distribution function

$$G(t|\underline{\mu}) = \Phi\left[\frac{1}{\alpha} \left(\sqrt{\frac{t}{\beta}} - \sqrt{\frac{\beta}{t}} \right) \right] \tag{5.3.9}$$

where

$$\alpha = \sigma/\sqrt{\mu_1(d_c-\mu_0)},$$
$$\beta = (d_c-\mu_0)/\mu_1.$$

Whichever of (5.3.6) or (5.3.8) is chosen, the unconditional life distribution is given by

$$F_T(t) = \iint G(t|\underline{\mu})\ f_{\underline{\mu}}(\underline{\mu})\ d\mu_0\ d\mu_1, \tag{5.3.10}$$

where $f_{\underline{\mu}}(\underline{\mu})$ denotes the joint probability density for $\underline{\mu}$, and $G(t|\underline{\mu})$ is given by (5.3.7) or (5.3.9) depending on which approach is chosen. In principle, the integration in (5.3.10) is taken over $(0,\infty)x(0,\infty)$. However, $G(t|\underline{\mu})$ is not defined for $\mu_0 > d_c$ in (5.3.7) or (5.3.9). Hence, if $P(\mu_0 > d_c)$ is not negligible with the parameter estimates used, the probability distribution for $\underline{\mu}$ should be truncated accordingly, and the integration should be taken over $(0,d_c)x(0,\infty)$. In any case, with the chosen bivariate lognormal distribution for $\underline{\mu}$, the integral cannot be solved explicitly. In each practical case, the distribution of T must be assessed by Monte Carlo simulations and/or approximations. This will not be carried out any further in this report.

5.4 VALVE RELIABILITY - MODEL 1 VERSUS MODEL 2

The estimated E(D(t)) and Var(D(t)) found above for t=13908 cycles are summarized in Table 5.4.1. Estimates for E(D(t)) and Var(D(t)) at t=13756 cycles are also shown in the table, with approximate 90% confidence intervals. Figure 5.3.1 shows E(D(t)) as function of t for the two models, based on (5.2.3) and (5.3.3) with the estimated parameter values. The curves $E(D(t)) \pm \sqrt{Var(D(t))}$ based on (5.2.4) and (5.3.4) are also included.

Table 5.4.1. Some estimated values of E(D(t)) and Var(D(t)).

	t = 13908 cycles, estimates from the preceding sections		t = 13756 cycles, based on the measured values at t = 13756 cycles	
	Model 1	Model 2	Estimate [1]	Approximate 90% confidence interval [2]
E(D(t))	55.84	58.36	52.8	(15.7, 89.9)
Var(D(t))	39.68^2	40.62^2	38.93^2	$(25.27^2, 92.39^2)$

---

1) Obtained with the estimators

$$\hat{E}(D(t)) = \overline{D(t)} = \frac{1}{r}\sum_{j=1}^{r} D_j(t)$$

and

$$\hat{Var}(D(t)) = \frac{1}{r-1}\sum_{j=1}^{r} [D_j(t) - \overline{D(t)}]^2.$$

2) Assuming that $D_1(t), \ldots, D_r(t)$ are normally distributed. In fact they are only independent, identically, not normally distributed. Hence, the obtained confidence intervals are only approximations.

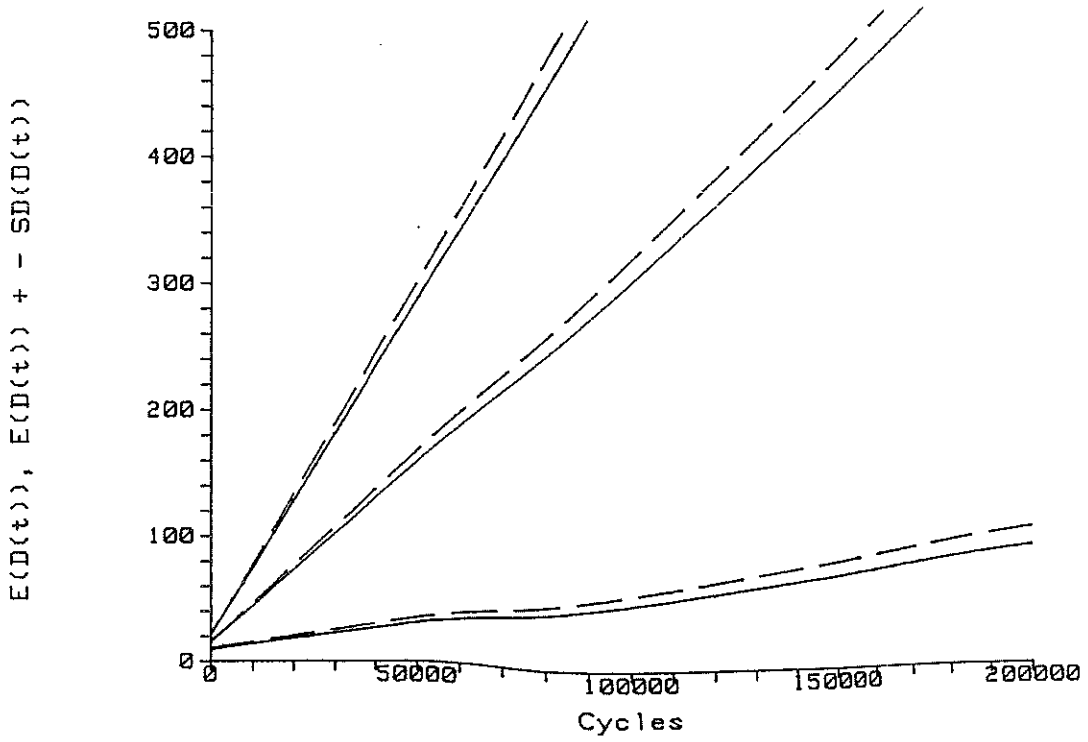

Figure 5.3.1. Estimated E(D(t)) and $E(D(t)) \pm \sqrt{Var(D(t))}$ for Model 1 (solid curves) and Model 2 (dotted curves).

Table 5.3.1 and Figure 5.3.1 show that the estimated E(D(t)) and Var(D(t)) do not differ much between the two models. Calculations are easier in Model 1 than in Model 2. Further, as noted in Chapter 3, Model 1 fits the valve leakage data somewhat better than Model 2.

In the last chapter, which covers component acceptance testing, only Model 1 will be considered in detail.

6. ACCEPTANCE TESTING

6.1 INTRODUCTION

In many applications of control valves, especially in subsea oil/gas production sites, the cost of repairing or replacing a valve far exceeds the purchase cost of a valve. In these cases, valves are acceptance tested, and only those satisfying rather strict requirements are installed. For example, the Underwater Manifold Centre (UMC) at the Cormorant Field in the North Sea contains about 250 control valves. During the acceptance testing, about 15% of the purchased control valves were discharged, due to leakage or other measurements being outside given limits. All these valves were fully capable of performing their function, but were discharged due to the risk that they could deteriorate rather fast.

The results obtained through the tests described in this report, may be used as a basis for acceptance testing with respect to leakage deterioration. Such acceptance testing may be performed in alternative ways, such as:

i) Measure the leakage through the new valves, D(0). Discharge the valves with initial leakage above a given limit.

ii) Measure the leakage through new valves, D(0), and also the leakage after a given number of cycles, $D(t_1)$. Discharge the valves with lowest predicted future reliability.

iii) As alternative ii), but in addition with measurements at one or more intermediate points in time between 0 and t_1.

In alternative i), the obvious acceptance criterion is $D(0) \leq k$, determined by a critical value k. In alternatives ii) and iii), the selection criteria are not so obvious. In Section 6.2 below, the class of reasonable linear criteria for case ii) is derived. In Section 6.3, a procedure for choosing the approximately "best" among the linear criteria is developed and described.

6.2 A CLASS OF LINEAR ACCEPTANCE CRITERIA

In this section, a class of linear acceptance criteria for case ii) above is derived.

Assume that the reliability is measured in terms of the leakage distribution at the end of the planned working life of the valve. If the planned working life is t_{max}, then a valve having passed this acceptance test will have age $t_1 + t_{max}$ at the end of the working life. Any acceptance criterion in alternative ii) may stated as to accept the valve if

$$f(D(0),D(t_1)) \leq k, \tag{6.2.1}$$

where the function f and the constant k determine the criterion.

What sort of functions f give reasonable acceptance criteria? Consider 3 valves, with measured values og $D(0)$ and $D(t_1)$ as illustrated in Figure 6.2.1. It seems quite obvious to give the following "ranking" of these valves:

i) Valve 1 seems better than valve 2.

ii) Valve 1 seems better than valve 3.

iii) It is not possible to rank Valve 2 and 3 relative to each other without more information available.

Rewriting criterion (6.2.1) in terms of another function f_1 as

$$f_1(D(0),D(t_1)-D(0)) \leq k, \tag{6.2.2}$$

statements i) and ii) above mean that f_1 ought to be strictly increasing in its first and second argument, respectively. Note that for a fixed value of $D(t_1)$, f_1 needs not be an increasing function of $D(0)$.

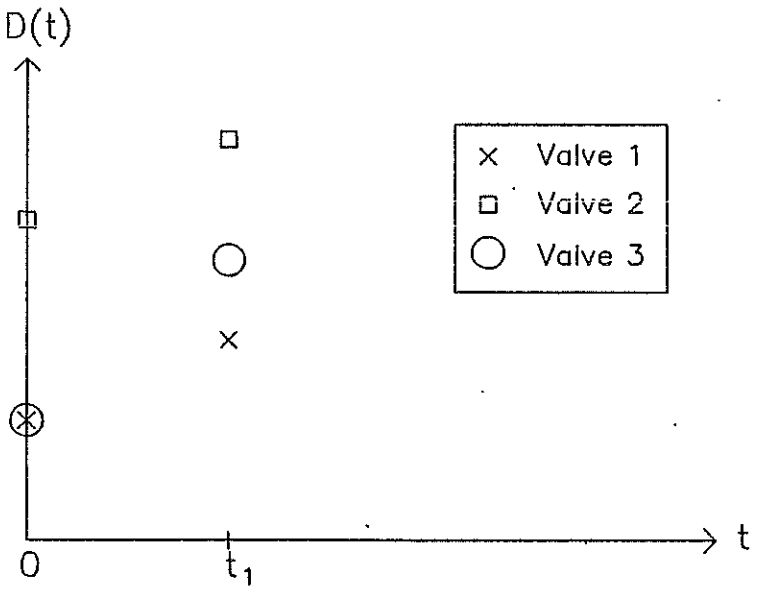

Figure 6.2.1. Comparison of possible leakage measurements at time 0 and t_1.

For simplicity, we shall confine ourselves to linear functions f_1, that is, acceptance criteria of the type

$$a_1 D(0) + b_1[D(t_1) - D(0)] \leq c_1, \quad a_1 > 0, \; b_1 > 0. \tag{6.2.3}$$

This is equivalent to each of the criteria

$$a_2 D(0) + [D(t_1) - D(0)] \leq c_2, \quad a_2 > 0$$

$$(a_2 - 1)D(0) + D(t_1) \leq c_2, \quad a_2 > 0$$

$$aD(0) + D(t_1) \leq c, \quad a > -1. \tag{6.2.4}$$

Since $D(t_1)$ is the measurement closest to $t_1 + t_{max}$, it seems reasonable to consider only criteria with more weight on $D(t_1)$ than on $D(0)$. That is, we consider only criteria with $a < 1$. Hence, the class of criteria to consider becomes

$$aD(0) + D(t_1) \leq c, \quad -1 < a < 1. \tag{6.2.5}$$

In order to obtain a better understanding of acceptance criterion (6.2.5), it may be illustrated as follows: Plot the points $(0,D(0))$ and $(t_1,D(t_1))$ in a coordinate system with linear axes. Draw the straight line through these two points. This line has the equation

$$d(t) = D(0) + \frac{D(t_1) - D(0)}{t_1}\, t. \qquad (6.2.6)$$

Let $t_{crit} = t_1/(a+1)$ and $d_{crit} = c/(a+1)$. Then, criterion (6.2.5) is equivalent to

$$d(t_{crit}) \le d_{crit}, \quad t_{crit} > t_1/2. \qquad (6.2.7)$$

This criterion is illustrated in Figure 6.2.2. Note that

$$a < 0 \Leftrightarrow t_{crit} > t_1$$
$$a = 0 \Leftrightarrow t_{crit} = t_1$$
$$a > 0 \Leftrightarrow t_1/2 < t_{crit} < t_1.$$

In the example illustrated in Figure 6.2.2, $a < 0$, and $t_{crit} > t_1$.

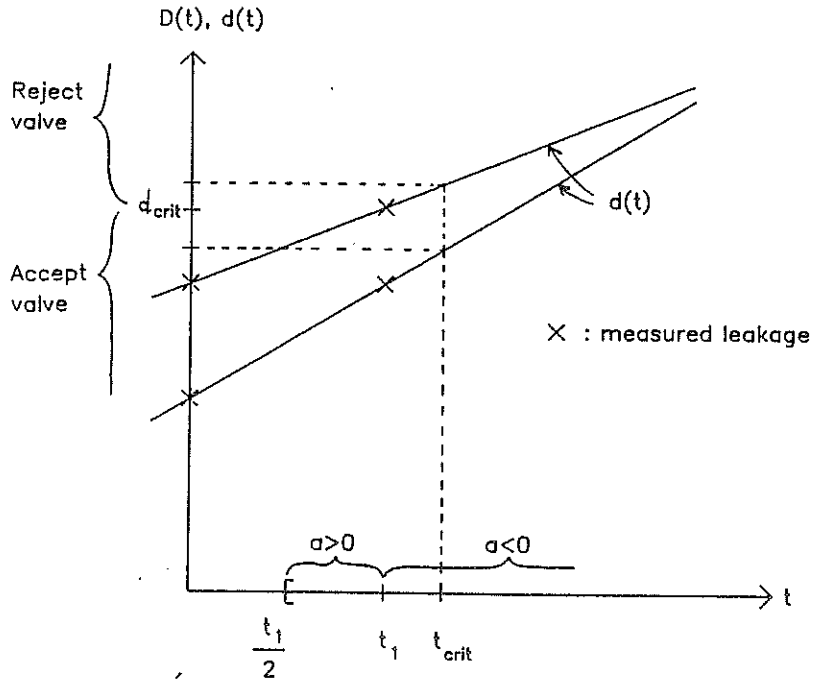

Figure 6.2.2. An example on the acceptance criterion given by Equation (6.2.7). The valves with $d(t_{crit}) < t_{crit}$ are accepted.

6.3 A PROCEDURE FOR CHOOSING A LINEAR ACCEPTANCE CRITERION

In this section, a procedure is developed and described, for choosing the approximately "best" among linear criteria like those described in the previous section. First, the procedure is explained in detail for the case where leakage is measured at two points in time. Secondly, this procedure is performed for a numerical example, including some studies of the "optimality" of the procedure. At the end, a scheme for the procedure in a more general situation is given.

Application of Multinormal Distribution Results

Assume that the valve leakage $D(0)$ and $D(t_1)$ is measured at time 0 and t_1. Based on these measurements, the valves with lowest predicted leakage at time $t_1 + t_{max}$ will be accepted. For the valve population considered, the following parameters are known (or have been estimated):

$$E(\underline{\mu}) = \underline{\theta}$$

$$V(\underline{\mu}) = \Lambda = \begin{bmatrix} \lambda_{00} & \lambda_{01} \\ \lambda_{10} & \lambda_{11} \end{bmatrix}$$

$$\mathrm{Var}(D(t)|\underline{\mu}) = \sigma^2$$

First, fit a normal distribution to $(\log(\mu_0), \log(\mu_1))$ using (5.1.10) to (5.1.12). If the estimates give a correlation coefficient with absolute value greater than 1, adjust them to make it less than 1. Now, consider the probability distribution of the stochastic vector $(D(0), D(t_1), D(t_1 + t_{max})'$. For convenience, we shall use the notation

$$t_2 = t_1 + t_{max},$$
$$D_0 = D(0),$$
$$D_1 = D(t_1),$$
$$D_2 = D(t_2),$$

and

$$\underline{D} = \begin{bmatrix} D_0 \\ D_1 \\ D_2 \end{bmatrix}. \tag{6.3.1}$$

In our model, we have

$$\begin{bmatrix} D_0 \\ D_1 \\ D_2 \end{bmatrix} = \begin{bmatrix} \mu_0 + \sigma U_0 \\ \mu_0 + \mu_1 t_1 + \sigma U_1 \\ \mu_0 + \mu_1 t_2 + \sigma U_2 \end{bmatrix}$$

$$= \begin{bmatrix} 1 & 0 \\ 1 & t_1 \\ 1 & t_2 \end{bmatrix} \begin{bmatrix} \mu_0 \\ \mu_1 \end{bmatrix} + \sigma \begin{bmatrix} U_0 \\ U_1 \\ U_2 \end{bmatrix} \tag{6.3.2}$$

$$= T\underline{\mu} + \sigma\underline{U},$$

where $(\log(\mu_0), \log(\mu_1))$ is binormally distributed, and U_0, U_1, U_2 are independent standard normally distributed and independent of $\underline{\mu}$. From (6.3.2), the expectation and variance-covariance matrix of $\underline{D}$ are found to be:

$$E(\underline{D}) = T\,E(\underline{\mu}) = \begin{bmatrix} 1 & 0 \\ 1 & t_1 \\ 1 & t_2 \end{bmatrix} \begin{bmatrix} \theta_0 \\ \theta_1 \end{bmatrix} \tag{6.3.3}$$

and

$$V(\underline{D}) = V(T\underline{\mu}) + V(\sigma\underline{U})$$

$$= T\,V(\underline{\mu})\,T' + \sigma^2 I_3$$

$$= \begin{bmatrix} 1 & 0 \\ 1 & t_1 \\ 1 & t_2 \end{bmatrix} \begin{bmatrix} \lambda_{00} & \lambda_{01} \\ \lambda_{01} & \lambda_{11} \end{bmatrix} \begin{bmatrix} 1 & 1 & 1 \\ 0 & t_1 & t_2 \end{bmatrix} + \sigma^2 I_3$$

$$= \begin{bmatrix} \lambda_{00}+\sigma^2 & & \text{(Symmetric matrix)} \\ \lambda_{00}+t_1\lambda_{01} & \lambda_{00}+2t_1\lambda_{01}+t_1{}^2\lambda_{11}+\sigma^2 & \\ \lambda_{00}+t_2\lambda_{01} & \lambda_{00}+(t_1+t_2)\lambda_{01}+t_1t_2\lambda_{11} & \lambda_{00}+2t_2\lambda_{01}+t_2{}^2\lambda_{11}+\sigma^2 \end{bmatrix}. \tag{6.3.4}$$

We are interested in the conditional distribution of $(D_2 \mid D_0=d_0,\ D_1=d_1)$. Each of the random variables D_0, D_1, and D_2 equal a sum of one or two lognormally distributed variables, and a normally distributed variable. Hence, finding an explicit expression for the distribution of $(D_2 \mid D_0=d_0,\ D_1=d_1)$ does not seem feasible.

Partition $\underline{D}$ and its variance-covariance matrix as follows:

$$\underline{D} = \begin{bmatrix} \underline{D}_1 \\ \underline{D}_2 \end{bmatrix} \tag{6.3.5}$$

where

$$\underline{D}_1 = \begin{bmatrix} D_0 \\ D_1 \end{bmatrix}, \qquad \underline{D}_2 = [\, D_2 \,],$$

and

$$\mathrm{Var}(\underline{D}) = \begin{bmatrix} \Gamma_{11} & \Gamma_{12} \\ \Gamma_{21} & \Gamma_{22} \end{bmatrix}, \tag{6.3.6}$$

In (6.3.6), Γ_{11} is the variance-covariance matrix of $\underline{D}_1$, and is made up of the upper left 2x2 elements in (6.3.4). Further, Γ_{22} is the

variance of $\underline{D}_2$, and $\Gamma_{12} = \Gamma_{21}'$ are the covariances between $\underline{D}_1$ and $\underline{D}_2$, which are the two first entries of the last row in (6.3.4).

If $\underline{D}$ was multinormally distributed with the expectation and variance-covariance matrices given above, then conditional distribution of $\underline{D}_2$ given $\underline{D}_1=\underline{d}_1$ would be multinormal with mean and variance:

$$E(\underline{D}_2 \mid \underline{D}_1=\underline{d}_1) = E(\underline{D}_2) + \Gamma_{21}\Gamma_{11}^{-1}(\underline{d}_1 - E(\underline{D}_1)) \tag{6.3.7}$$

$$Var(\underline{D}_2 \mid \underline{D}_1=\underline{d}_1) = \Gamma_{22} - \Gamma_{21}\Gamma_{11}^{-1}\Gamma_{12} \tag{6.3.8}$$

The above result is given i.e. in Mardia & al (1979) p 63. However, $\underline{D}$ is not multinormally distributed. Still, (6.3.7) and (6.3.8) may provide reasonably good approximations. In fact, (6.3.7) gives the best linear predictor for $\underline{D}_2$ under squared error loss for all distributions, as seen by the following argument:

Let ξ be any linear predictor for D_2, that is, let

$$\xi = E(D_2) + a'[\underline{D}_1 - E(\underline{D}_1)] \tag{6.3.9}$$

for some column vector a with the same dimension as $\underline{D}_1$. The squared prediction error is

$$\begin{aligned} L^2 &= (D_2 - \xi)^2 \\ &= (D_2 - \{E(D_2) + a'[\underline{D}_1 - E(\underline{D}_1)]\})^2 \\ &= (\{[D_2 - E(D_2)] - a'[\underline{D}_1 - E(\underline{D}_1)]\})^2. \end{aligned} \tag{6.3.10}$$

The expected squared error loss is

$$E(L^2) = VarD_2 - 2a'\Gamma_{12} + a'\Gamma_{11}a. \tag{6.3.11}$$

The derivative with respect to a, that is the vector of partial derivatives with respect to the components of a, is

$$\frac{\partial E(L2)}{\partial a} = -2\Gamma_{12} + 2\Gamma_{11}a. \tag{6.3.12}$$

Setting (6.2.12) equal to the zero vector yields

$$a = \Gamma_{11}^{-1}\Gamma_{12},$$
$$a' = \Gamma_{12}\Gamma_{11}^{-1}. \tag{6.3.13}$$

Inserting (6.3.13) into (6.3.9) yields the right side of (6.3.7). The minimal expected squared prediction error is obtained by entering (6.3.13) into (6.3.11), giving the right side of (6.3.8).

Inserting (6.3.3) and (6.3.4) into (6.3.6), and performing the required matrix operations yields

$$E(\underline{D}_1) = \begin{bmatrix} \theta_0 \\ \theta_0 + \theta_1 t_1 \end{bmatrix} \tag{6.3.14}$$

$$E(\underline{D}_2) = \theta_0 + \theta_1 t_2 \tag{6.3.15}$$

and

$$\Gamma_{21}\Gamma_{11}^{-1} = [g_1, g_2]/g_3 \tag{6.3.16}$$

where

$$g_1 = t_1^2\lambda_{00}\lambda_{11} - t_1^2\lambda_{01}^2 + t_1t_2\lambda_{01}^2 - t_1t_2\lambda_{00}\lambda_{11} + t_2\lambda_{01}\sigma^2 + \lambda_{00}\sigma^2$$

$$g_2 = t_1t_2\lambda_{00}\lambda_{11} - t_1t_2\lambda_{01}^2 + t_1t_2\lambda_{11}\sigma^2 + t_1\lambda_{01}\sigma^2 + t_2\lambda_{01}\sigma^2 + \lambda_{00}\sigma^2$$

$$g_3 = t_1^2[\lambda_{11}(\lambda_{00} + \sigma^2) - \lambda_{01}^2] + 2t_1\lambda_{01}\sigma^2 + 2\lambda_{00}\sigma^2 + \sigma^4.$$

A Numerical Example

In Section 5.1, estimated parameters in the binormal distribution of $(\log(\mu_0),\log(\mu_1))$ were calculated, and $\tau_{01} = \mathrm{Cov}(\log(\mu_0),\log(\mu_1))$ was adjusted to make the absolute value of the correlation less than 1. The corresponding adjusted value of λ_{01} was obtained by inserting (4.1.17)

and the rest of the parameters in (4.1.14) into (4.1.9), which gives $\lambda_{01} = 0.01311$. Hence, the set of basic parameters in the model becomes:

$$\begin{aligned} \theta_0 &= 15.93 \\ \theta_1 &= 0.00287 \\ \lambda_{00} &= 5.647^2 \\ \lambda_{11} &= 0.00245^2 \\ \lambda_{01} &= 0.01311 \\ \sigma^2 &= 3.273^2 \end{aligned} \tag{6.3.17}$$

Here, the notation θ_0, θ_1, ..., is used instead of $\hat{\theta}_0$, $\hat{\theta}_1$, ..., for convenience, even though strictly, they are estimates.

In order to get a feeling for how good the model and the approximations are, we use two times for which we have observations:

$$\begin{aligned} t_1 &= 2500 \\ t_2 &= 16408 \end{aligned}$$

Hence, we use the value $t_{max} = t_2 - t_1 = 13908$ in the example. Inserting these values into the appropriate equations above gives

$$\begin{aligned} E(D_0) &= 15.93 \\ E(D_1) &= 23.105 \\ E(D_2) &= 63.02 \\ \Gamma_{21}\Gamma_{11}^{-1} &= [0.96748,\ 3.18144] \end{aligned}$$

Hence,

$$\begin{aligned} E(D_2|(D_0,D_1)) &= 63.02 + 0.96748(D_0 - 15.93) + 3.18144(D_1 - 23.105) \\ &= 0.96748D_0 + 3.18144D_1 - 25.90 \\ &= aD_0 + bD_1 + c. \end{aligned} \tag{6.3.18}$$

Accepting a valve if (6.3.18) does not exceed a given value, gives a linear acceptance criterion agreeing with (6.2.5), since $|0.96748| < 3.18144$. Further, (5.3.5) and (6.3.8) give

$$Var(D_2) = 45.62^2$$

and

$$\mathrm{Var}(D_2|(d_0,d_1)) = 13.294^2.$$

Table 6.3.1 gives the results when inserting the measured leakages of the five valves into (6.3.18). These results agree well with the measured leakages D_2.

Table 6.3.1. Conditional expectation of D_2 from (6.3.18), and measured values of D_2.

d_0	d_1	$E(D_2\|(d_0,d_1))$	d_2
9.2	13.8	26.90	22
19.6	20.0	56.69	58
22.0	50.4	155.73	148
19.0	25.2	71.69	56
11.6	17.2	40.05	46

Continuing this example, assume that this type of valves will be accepted by the following criterion: The probability that the leakage after 13908 cycles in use shall exceed 100 ml/min, must be lower than a given, low probability α, say, $\alpha = 0.01$. That is, we require that

$$P(D(13908) > 100) \leq \alpha. \qquad (6.3.19)$$

For the given valve population, (5.2.5) gives $\mathrm{Var}(D(13908))\ 39.68^2$, and

$$P(D(13908) > 100) \approx 1 - \Phi\left(\frac{100 - (15.93 + 0.00287 \cdot 13908)}{39.68}\right) = 0.132,$$

which does not satisfy (6.3.19) for "low" values of α. In order to meet the requirement, the valves are tested and accepted as follows: Test the valves for time t_1=2500 cycles, and measure the leakage at times 0 and t_1. Find a criterion value c_α, and accept only the valves with $D_0=d_0$ and $D_1=d_1$ such that

$$E(D_2 \mid d_0,d_1) \approx ad_0 + bd_1 + c \leq c_\alpha, \qquad (6.3.20)$$

where $D_2 = D(2500 + 13908)$, and a, b, and c are given in (6.3.18). The criterion value c_α is set such that

$$P(D_2 > 100 \mid ad_0 + bd_1 + c \le c_\alpha) \le \alpha. \tag{6.3.21}$$

Now, we only want to accept valves with d_0, d_1 such that

$$P(D_2 > 100 \mid (d_0, d_1) \in \text{Acceptance region}) \le \alpha.$$

In the multivariate normal approximation, we have

$$E(D_2 \mid d_0, d_1) = ad_0 + bd_1 + c,$$
$$\text{Var}(D_2 \mid d_0, d_1) = 13.294^2,$$

and

$$P(D_2 > 100 \mid d_0, d_1) \approx 1 - \Phi\left(\frac{100 - ad_0 + bd_1 + c}{13.294}\right) \le \alpha$$

gives

$$ad_0 + bd_1 + c \le 100 - 13.294u_\alpha \tag{6.3.22}$$

where u_α is the upper α percentile of the standard normal distribution. Hence,

$$c_\alpha = 100 - 13.294u_\alpha. \tag{6.3.23}$$

Using this acceptance criterion, the probability that a random valve will be accepted, is

$$p_\alpha = P(aD_0 + bD_1 + c \le c_\alpha) \approx \Phi\left(\frac{c_\alpha - 63.02}{43.725}\right). \tag{6.3.24}$$

The normal distribution approximations used in (6.3.22) and (6.3.24) are probably poorest near the distribution tail, i.e. for values of α near 0. Table 6.3.2 gives c_α and p_α for some values of α.

Table 6.3.2. Some values of c_α and p_α calculated from (6.3.22) and (6.3.24). Some results from Monte Carlo simulation of 2000 valves are also given.

Based on the normal distribution approximations (6.3.22) and (6.3.24)			Results from Monte Carlo simulations with acceptance limit c_α	
α	c_α	p_α	P(Accept valve)	$P(D_2>100 \mid \text{Accepted})$
0.1	82.957	0.676	0.725	0.00344
0.05	78.131	0.635	0.694	0.00144
0.025	73.944	0.597	0.658	0.00076
0.01	69.078	0.555	0.616	0
0.005	65.755	0.525	0.586	0
0.001	58.922	0.462	0.523	0

In order to check how well the above results, based on the multivariate normal distribution, agree with the model composed of lognormal and normal distributions, 2000 valves were Monte Carlo simulated according to the model. Figure 6.3.1 shows a normal probability plot of the distribution of D_2 (leakage after 16408 cycles). It appears that the distribution of D_2 in this case differs significantly from the normal distribution. This was expected, since $D_2 = \mu_0 + \mu_1 t_2 + \sigma^2 U_2$, and the main contribution to the variance of D_2 comes from $\text{Var}(\mu_1 t_2) = t^2 \lambda_{11} = 16408^2 \cdot 0.00245^2 = 40.20^2$. The coefficient μ_1 is lognormally distributed, and D_2 is approximately lognormally distributed. This has been confirmed by a lognormal plot of the simulated values of D_2, not shown here. Since the distribution of D_2 differs significantly from the normal distribution, we may also expect the distribution of $D_2 \mid (ad_0+bd_1+c)$ to differ from the normal distribution. This may explain the relatively large differences between p_α and simulated P(Accept valve) in Table 6.3.2.

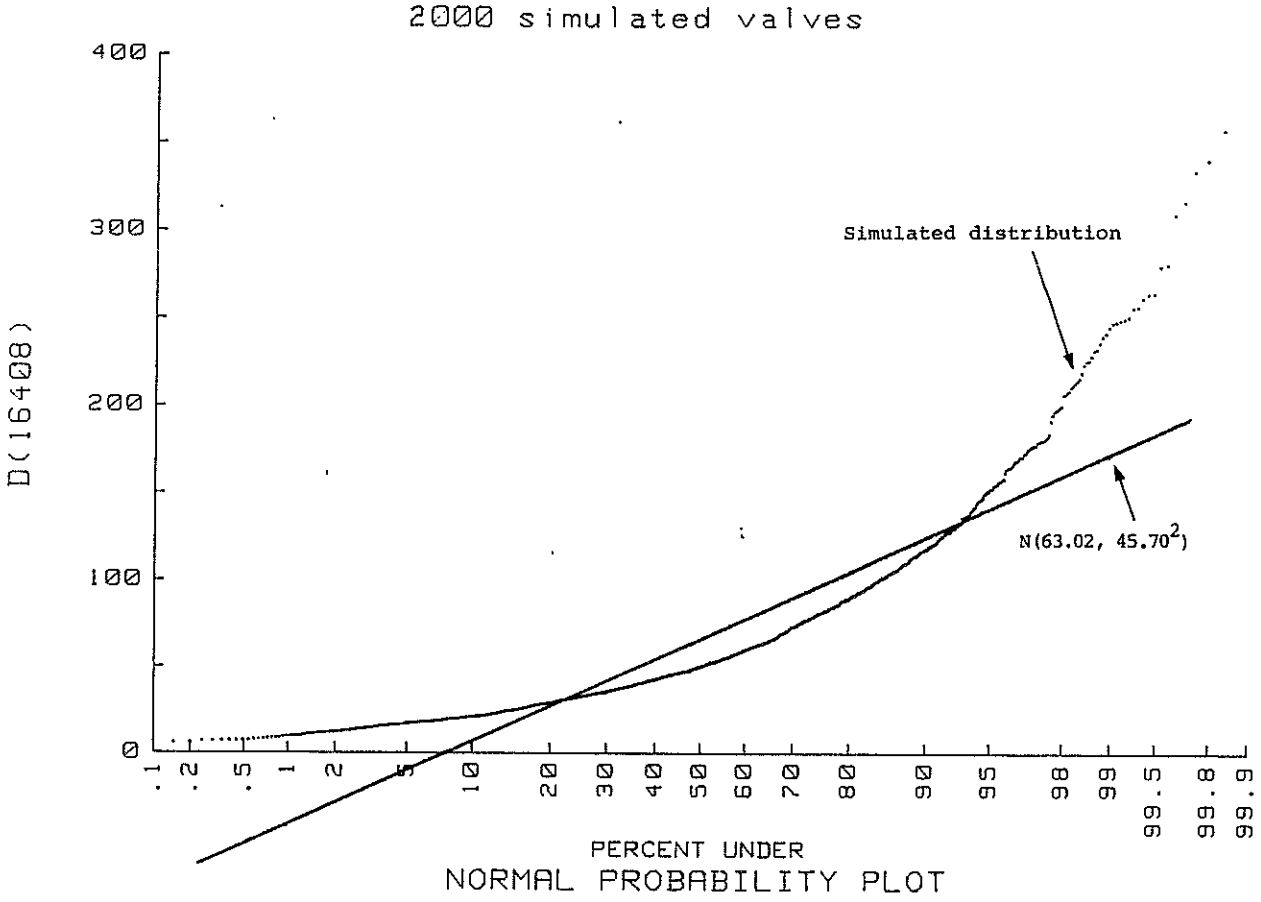

Figure 6.3.1. Normal probability plot of the simulated distribution of D_2 (2000 simulations). The solid line shows the normal distribution function with mean 63.02 and variance 45.70^2.

Further, note that in Table 6.3.2,

$$\alpha \approx P(D_2 > 100 \mid ad_0 + bd_1 + c = c_\alpha)$$

is based on the multinormal distribution approximation, and

$$P(D_2>100|\text{Accepted}) = P(D_2 > 100 \mid ad_0 + bd_1 + c \leq c_\alpha)$$

is based on the Monte Carlo simulations. I order to compare the simulation results to the normal approximation values, it would be interesting to find the values of

$$P(D_2 > 100 \mid ad_0 + bd_1 + c = c_\alpha)$$

for the simulated valves, and compare them to the values of α in Table 6.3.2. However, this cannot be done directly. The variable $aD_0 + bD_1 + c$ is continuously distributed. Hence, we can hardly obtain many simulations with $ad_0 + bd_1 + c \approx c_\alpha$ for a given c_α. However, it is possible to get a rough feeling for the agreement between α and the corresponding values for the simulated valves. From Table 6.3.2, we should expect $P(D_2 > 100 \mid ad_0 + bd_1 + c)$ to be in the interval (0.05, 0.1), or near this interval, for the valves with $78.131 \leq ad_0 + bd_1 + c \leq 82.957$. The detailed simulation results (not included here) show that among 60 valves with $78.131 \leq ad_0 + bd_1 + c \leq 82.957$, 3 valves had $d_2 > 100$. This gives an estimated probability equal to $3/60 = 0.05$, which agrees well with what we expected.

The distributions of D_2, and of $D_2|(d_0,d_1)$, are "in between" normal and lognormal, but "closest to" the latter. Alternative computations of p_α, using lognormal instead of normal distribution, gave values about as different from the simulated P(Accept valve) as the ones given in Table 6.3.2, on the other side of P(Accept valve).

As derived in Section 6.2, a linear acceptance criterion for a valve should be to accept the valve if

$$aD_0 + D_1 \leq c, \qquad -1 < a < 1, \tag{6.3.25}$$

where the parameters a and c determine the criterion. The criterion used above is of this type, with $a = 0.96748/3.18144 = 0.30410$. The acceptance limit c determines the fraction of the valves to accept. Figure 6.3.2 shows $P(D_2>100|\text{Accepted})$ as a function of P(Accept) for the simulated valves. Note that P(Accept) is a strictly increasing function of c.

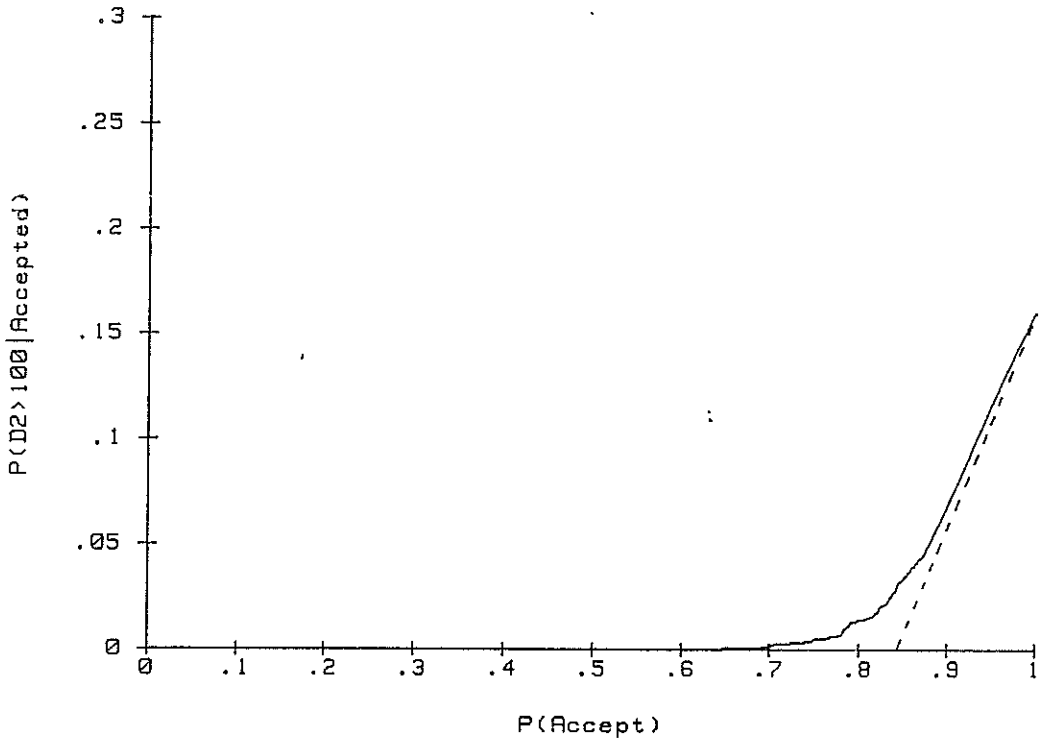

Figure 6.3.2: $P(D_2>100|\text{Accepted})$ as a function of P(Accept) for the simulated valves, with a valve acceptance criterion based on $0.30410D_0 + D_1$. The dotted line shows the corresponding function for a hypothetical, "perfect" criterion (6.3.26).

For the 2000 simulated valves, $p_e = P(D_2>100) = 0.160$. If a "perfect" acceptance criterion had existed, we would, based on an observed set (d_0, d_1), give a perfect prediction for whether D_2 is above or below 100. Hence, for that "perfect" criterion, $\gamma = P(D_2>100|\text{Accepted})$ as a function of $\beta = P(\text{Accept})$ would have been:

$$\gamma(\beta) = \begin{cases} 0 & \text{for } 0 \le \beta \le 1 - p_e \\ \beta - (1 - p_e) & \text{for } 1 - p_e \le \beta \le 1 \end{cases} \qquad (6.3.26)$$

The function 6.3.20 is also shown in Figure 6.3.2. The two functions are so close that the derived acceptance criterion seem reasonably satisfactory.

The value a = 0.30410 in (6.3.25) was derived as the best acceptance criterion using multinormal distribution theory. Our model is not multinormal, and another value may provide a better criterion. Several values of a were tried out on the 2000 simulated valves. For each value of a, we may define the function $\gamma(\beta)$ where β = P(Accept valve) and γ = $P(D_2>100|\text{Accepted})$. This function was drawn for each value of a, and some of them are shown in Figure 6.3.3. If one criterion gives a function $\gamma(\beta)$ below that of another criterion, the one with the lowest $\gamma(\beta)$ values is better. Visual comparisons between these functions, and the function for a = 0.30410, are summarized in Table 6.3.3.

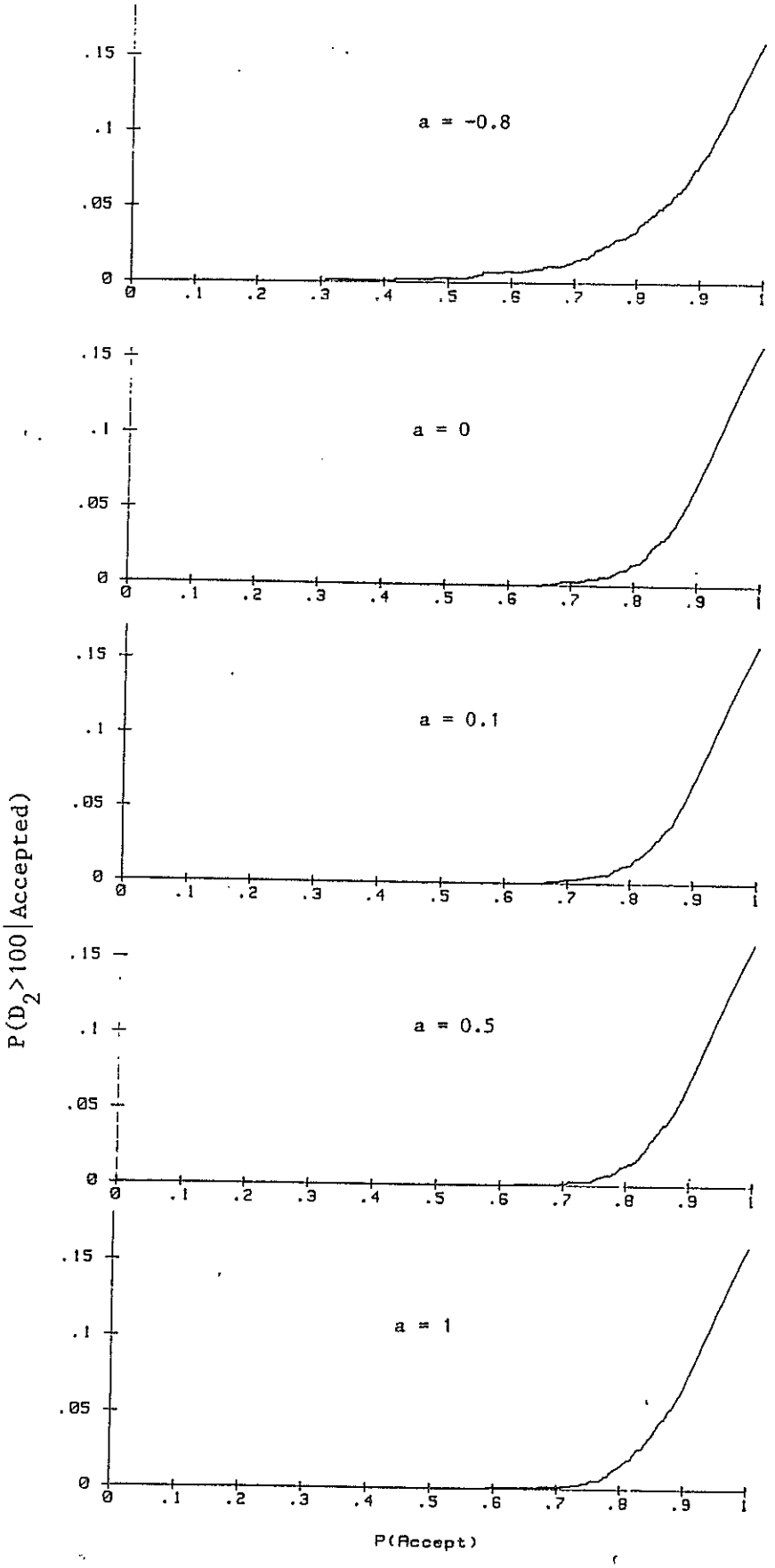

Figure 6.3.4: $P(D_2>100|\text{Accepted})$ as a function of P(Accept) for the simulated valves, with a valve acceptance criterion based on $aD_0 + D_1$, for some values of a.

Table 6.3.3. Comparison between acceptance criteria based on $aD_0 + D_1$, for several values of a, based on visual comparisons between Figures 6.3.4 and 6.3.5.

a	Compared to the criterion based on a = 0.30410
-0.8	Significantly worse
0	Perhaps slightly worse
0.1	Hardly any difference
0.30410	-
0.5	No difference is seen
1	Hardly any difference

Figure 6.3.4 and Table 6.3.3 tell us that even if a = 0.30410 may not give the optimal linear criterion, hardly anything is gained by choosing another value of a. In fact, hardly any difference was seen over a large range for a, including the range from 0 to 1. This is probably due to the model structure (6.3.2) of $\underline{D}$, and the parameter values used: If $D_1=d_1$ is known, then the value of $D_0=d_0$ will not provide much more information on D_2. In other words, the conditional distribution of $D_2|D_1=d_1$ probably does not differ much from the conditional distribution of $D_2|(d_0,d_1)$.

It is probably correct to draw this conclusion even further, at least for the model and parameter values used: It seems likely that the criterion will not improve much, if anything at all, if it is changed to a non-linear criterion "not very far away" from $0.30410D_0 + D_1$. Since a possibly optimal, non-linear acceptance criterion probably will not be "very far" away from the best linear criterion, not much is gained by looking at non-linear criteria.

The above conclusion is not necessarily the true for other parameter values.

A General Algorithm for the Procedure

The multinormal distribution approach may also be used when leakage is measured at more than points in time. It may be generalized as follows:

1) Find the expectation and the variance-covariance matrix of $\underline{D} = (D(0), \ldots, D(t_1), D(t_{max}))$.

2) Calculate the conditional expectation and variance $D(t_{max})|(D(0), \ldots, D(t_1))$, as if $\underline{D}$ had been multinormally distributed. This is performed by straightforward matrix multiplications, using results from multivariate analysis. The conditional expectation is some linear function of $D(0), \ldots, D(t_1)$, say, $a_0D(0) + \ldots + a_1D(t_1)$.

3) The distribution of D(t) for t=0 may agree less well with the model than for $t > 0$. In order to reduce the effect of this model discrepancy, modify $a_0D(0) + \ldots + a_1D(t_1)$ by reducing reduce the (absolute value) of a_0.

4) The criterion is to accept the valve if $a_0D(0) + \ldots + a_1D(t_1) \leq k$, where k is the critical value. The critical value k may be found using results based on the multinormal distribution assumption, or better, based on Monte Carlo simulations from the true distribution of $\underline{D}$.

REFERENCES

Cox, D. R. & Miller, H. D.: (1965) "The Theory of Stochastic Processes". Chapman and Hall, London.

Ditlevsen, O. & Olesen, R.: (1986) "Statistical Analysis of the Virkler Data on Fatigue Crack Growth". Engineering Fracture Mechanics, Vol 25, No 2, 1986, pp 177 - 195.

Hudak, S. J. Jr, Saxena, A., Bucci, R. J., & Malcolm, R. C..: (1978) "Development of Standard Methods for Testing and Analyzing Fatigue Crack Growth Rate Data". AMFL-TR-78-40.

Iuculano, G. & Zanini, A.: (1986) "Evaluation of Failure Models through Step-stress Tests". IEEE Transactions on Reliability, Vol R-35, No 4, October 1986, pp 409 - 413.

Johnson, N. L. & Kotz, S.: (1970) "Continuous Univariate Distributions-1". Houghton Mifflin, New York.

Kielland, G. G., Lydersen, S., Onsøyen, E., & Slind, T.: (1985) "Subsea Control Valves. Accelerated Life Testing. Phase I - Final Report." SINTEF Report STF18 F85507 (Restricted).

Kielland, G. G., Lydersen, S., & Rausand, M.: (1986) "SERA. Subsea Equipment Reliability and Availability. Preliminary Report from the Project". SINTEF Project Memo, Project no 757003.20, 1986-04-04.

Lydersen, S., Onsøyen, E., Renolen, P., & Slind, T.: (1986) "Subsea Control Valves. Accelerated Life Testing. Phase II." SINTEF Report STF18 F86036 (Restricted).

Lydersen, S., Sæther, F., & Ørjasæter, O.: (1987) "Accelerated Life Testing of Pilot Valves". SINTEF Report STF18 F87040 (Restricted).

Mardia, K. V., Kent, J. T., & Bibby, J. M.: (1979) "Multivariate Analysis". Academic Press, London.

Narbuvoll, H.: (1987) "Regresjonsmodeller med stokastiske koeffisienter for analyse av sprekkvekst i stål" (Regression models with stochastic coefficients for analysis of fatigue crack growth in steel. In Norwegian). M.Sc. thesis at NTH, Department of Mathematical Statistics.

Spjøtvoll, E.: (1977) "Random Coefficients Regression Models. A Review." Math. Operationsforsch. Statist., Ser. Statistics, Vol. 8, No. 1, pp 69 - 93.

Virkler, D. A., Hillberry, B. M., & Goel, P. K.: (1979) "The Statistical Nature of Fatigue Crack Propagation". Transactions of the ASME, Vol 101, April 1979, pp 148 - 153.

Ørjasæter, O., Grøvlen, M., & Sæther, F.: (1985) "Scatter in Fatigue Crack Growth Data of C-MN Steel". SINTEF Report STF18 A85091.

STIAN LYDERSEN

RELIABILITY TESTING BASED ON DETERIORATION MEASUREMENTS
PART III: HEAT AGEING OF ELASTOMER FOIL

DOKTOR INGENIØRAVHANDLING 1988:32
NTH, INSTITUTT FOR MATEMATISKE FAG
TRONDHEIM 1988

ABSTRACT

Results from a heat ageing test of elastomer foil, where standard test pieces of foil were exposed to elevated temperatures, have been analyzed. The test pieces had been destructively tested, to measure breaking force and elongation at break.

The Arrhenius model has included in an accelerated time model for breaking force, and fitted to the data using non-linear least squares estimation. The foil is considered useful for its purpose as long as the breaking force for a standard test piece is above 12 kp. The lifetime distribution, with respect to this criterion, at normal use temperature has been estimated.

Contents of Part III

SUMMARY AND CONCLUSIONS

SINTEF, Division of Materials and Processes, has performed a number of tests on elastomer foils used as humidity stopper in building walls. The test series considered in this report, included a foil specially manufactured without heat stabilizer, unlike commercially available foils. The foil is considered useful for its purpose as long as the breaking force for a standard test piece is above 12 kp.

Pieces of foil were hung in heat chambers, and at certain points in time, standard test pieces were cut off and tested. Breaking force and elongation at break were measured. Breaking force tended to decrease as the foil deteriorated. Elongation tended to decrease until it was around 2.5 cm for a standard test piece, and then increased somewhat as it deteriorated further. Figure 1 shows the measured breaking force of the test pieces, as function of time.

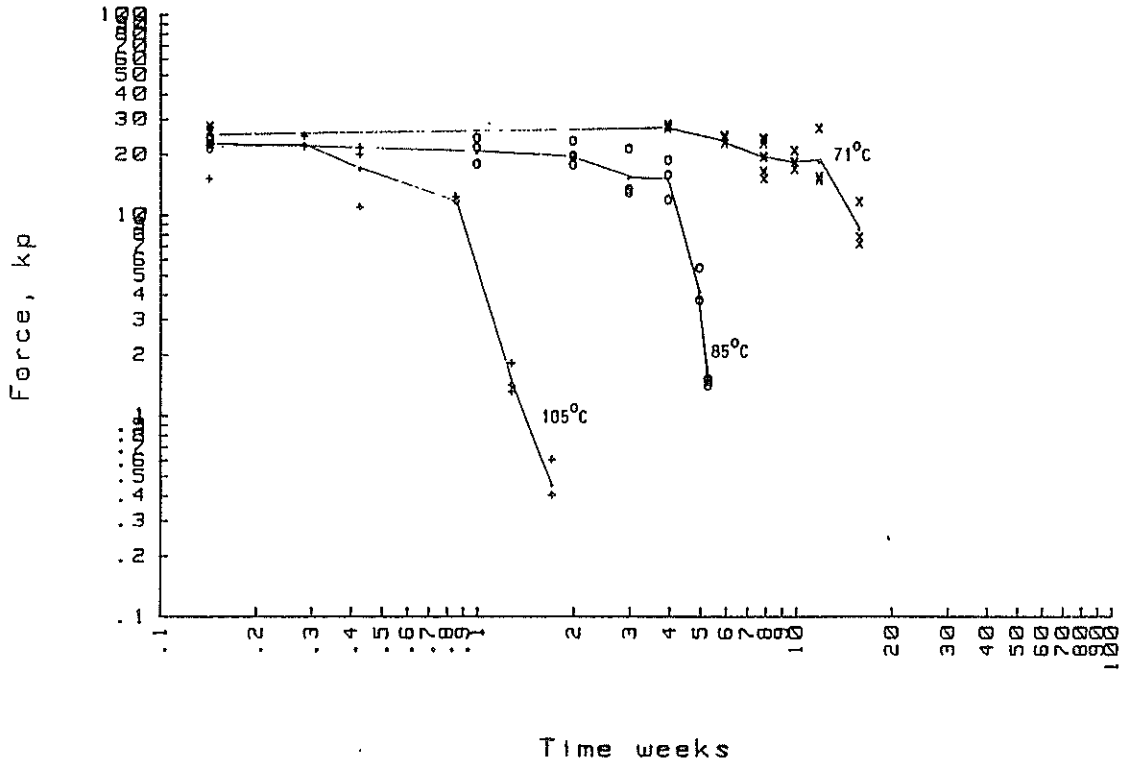

Figure 1: Measured breaking force as function of exposure time for each temperature. The solid lines show average measurements. Logarithmic scales.

The logarithms of the breaking force for each test piece are assumed independent, normally distributed with expectation

$$E(Y;\theta,t) = \beta_0 - \beta_1 \exp(A\, e^{-B/\theta}\, t)$$

and variance

$$Var(Y;\theta,t) = \sigma^2,$$

where Y is log(force), θ is absolute temperature, and t is exposure time. The model parameters, β_0, β_1, A, B, and σ, have been estimated using non-linear least squares estimation. According to the model, exposing the foil to temperature θ for time t has the same effect as exposing it to temperature θ_0 for time t' if

$$t' = a(\theta)\, t$$

where

$$a(\theta) = \exp[-B(1/\theta - 1/\theta_0)].$$

With θ_0 = 293.15 K (= 20°C), using the obtained parameter estimates, these acceleration factors $a(\theta)$ are obtained for the test temperatures:

71°C:	$t' = 260\, t$
85°C:	$t' = 910\, t$
105°C:	$t' = 4600\, t$.

Using these acceleration factors, equivalent times at 20°C for the test pieces have been calculated. Figure 2 shows measured breaking force as function of equivalent time av 20°C, including the fitted regression curve (estimated median breaking force). The model seems to fit the data reasonably well. There are, however, indications that other deterioration mechanisms dominate at the highest exposure times at 85°C and 105°C. A reduced data set is obtained by removing these observations. The fitted regression curve for the reduced data set is also shown in Figure 2.

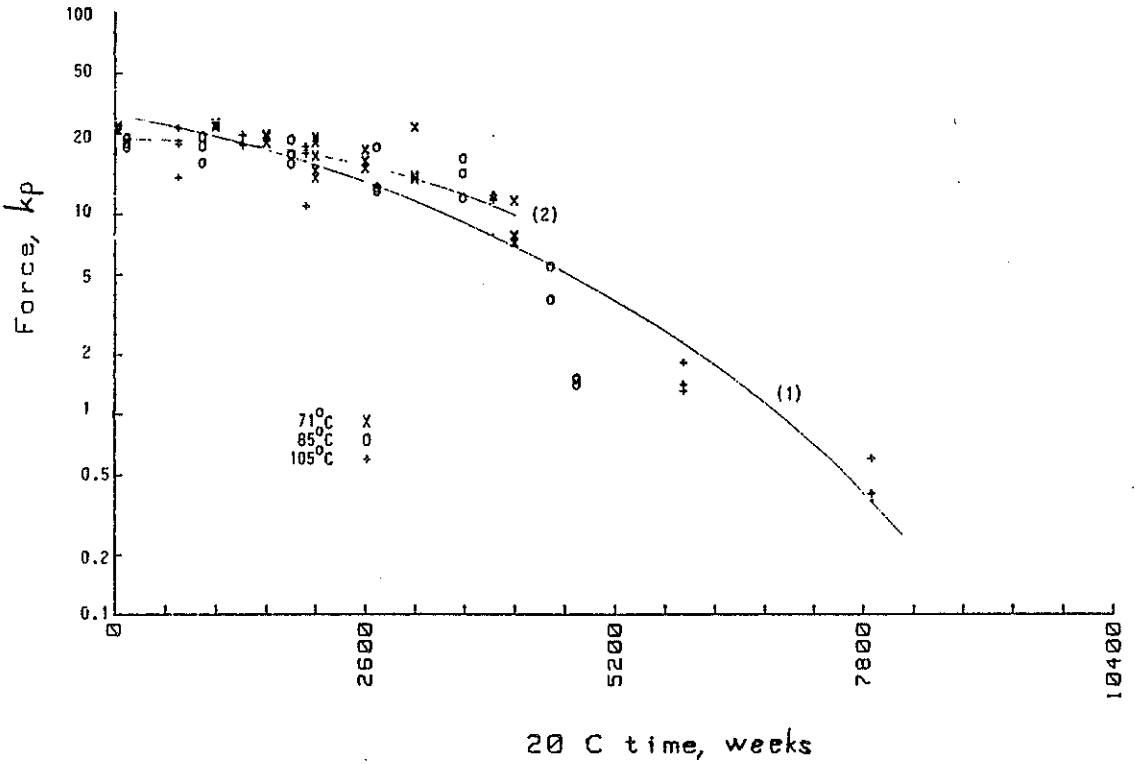

Figure 2: Breaking force as a function of estimated equivalent time at 20°C. Regression curve for the median breaking force, fitted to the whole data set (1), and fitted to the reduced data set (2).

The lifetime distribution at 20°C, for the time T until a standard test piece it reaches a breaking force of 12 kp, is given by

$$F_T(t) = P(T \leq t;\ \theta) = P(Y \leq \log(12);\theta_0, t).$$

Estimated probability densities based on the complete data set, and on the reduced data set, are shown in Figure 3. The two distributions are somewhat different, especially in the left tail. For example, the percentile $t_{0.98}$, is the time such that $P(T > t_{0.98}) = 0.98$. The estimates for this percentile are 9.5 years based on the complete data set and 49.6 years based on the reduced data set. The medians of the two distributions are 58.4 years and 72.2 years, respectively.

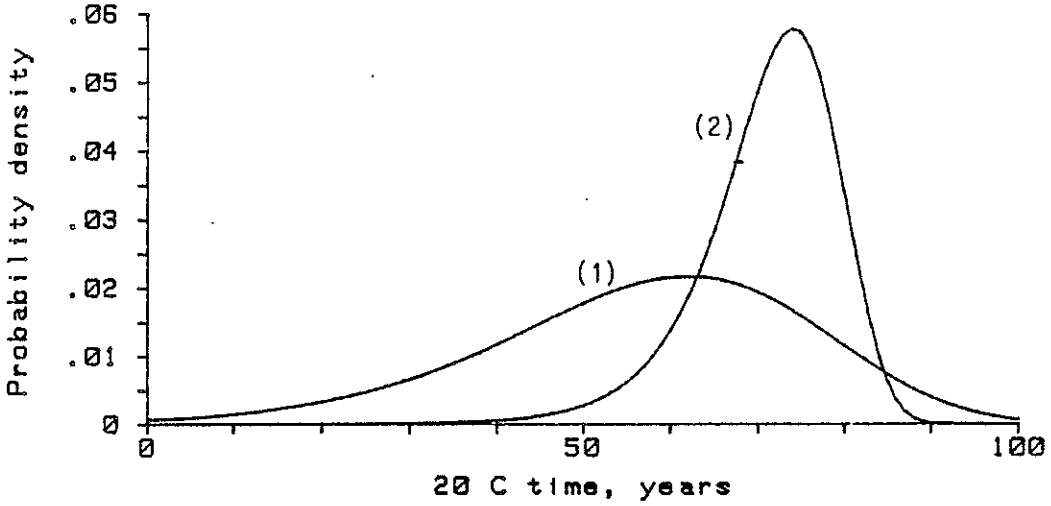

Figure 3: Estimated probability density for the lifetime distribution at 20°C, based on the whole data set (1) and on the reduced data set (2).

Even the with the lifetime distribution based on the reduced data set, the performance is far too poor for a humidity stopper in building walls. These results confirm that the tested type of foil without heat stabilizer does not seem suitable for this application.

1. INTRODUCTION

SINTEF, Division of Materials and Processes, has performed a number of tests on elastomer foils used as humidity stopper in building walls. The foil is considered useful for its purpose as long as the breaking force for a standard test piece is above 12 kp.

In this report, results from a laboratory test series are used to study deterioration function of time, within a stochastic deterioration model. Especially, the lifetime distribution at use temperature 20°C is studied. The tested foil was specially manufactured without heat stabilizer, unlike commercially available foils.

2. LABORATORY TEST RESULTS

Table 2.1 shows data from an ageing experiment of elastomer foil. This kind of foil is used as humidity stopper in building walls. In the experiment, pieces of foil were hung in heat chambers, and at certain points in time, standard test pieces were cut off the foil and tested with respect to breaking force and elongation at break. The purpose of the experiment was to assess the useful lifetime of the foil at use temperature, which is approximately 20°C. The foil is considered useful as long as the breaking force for a standard test piece is above 12 kp. The limit of 12 kp has been set on a somewhat ad hoc basis.

Table 2.2 shows the average values of the measurements, for each temperature and time combination.

Plots of corresponding values of elongation and breaking force are given in Figures 2.1 to 2.4. The trend seems to be the same for all the temperatures: Both force and elongation tend to decrease until an elongation "minimum" is achieved, then elongation tends to increase somewhat while the force still decreases. For modelling and computational convenience, the further analysis will be done on the force data, since these data seem to have a monotone time trend.

Figures 2.5 to 2.7 show the measured breaking force as function of time, plotted on linear and logarithmic axes.

Table 2.1: Heat ageing of elastomer foil. Breaking force and elongation at break for standard test pieces.

OBS#	Variable # 1 (Force, kp)	Variable # 2 (Elong, cm)	Variable # 3 (Time weeks)	Variable # 4 (Temp, C)
1	15.00000	3.36000	.14286	105.00000
2	26.50000	4.22000	.14286	105.00000
3	22.10000	3.93000	.14286	105.00000
4	24.50000	4.19000	.28571	105.00000
5	21.80000	4.00000	.28571	105.00000
6	21.70000	3.80000	.28571	105.00000
7	21.40000	3.80000	.42857	105.00000
8	10.80000	2.74000	.42857	105.00000
9	19.80000	3.72000	.42857	105.00000
10	12.20000	2.83000	.85714	105.00000
11	11.70000	2.78000	.85714	105.00000
12	11.60000	2.75000	.85714	105.00000
13	1.40000	2.65000	1.28571	105.00000
14	1.80000	2.62000	1.28571	105.00000
15	1.30000	2.58000	1.28571	105.00000
16	.40000	3.00000	1.71429	105.00000
17	.40000	2.96000	1.71429	105.00000
18	.60000	3.00000	1.71429	105.00000
19	21.30000	3.70000	.14286	85.00000
20	22.40000	3.76000	.14286	85.00000
21	23.70000	4.07000	.14286	85.00000
22	17.80000	3.80000	1.00000	85.00000
23	21.50000	4.30000	1.00000	85.00000
24	24.00000	4.08000	1.00000	85.00000
25	23.20000	4.25000	2.00000	85.00000
26	19.50000	3.80000	2.00000	85.00000
27	17.60000	3.72000	2.00000	85.00000
28	13.30000	3.31000	3.00000	85.00000
29	12.80000	3.20000	3.00000	85.00000
30	21.20000	4.08000	3.00000	85.00000
31	18.60000	3.83000	4.00000	85.00000
32	15.70000	3.57000	4.00000	85.00000
33	11.80000	3.00000	4.00000	85.00000
34	3.70000	2.75000	5.00000	85.00000
35	5.40000	2.67000	5.00000	85.00000
36	3.70000	2.56000	5.00000	85.00000
37	1.50000	2.70000	5.30000	85.00000
38	1.40000	2.77000	5.30000	85.00000
39	1.50000	2.79000	5.30000	85.00000
40	27.50000	4.40000	.14286	71.00000
41	26.20000	4.52000	.14286	71.00000
42	25.70000	4.34000	.14286	71.00000
43	27.50000	4.45000	4.00000	71.00000
44	26.80000	4.50000	4.00000	71.00000
45	28.00000	4.73000	4.00000	71.00000
46	24.60000	4.22000	6.00000	71.00000
47	22.60000	4.08000	6.00000	71.00000
48	24.10000	4.14000	6.00000	71.00000
49	16.30000	3.48000	8.00000	71.00000
50	19.30000	3.76000	8.00000	71.00000
51	23.70000	4.32000	8.00000	71.00000
52	23.90000	4.22000	8.00000	71.00000
53	15.00000	3.17000	8.00000	71.00000
54	22.60000	3.95000	8.00000	71.00000
55	16.70000	3.56000	10.00000	71.00000
56	18.20000	3.63000	10.00000	71.00000
57	20.70000	3.78000	10.00000	71.00000
58	14.70000	3.35000	12.00000	71.00000
59	15.30000	4.15000	12.00000	71.00000
60	26.70000	3.78000	12.00000	71.00000
61	7.10000	2.33000	16.00000	71.00000
62	11.50000	2.67000	16.00000	71.00000
63	7.70000	2.28000	16.00000	71.00000

Table 2.2: Heat ageing of elastomer foil. Average breaking force and average elongation at break for per temperature-time combination.

Foil

Data type is: Raw data

OBS#	Variable # 1 (Force, kp)	Variable # 2 (Elong, cm)	Variable # 3 (Time weeks)	Variable # 4 (Temp, C)
1	21.20000	3.83667	.14286	105.00000
2	22.66667	3.99667	.28571	105.00000
3	17.33333	3.42000	.42857	105.00000
4	11.83333	2.78667	.85714	105.00000
5	1.50000	2.61667	1.28571	105.00000
6	.46667	2.98667	1.71429	105.00000
7	22.46667	3.84333	.14286	85.00000
8	21.10000	4.06000	1.00000	85.00000
9	20.10000	3.92333	2.00000	85.00000
10	15.76667	3.53000	3.00000	85.00000
11	15.36667	3.46667	4.00000	85.00000
12	4.26667	2.66000	5.00000	85.00000
13	1.46667	2.75333	5.30000	85.00000
14	26.46667	4.42000	.14286	71.00000
15	27.43333	4.56000	4.00000	71.00000
16	23.76667	4.14667	6.00000	71.00000
17	20.13333	3.81667	8.00000	71.00000
18	18.53333	3.65667	10.00000	71.00000
19	18.90000	3.76000	12.00000	71.00000
20	8.76667	2.42667	16.00000	71.00000

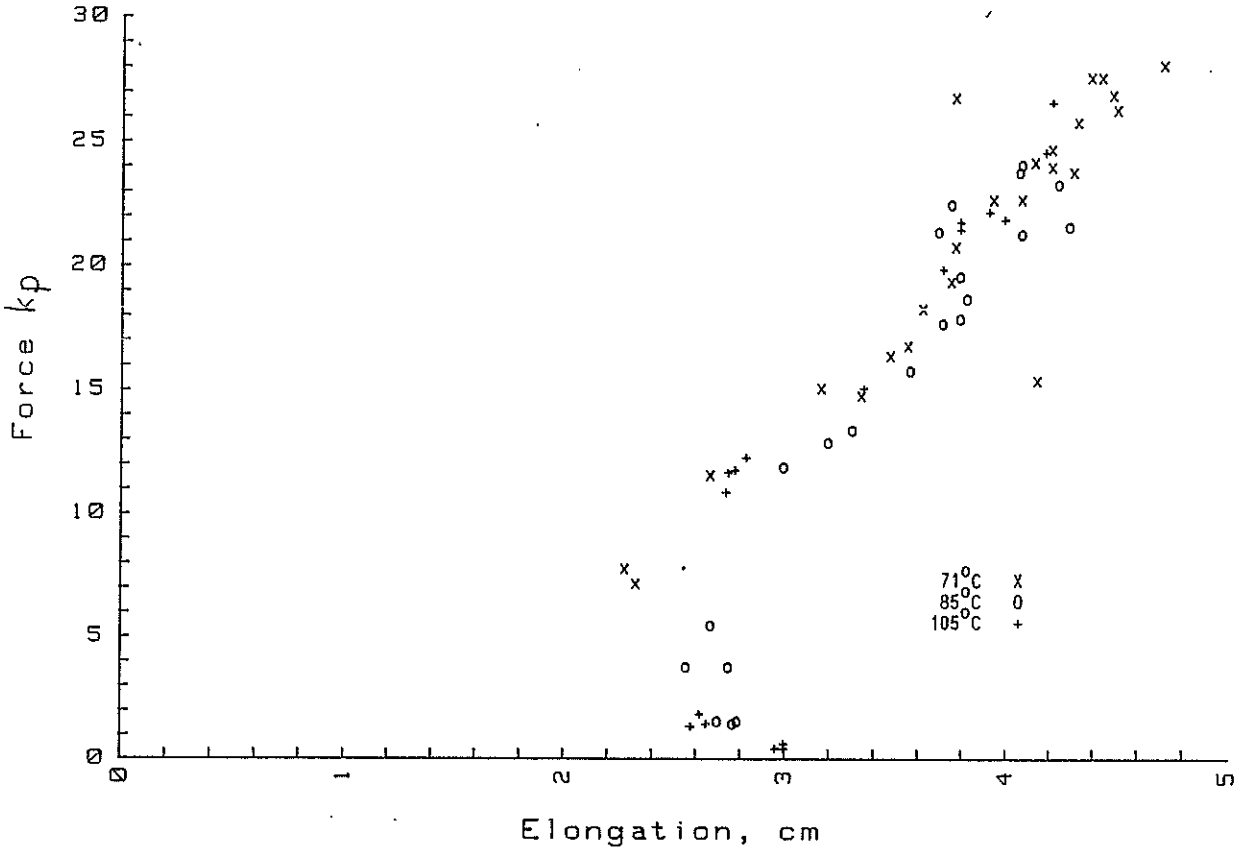

Figure 2.1: Scatter plot of force and elongation - all data.

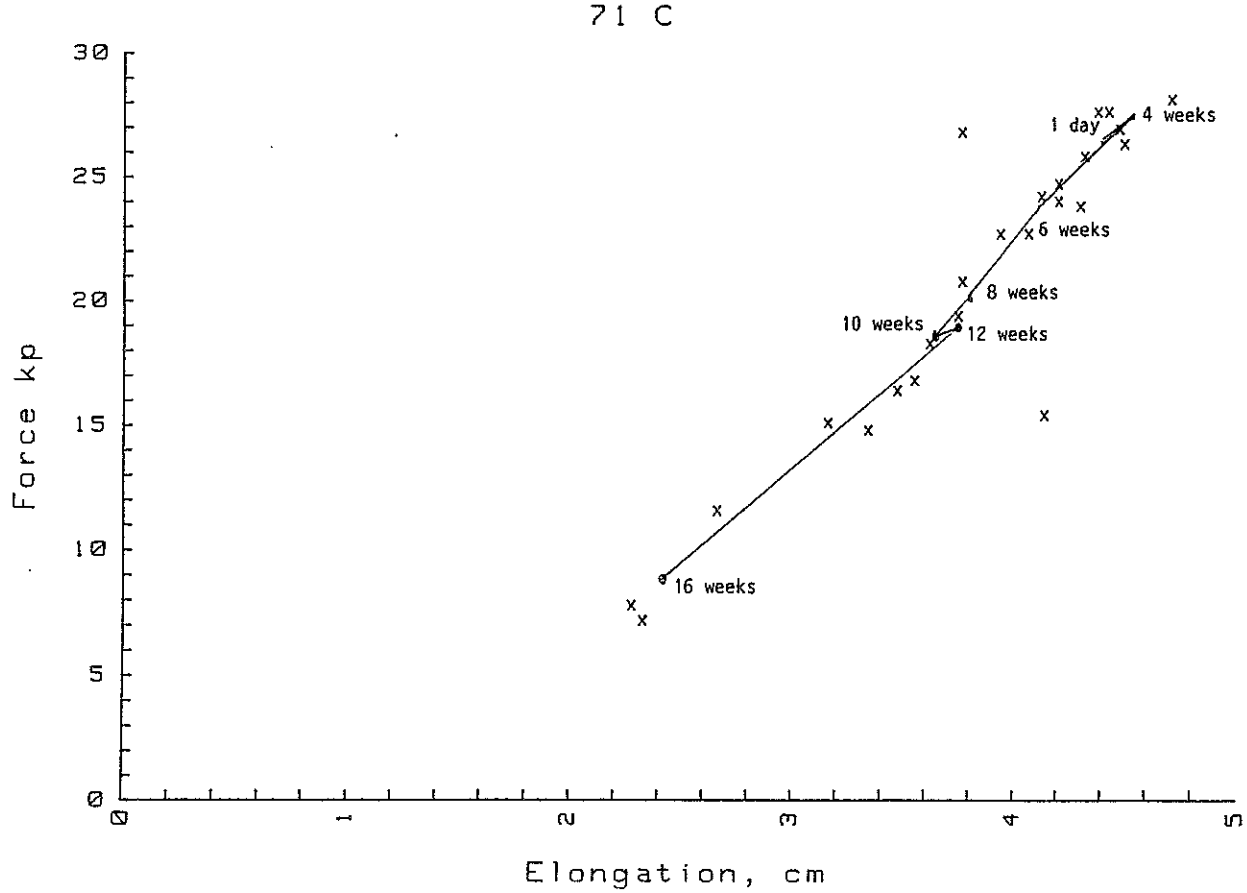

Figure 2.2: Scatter plot of force and elongation - foil exposed to 71°C.

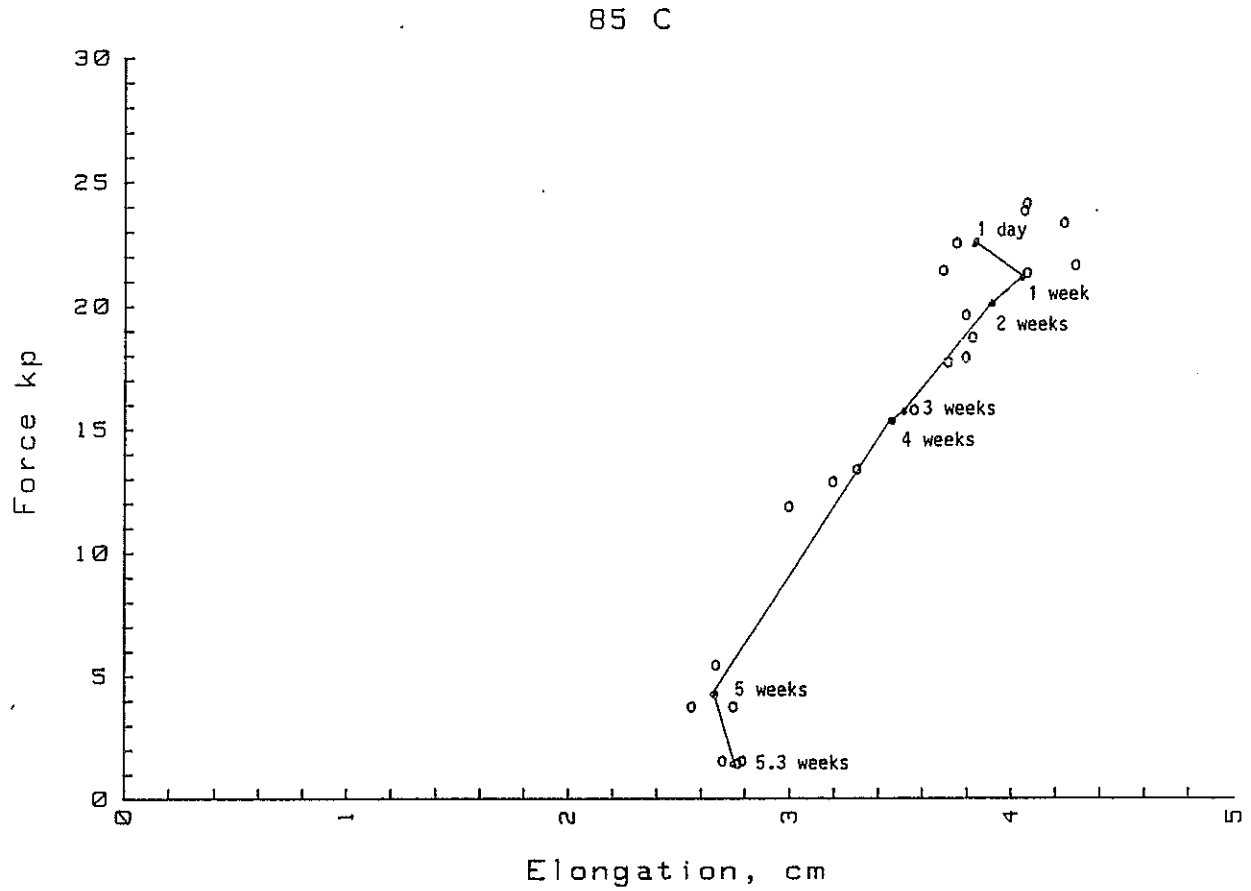

Figure 2.3: Scatter plot of force and elongation - foil exposed to 85°C.

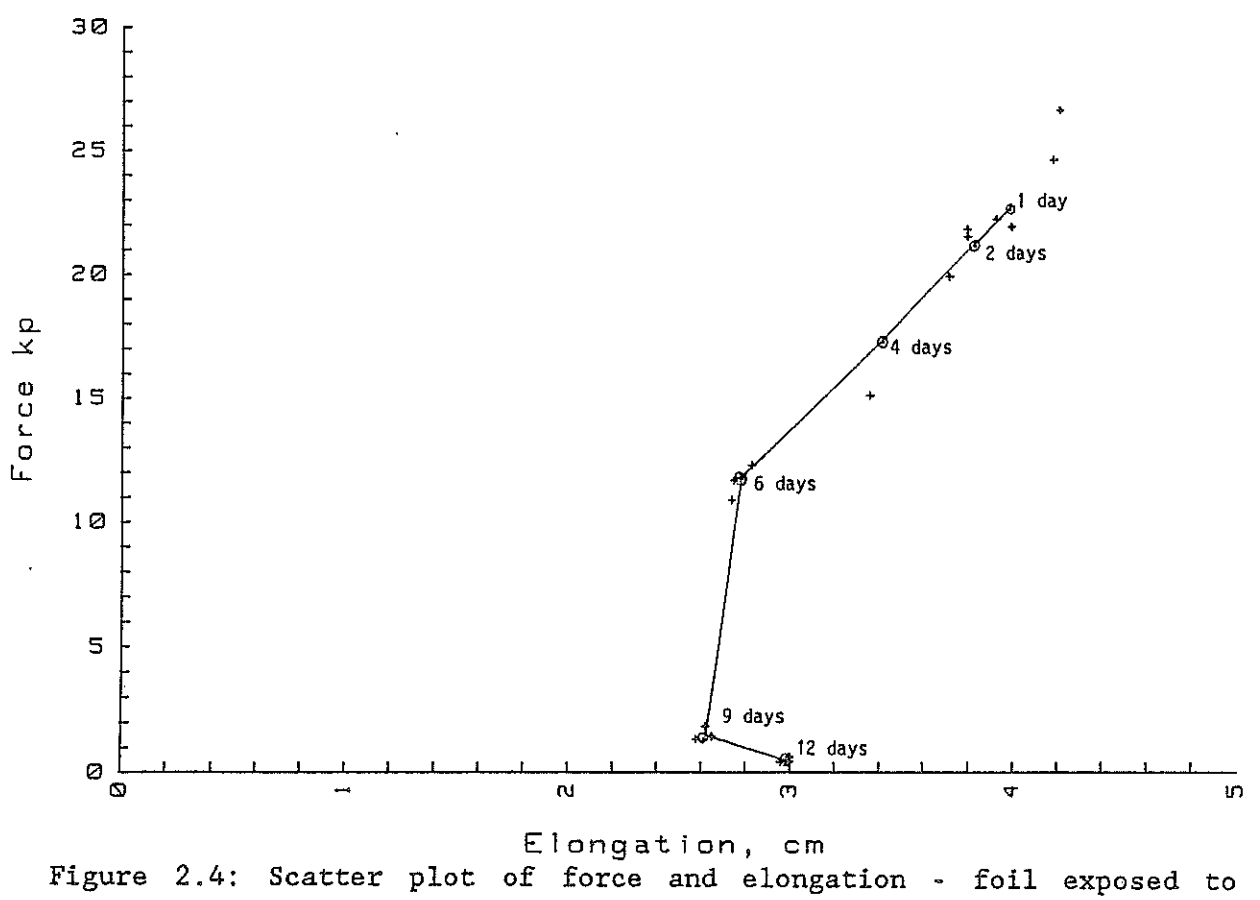

Figure 2.4: Scatter plot of force and elongation - foil exposed to 105°C.

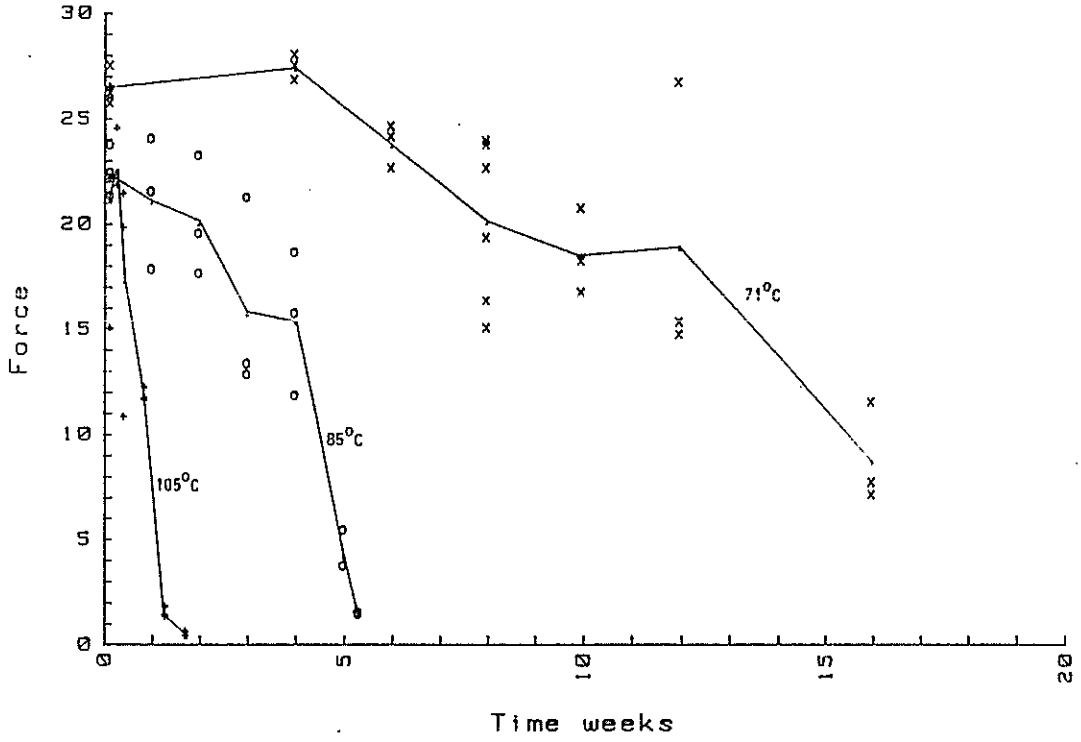

Figure 2.5: Measured breaking force as function of exposure time for each temperature (from Table 2.1). The solid lines show average measurements (from Table 2.2). Linear scales.

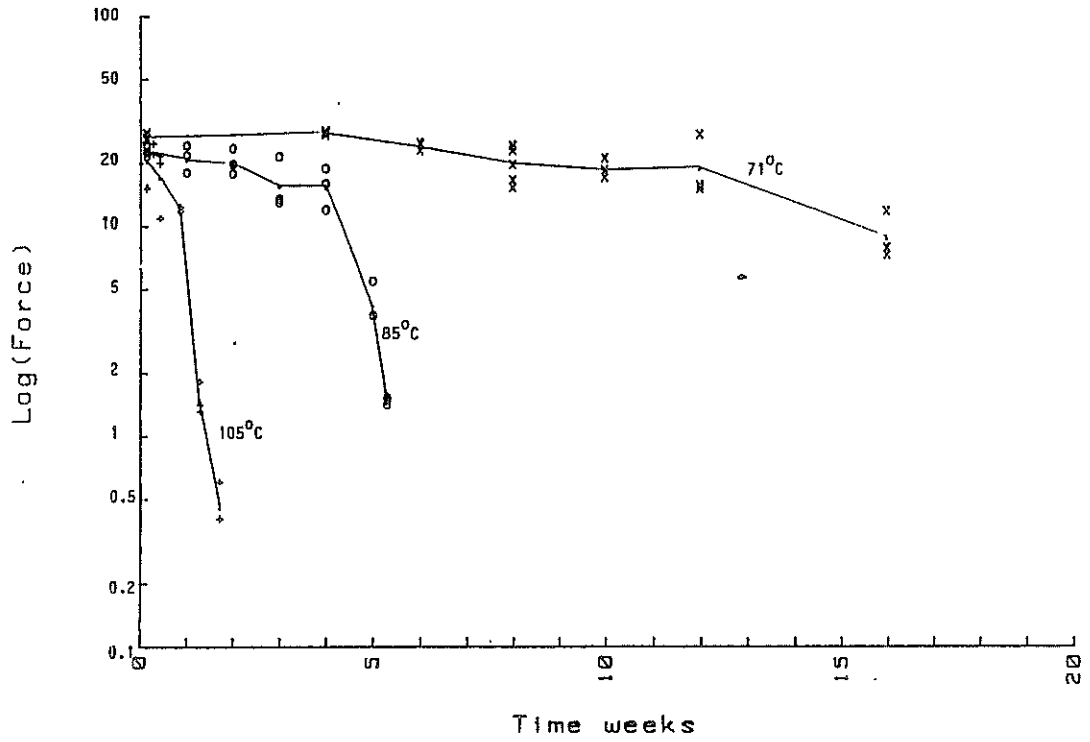

Figure 2.6: Measured breaking force as function of exposure time for each temperature (from Table 2.1). The solid lines show average measurements (from Table 2.2). Linear time scale and logarithmic force scale.

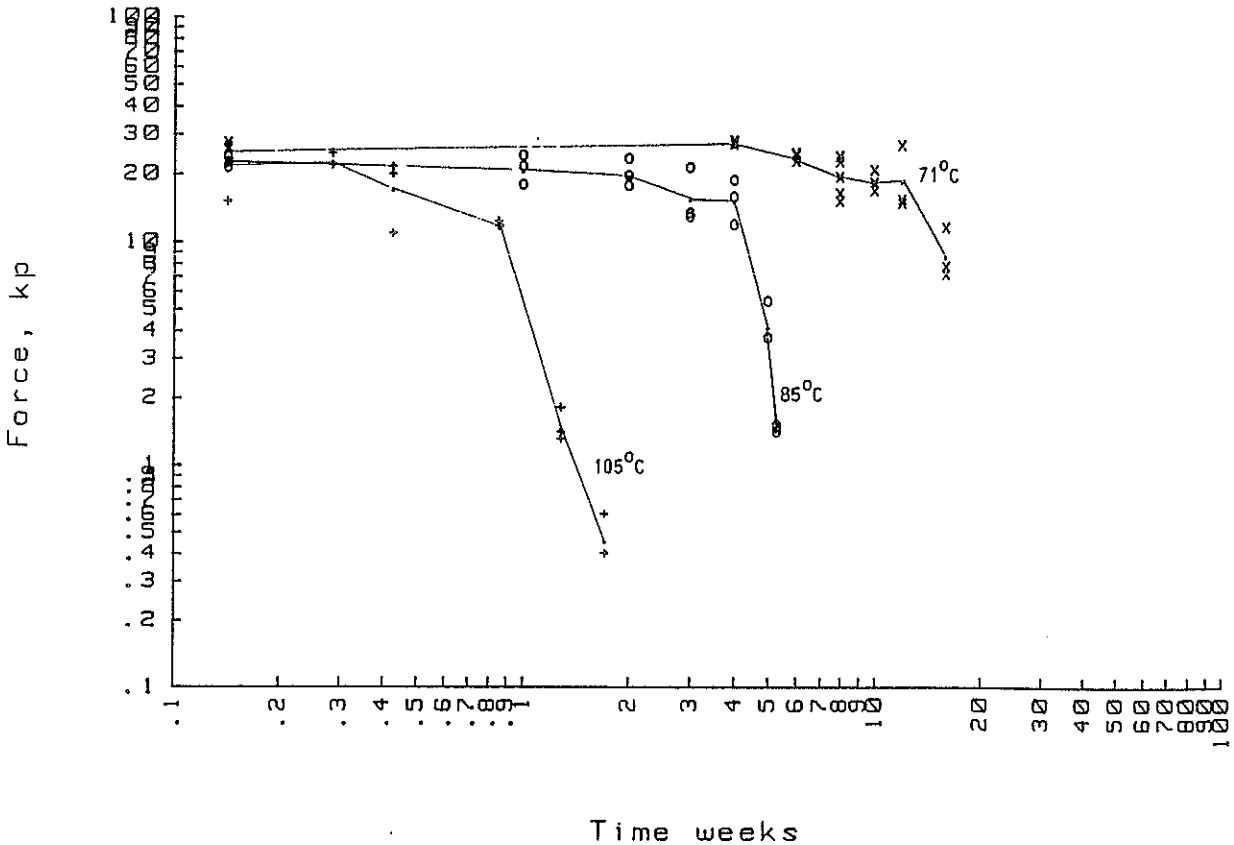

Figure 2.7: Measured breaking force as function of exposure time for each temperature (from Table 2.1). The solid lines show average measurements (from Table 2.2). Logarithmic scales.

3. STOCHASTIC MODELLING

Modelling will be performed on the logarithm of the force, log(force), rather that on the force itself, for two reasons:

1) When least squares estimation is to be performed, it is advantageous to have homoscedastic data. The force variance seems to be smaller for temperature-time combinations giving smaller expected force (Figure 2.5). Plots with force on a logarithmic scale (figures 2.5 and 2.7), however, indicate that the variance of log(force) seems to be approximately the same for all temperature-time combinations.

2) The normal distribution model, which gives computational convenience, assigns positive probability to both positive and negative values. Force itself is always positive, while log(force) can be both positive and negative. The normal distribution model may, thus, be applied on log(force).

Let the random variable Y denote the measured log(force) of a test piece exposed to temperature θ for time t. Throughout the report, log(·) denotes the natural logarithm. The data shall be fitted to some model

$$P(Y \leq y \; ; \; \theta, t \;) = F(y;\theta,t) \qquad (3.1)$$

A total of 4 assumptions will be set for this model.

Assumption 1:

The distribution depends on time and temperature only through $k(\theta)\cdot t$, where k is a function of θ only. That is, (3.1) may be written on the form

$$F(y;\theta,t) = F_1(y;k(\theta)t), \tag{3.2}$$

or

$$F(y;\theta,t) = F_1(y;u), \tag{3.3}$$

where

$$u = k(\theta)t. \tag{3.4}$$

The quantity u may be thought of as operational age, being the equivalent time at the (theoretical) temperature $\theta_0 = k^{-1}(1)$, that is, the temperature where the reaction rate $k(\theta)$ is 1.

It is easily checked out graphically whether (3.2) seems to agree with the data, since, alternatively, (3.2) may be written

$$\begin{aligned} F(y;\theta,t) &= F_1(y;\exp[\log(k(\theta)) + \log(t)]) \\ &= F_2(y,\log(k(\theta)) + \log(t)). \end{aligned} \tag{3.5}$$

Equation (3.5) states that the temperature effect on the distribution $F(\cdot)$ is to add a constant to log(t). Figure 2.7 shows the force - time data plotted on logarithic scales. Indeed, it seems plausible that changing the temperature only shifts the log(time) scale to the left or right, it does not seem to change the shape of the curve significantly. This indicates that (3.3) seems to agree well with the data.

Assumption 2:

The reaction rate, $k(\theta)$, follows the Arrhenius law, that is,

$$k(\theta) = A \exp(B/\theta), \tag{3.6}$$

where A and B are constants and θ is given as absolute temperature.

A rough estimate for the constant B may be found by examining Figure 2.7, even without extra model assumptions. According to Assumptions 1 and 2, exposing the foil to temperature θ_1 for time t_1 has the same effect as exposing it to temperature θ_2 for time t_2 if

$$A \exp(B/\theta_1)\ t_1 = A \exp(B/\theta_2)\ t_2. \tag{3.7}$$

It follows from this equation that

$$B = \log(t_2/t_1)/(1/\theta_2 - 1/\theta_1) \tag{3.8}$$

For example, Figure 2.7 shows that average breaking force is approximately 10 kp after $t_1 \approx 0.9$ when $\theta_1 = 105^{\circ}C$, and after $t_2 \approx 15$ when $\theta_2 = 71^{\circ}C$. Inserting these values into (3.8) gives $B \approx 1.1 \cdot 10^4$. The effect of the parameter B may be interpreted as follows, according to (3.7): Exposing the foil in $20^{\circ}C$ for time t' has the same effect as exposing it in temperature θ for time t if

$$t' = a(\theta)\ t \tag{3.9}$$

where

$$a(\theta) = \exp[-B(1/\theta - 1/\theta_0)] \tag{3.10}$$

and $\theta_0 = 293.15$ K. The function $a(\theta)$ in (3.9) is commonly referred to as the acceleration factor. In our case, this factor may be estimated by inserting the estimate for B into (3.10). For the temperatures at which

the foil has been tested, and with $B = 1.1 \cdot 10^4$, equation (3.9) with estimated acceleration factor becomes:

$$\begin{aligned} 71^{\circ}C: &\quad t' = 260\ t \\ 85^{\circ}C: &\quad t' = 910\ t \\ 105^{\circ}C: &\quad t' = 4600\ t \end{aligned} \tag{3.11}$$

The interpretation of equations (3.11) is that, for example, breaking force deterioration goes 260 times faster at 71°C than at 20°C.

Assumption 3:

The log(force) data follow a homoscedastic normal model, that is,

$$Y \sim N(m(u), \sigma^2) \tag{3.12}$$

where m(u) is a function of u, and σ^2 does not depend on u.

We recall from Assumptions 1 and 2 that

$$u = k(\theta)t = A \exp(B\theta)\ t. \tag{3.13}$$

The function m(u) is the expected log(force) after time t in temperature θ. Figures 2.6 and 2.7 indicate a somewhat complex functional form of m(u): The force seems constant, or slowly decreasing in the beginning, then it starts to decrease more rapidly. The physical ageing mechanisms are not well enough known to provide background for setting up a function m(u). However, this does not impose any serious problem: The purpose is to predict how long the force keeps above 12 kp at 20°C. In order to do this, it is not necessary to extrapolate outside the force range for which data exists, only outside the temperature range for which we have data. As long as Assumptions 1 and 2 about the temperature effect hold, the results will be rather insensitive to which model m(u) is used, as long as the chosen m(u) fits reasonably well to the data.

Assumption 4

The following model will be used for expected log(force) after time t in temperature θ:

$$m(u) = \beta_0 - \beta_1 \exp(\beta_2 \cdot u) \tag{3.14}$$

Combining (3.14) with (3.13), deleting excess parameters, yields

$$m(u) = E(Y;\theta,t) = \beta_0 - \beta_1 \exp(A\, e^{-B/\theta}\, t). \tag{3.15}$$

Hence, the complete model may be written

$$\log(Y_i) = \beta_0 - \beta_1 \exp(A\, e^{-B/\theta_i}\, t_i) + \sigma U_i \tag{3.16}$$

where Y_i is the measured breaking force of test specimen number i, after time t_i at temperature θ_i. The parameters to be estimated are β_0, β_1, A, B, and σ. We shall take Y_i to be measured in kp, t_i in weeks, and absolute temperature θ_i in K.

4. MODEL PARAMETERS

Least squares estimates (LSE) for the parameters are be found by minimizing the function

$$Q(\beta_0,\beta_1,A,B) = \sum_{i=1}^{n} [\ y_i - E(Y_i;\theta_i,t_i)\ ]^2 \qquad (4.1)$$

The minimization is readily done numerically, by a computer code with a proper search procedure. Rough initial estimates for the search procedure may, for example, be found from Figure 2.7. Initially, the mean breaking force seems to be around 27 kp, that is, $\beta_0 \approx \log(27) \approx 3.3$. Using two of the mean values for 105°C from Table 2.2, we obtain

$$E(Y;105^oC,\ 0.86) \approx \log(11.83) = 2.47$$
$$E(Y;105^oC,\ 1.71) \approx \log(0.467) = -0.76$$

These values, together with the obtained rough estimates for B and β_0, gives two equations for β_1 and A:

$$2.47 = 3.3 - \beta_1 \exp[\ A \exp(\ -1.1\cdot10^4/(273.15+105)\ )\ 0.86\ ]$$
$$-0.76 = 3.3 - \beta_1 \exp[\ A \exp(\ -1.1\cdot10^4/(273.15+105)\ )\ 1.71\ ]$$

These equations are readily solved, giving $\beta_1 = 0.167$ and $A = 8.02\cdot10^{12}$. Thus, the initial set of parameter estimates is:

$$\beta_0 = 3.3$$
$$\beta_1 = 0.167$$
$$A = 8.02\cdot10^{12}$$
$$B = 1.1\cdot10^4$$

The results below were obtained by a statistical analysis program package (HP, 1982). This program package utilizes the Marquandt algorithm (Marquandt, 1963) for nonlinear least squares estimation. These estimates and confidence intervals were obtained:

Parameter	Estimate	One at a time 90% confidence intervals:
β_0	4.63	(4.24 , 5.02)
β_1	1.17	(0.848 , 1.49)
A	$3.93 \cdot 10^{12}$	$(3.06 \cdot 10^{12}$, $5.04 \cdot 10^{12})$
B	10999.5	(10996.2 , 11002.8)
σ	0.414	

A more detailed calculation output is given in Table 4.1. Predicted observations are estimated expectations, obtained by inserting the parameter estimates:

$$\hat{Y} = \hat{E}(Y_i;\theta_i,t_i) = \hat{\beta}_0 - \hat{\beta}_1 \exp(\hat{A}\, e^{-\hat{B}/\theta_i}\, t_i).$$

The difference between observed and predicted Y values,

$$Y_i - \hat{Y}_i,$$

are called residuals. Table 4.2 gives observed Y, predicted Y, and residuals for the log(force) data. Figure 4.1 shows the residuals plotted versus time. The residuals seem to indicate a reasonable fit between the data and the assumed model.

Note that the final estimate of the temperature dependence parameter, B, happens to be equal to the initial estimate, $\hat{B} = 1.1 \cdot 10^4$. The calculated acceleration factors (3.11) are, thus, also valid for final parameter estimates. To provide a visual check on model fit, force is plotted on a logarithmic scale, as a function of estimated equivalent time at 20°C, t', in Figure 4.2. The regression curve is also shown in the figure. From looking at this figure, and at the table of residuals, the model seems to provide a reasonably well fit with the data, perhaps except the data for the longest exposure time in 85°C. The measured breaking forces after 5.3 weeks in this temperature are somewhat lower than our model would predict. This fact will not be examined further, since the matter of interest is time to reach a breaking force of 12 kp, and we are primarily interested in a reasonably good fit in that area.

Table 4.1: Computer printout, least squares estimation. Note that the computations were performed on the transformed model

$$E(Y) = \beta_0 - \beta_1 \exp[\ \exp(A'-B'/\theta')\ t\ ],$$

where $A'=\log(A)$, $B'=B/1000$, and $\theta'=\theta/1000$ is absolute temperature given in 1000K. This transformation was performed because the computer code did not accept parameter values too many orders of magnitude away from 1.

```
NON-LINEAR REGRESSION ON DATA SET:
  Foil

**********************************************************************

--where:  Dependent variable = (8)ln(Force)
          Independent variable(s) = (10)Temp 1000K
                                    (3)Time weeks

**********************************************************************

Delta(Convergence criteria)=  .0001

THE INITIAL VALUES OF PARAMETERS ARE :
          PARAMETER 1 = 3.3
          PARAMETER 2 = .167
          PARAMETER 3 = 29.7
          PARAMETER 4 = 11

ITERATION              ESTIMATED PARAMETER VALUES              S.S.RESIDUALS

     0        3.30000        .16700       29.70000       11.00000       17.96
     1        3.57967        .36555       29.50891       11.00147       12.09
     2        4.25274        .81678       29.16174       11.00275
     3        4.53043       1.08428       29.00394
     4        4.55175       1.10558       29.01[illegible]
     5        4.56890       1.12060                      ...00077       10.10
     6        4.58205                                    11.00066       10.10
     7        4.59[illegible]                            11.00054       10.10
     8                      ...9814       29.00267       11.00043       10.10
                            1.16893       29.00203       11.00031       10.10
              4.62729       1.16955       29.00147       11.00020       10.10
    19        4.62786       1.17002       29.00096       11.00009       10.10
    20        4.62831       1.17038       29.00051       10.99997       10.10
    21        4.62864       1.17064       29.00010       10.99986       10.10
    22        4.62888       1.17083       28.99972       10.99975       10.10
    23        4.62906       1.17096       28.99937       10.99963       10.10

**********************************************************************

THE ESTIMATED PARAMETER VALUES AFTER 23 ITERATIONS ARE :
          PARAMETER  1=       4.6291744 ( 4.6291744268E+00)
          PARAMETER  2=       1.1710486 ( 1.1710486052E+00)
          PARAMETER  3=      28.9990420 ( 2.8999041991E+01)
          PARAMETER  4=      10.9995179 ( 1.0999517908E+01)

**********************************************************************

          THE INITIAL VALUE OF SUM OF SQUARED RESIDUALS = 17.961084776
          AFTER 23 ITERATIONS THE SUM OF SQUARED RESIDUALS= 10.1028354859
          APPROXIMATE STANDARD ERROR FROM SQUARED RESIDUALS= .41380490543

**********************************************************************

               APPROXIMATE 90 % CONFIDENCE INTERVALS ON PARAMETERS

 PARAMETER       ONE-AT-A TIME C.I.                SIMULTANEOUS C.I.

           LOWER LIMIT       UPPER LIMIT       LOWER LIMIT       UPPER LIMIT
     1        4.2395            5.0188            3.9627            5.2957
     2         .8475            1.4946             .6176            1.7245
     3       28.7496           29.2484           28.5724           29.4257
     4       10.9962           11.0028           10.9938           11.0052

**********************************************************************
```

Table 4.2: Residual analysis on Y = log(force). The table shows observed Y, predicted Y, residual, standardized residual, and significance. Two (three) stars indicate a standardized residual greater than 2 (3).

OBS#	OBSERVED Y	PREDICTED Y	RESIDUAL	STANDARDIZED RESIDUAL	SIGNIF.
1	2.70805	3.29457	-.58652	-1.41738	
2	3.27714	3.29457	-.01743	-.04211	
3	3.09558	3.29457	-.19899	-.48088	
4	3.19867	3.10817	.09050	.21871	
5	3.08191	3.10817	-.02626	-.06346	
6	3.07731	3.10817	-.03086	-.07457	
7	3.06339	2.89574	.16765	.40515	
8	2.37955	2.89574	-.51619	-1.24743	
9	2.98568	2.89574	.08994	.21736	
10	2.50144	2.06327	.43817	1.05888	
11	2.45959	2.06327	.39632	.95775	
12	2.45101	2.06327	.38774	.93701	
13	.33647	.83101	-.49453	-1.19509	
14	.58779	.83101	-.24322	-.58777	
15	.26236	.83101	-.56864	-1.37418	
16	-.91629	-.99304	.07675	.18547	
17	-.91629	-.99304	.07675	.18547	
18	-.51083	-.99304	.48222	1.16532	
19	3.05871	3.42757	-.36886	-.89139	
20	3.10906	3.42757	-.31851	-.76970	
21	3.16548	3.42757	-.26209	-.63337	
22	2.87920	3.22672	-.34752	-.83982	
23	3.06805	3.22672	-.15867	-.38344	
24	3.17805	3.22672	-.04867	-.11761	
25	3.14415	2.94959	.19456	.47018	
26	2.97041	2.94959	.02083	.05033	
27	2.86790	2.94959	-.08169	-.19741	
28	2.58776	2.61769	-.02993	-.07233	
29	2.54945	2.61769	-.06825	-.16493	
30	3.05400	2.61769	.43631	1.05438	
31	2.92316	2.22021	.70295	1.69874	
32	2.75366	2.22021	.53345	1.28913	
33	2.46810	2.22021	.24789	.59904	
34	1.30833	1.74419	-.43586	-1.05329	
35	1.68640	1.74419	-.05779	-.13966	
36	1.30833	1.74419	-.43586	-1.05329	
37	.40547	1.58382	-1.17836	-2.84761	**
38	.33647	1.58382	-1.24735	-3.01434	***
39	.40547	1.58382	-1.17836	-2.84761	**
40	3.31419	3.44945	-.13526	-.32687	
41	3.26576	3.44945	-.18369	-.44390	
42	3.24649	3.44945	-.20295	-.49046	
43	3.31419	3.18911	.12507	.30225	
44	3.28840	3.18911	.09929	.23994	
45	3.33220	3.18911	.14309	.34579	
46	3.20275	3.03225	.17050	.41202	
47	3.11795	3.03225	.08570	.20710	
48	3.18221	3.03225	.14996	.36240	
49	2.79117	2.85830	-.06714	-.16224	
50	2.96011	2.85830	.10180	.24602	
51	3.16548	2.85830	.30717	.74231	
52	3.17388	2.85830	.31558	.76262	
53	2.70805	2.85830	-.15025	-.36310	
54	3.11795	2.85830	.25965	.62746	
55	2.81541	2.66541	.15000	.36250	
56	2.90142	2.66541	.23602	.57035	
57	3.03013	2.66541	.36473	.88140	
58	2.68785	2.45150	.23635	.57116	
59	2.72785	2.45150	.27635	.66784	
60	3.28466	2.45150	.83317	2.01343	**
61	1.96009	1.95124	.00885	.02139	
62	2.44235	1.95124	.49110	1.18680	
63	2.04122	1.95124	.08998	.21744	

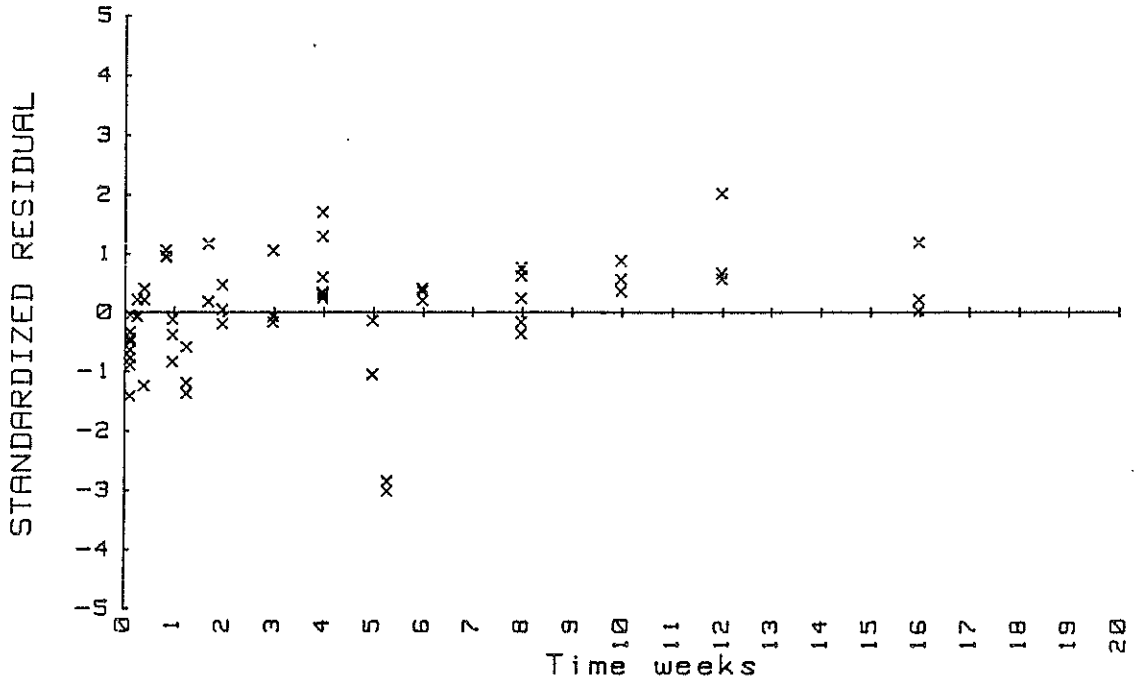

Figure 4.1: Residuals as function of time (weeks) for the fitted model.

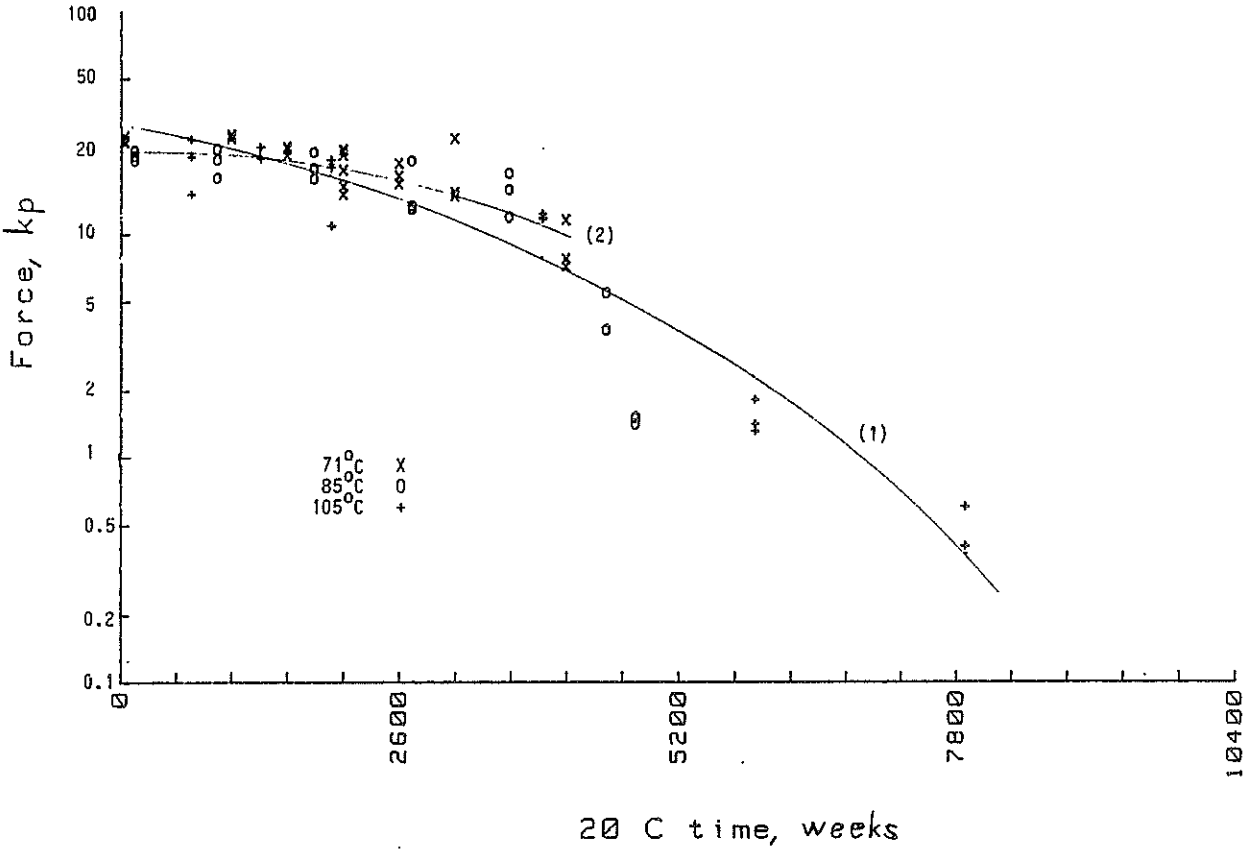

Figure 4.2: Breaking force as a function of estimated equivalent time at 20°C. Regression curve for the median breaking force, fitted to the whole data set (1), and fitted to the reduced data set (2).

5. LIFETIME DISTRIBUTION

For a standard test piece of elastomer foil, let T denote the time until it reaches a breaking force of 12 kp. If the breaking force is assumed to be a non-increasing function of time, we can set

$$F_T(t) = P(T \le t;\ \theta)$$

$$= P(Y \le \log(12);\theta,t)$$

$$= \Phi\left(\frac{\log(12) - [\beta_0 - \beta_1 \exp(\ A\ e^{-B/\theta}\ t)]}{\sigma} \right)$$

$$= \Phi\left(\frac{\beta_1 \exp(\ A\ e^{-B/\theta}\ t)] - [\beta_0 - \log(12)]}{\sigma} \right)$$

$$= \Phi\left(\frac{\exp(at) - b}{c} \right), \tag{5.1}$$

where

$$\begin{aligned} a &= A\ e^{-B/\theta} \\ b &= [\beta_0 - \log(12)]/\beta_1 \\ c &= \sigma/\beta_1, \end{aligned} \tag{5.2}$$

and $\Phi(x)$ is the standard normal distribution function.

The probability density of T is

$$f_T(t) = \frac{d}{dt} F_T(t)$$

$$= \varphi\left(\frac{\exp(at) - b}{c}\right) \cdot \exp(at) \cdot a \cdot \frac{1}{c}$$

$$= \frac{1}{\sqrt{2\pi}\cdot c} \exp\left[-\frac{1}{2} \left(\frac{\exp(at) - b}{c}\right)^2 \right] \exp(at) \cdot a \cdot \frac{1}{c} \tag{5.3}$$

where $\varphi(x)$ is the standard normal probability density. Inserting the

estimated parameters, and 20°C, into (5.2), yields the estimated time to failure distribution (5.3) at this temperature,

$$\hat{F}_T(t) = \Phi\left[\frac{\exp(\hat{a}t) - \hat{b}}{\hat{c}}\right], \tag{5.4}$$

where

$\hat{a} = 1.99 \cdot 10^{-4}$ weeks^{-1} = 0.01035 years^{-1}

$\hat{b} = 1.83$

$\hat{c} = 0.354$.

The probability density (5.3) with these parameters is shown in Figure 5.1.

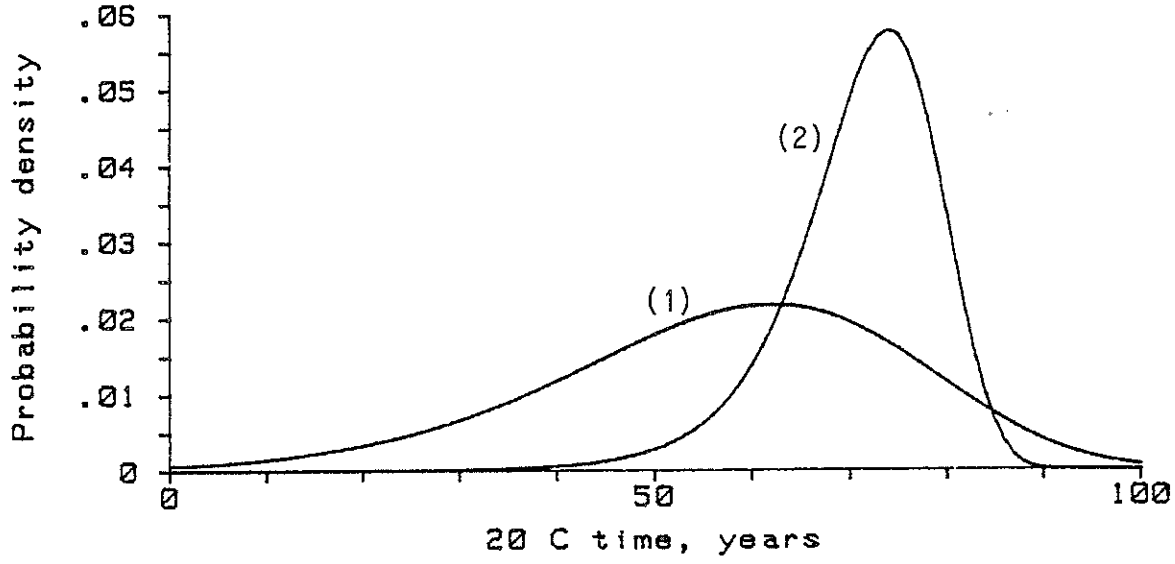

Figure 5.1: Estimated probability density for the lifetime distribution at 20°C, based on the whole data set (1) and on the reduced data set (2).

An interesting question is how sensitive the estimated time to failure distribution is towards the estimated regression curve. To give an indication about this, another regression curve will be fitted. From Figure 2.1, both elongation and force seem to follow an approximately linear trend as time increases, except for the longest exposed specimens at the highest temperatures. This could indicate that some other deterioration mechanism takes over approximately when the breaking force passes below 6 - 8 kp. A reduced, and perhaps more homogeneous, data set is created by deleting the observations for:

9 days, 105°C
12 days, 105°C
5 weeks, 85°C
5.3 weeks, 85°C

That is, a total of 12 observations are deleted, giving 51 observations in the reduced data set. The same model (16) was fitted to log(force) in the reduced data set, using LSE with the previous estimated parameters as initial estimates in the computer run. These final estimates were obtained:

Parameter	Estimate	One at a time 90% confidence intervals
β_0	3.19	(3.15 , 3.23)
β_1	0.0370	(0.0327 , 0.0413)
A	$1.39 \cdot 10^{13}$	$(1.34 \cdot 10^{13}$, $1.45 \cdot 10^{13})$
B	10968.0	(10967.6 , 10968.5)
σ	0.207	

Note that the estimate of the time dependence parameter, B, still equals the initial estimate, $\hat{B} = 1.1 \cdot 10^4$, to three digits. This regression curve is also drawn in Figure 4.2. In this case, the estimated parameters in the time to failure distribution (5.1) become

$\hat{a} = 7.84 \cdot 10^{-4}$ weeks^{-1} = 0.0408 years^{-1}
$\hat{b} = 19.06$
$\hat{c} = 5.59.$

The probability density (5.3) with these parameters is also shown in Figure 5.1.

Both the fitted regression curve, and the estimated time to failure distribution, depend quite a lot on whether estimation is based on the complete data set or on the reduced data set. Actually, the left tail of the time to failure distribution is shifted quite a lot to the right when the data set is reduced. This is better seen in Tables 5.1 and 5.2, which give some percentiles and survival probabilities for the estimated time to failure distributions. For example, the percentile $t_{0.98}$, is the time such that $P(T > t_{0.98}) = 0.98$. Table 5.2 shows that the estimates for this percentile are 9.5 years and 49.6 years, respectively. The medians of the two distributions are 58.4 years and 72.2 years, respectively.

Table 5.1: Some survival probabilities for the estimated time to failure distributions.

Time, years	Estimated survival probability	
	Based on complete data set	Based on reduced data set
20	0.955	0.999
40	0.815	0.994
60	0.456	0.910
80	0.098	0.102

Table 5.2: Some percentiles for the estimated time to failure distributions.

Survival probability	Estimated time, years	
	Based on complete data set	Based on reduced data set
0.98	9.5	49.6
0.95	21.4	56.1
0.9	30.9	60.7
0.5	58.4	72.2

As mentioned at the beginning of this chapter, there are good reasons to believe that different deterioration mechanisms have been present the highest exposure times at the highest temperatures, than for the reduced data set. First, the observed log(force) values tend to be higher than the predicted values from our model and estimates. Second, the elongation - force data do not follow the same approximately linear trend as for the rest of the data (Figure 2.1).

However, whether the the results based on the complete data set, or the results based on the reduced data set are accepted, the main conclusion turns out to be the same. Considering normal life-times for buildings, neither of the two probability densities shown in Figure 5.1 show a satisfactory performance for a humidity stopper in building walls.

REFERENCES

HP (1982): "Statistical Library for the HP Series 200 Computers. Manual Part No. 98820-13111". Hewlett-Packard Desktop Computer Division, 3404 East Harmony Road, Fort Collins, Colorado 80525.

Marquandt, D.: (1963) "An Algorithm for Least Squares Estimation of Nonlinear Parameters". J. Soc. Indust. and Appl. Math., Vol 11, No 2.

Renolen, P.: (1979) "Varmealdring av byggfolie" (Heat Ageing of Building Foil. In Norwegian). SINTEF Report STF16 F79052 (Restricted).

ISBN 82-7119-050-4